Biogeochemistry of dissolved domoic acid in the ocean: Sources, distribution and function

Dissertation

zur Erlangung des akademischen Doktorgrades der Naturwissenschaften

Doctor rerum naturalium

- Dr. rer. nat. -

an der

im Fachbereich Biologie/Chemie

im Fach Chemie

vorgelegt von

Jana Geuer

M.Sc. Biotechnologie

B.Sc. Naturwissenschaftliche Forensik

2020

Kolloquium: 27. Mai 2020

1. Gutachter: Prof. Dr. Boris Koch

2. Gutachter: Prof. Dr. Allan Cembella

Universität Bremen

Bremerhaven, 20.04.2020

Versicherung an Eides Statt

.

Ich, Jana Geuer,

versichere an Eides Statt durch meine Unterschrift, dass ich die vorstehende Arbeit selbständig und ohne fremde Hilfe angefertigt und alle Stellen, die ich wörtlich dem Sinne nach aus Veröffentlichungen entnommen habe, als solche kenntlich gemacht habe, mich auch keiner anderen als der angegebenen Literatur oder sonstiger Hilfsmittel bedient habe.
Ich versichere an Eides Statt, dass ich die vorgenannten Angaben nach bestem Wissen und Gewissen gemacht habe und dass die Angaben der Wahrheit entsprechen und ich nichts verschwiegen habe.
Die Strafbarkeit einer falschen eidesstattlichen Versicherung ist mir bekannt, namentlich die Strafandrohung gemäß § 156 StGB bis zu drei Jahren Freiheitsstrafe oder Geldstrafe bei vorsätzlicher Begehung der Tat bzw. gemäß § 161 Abs. 1 StGB bis zu einem Jahr Freiheitsstrafe oder Geldstrafe bei fahrlässiger Begehung.

Bremerhaven, den 20.04.2020

Jana Geuer

Acknowledgements

First, I cordially thank Prof. Dr. Boris Koch for giving me the opportunity to work on this exciting project. Thank you, Boris, for your continuous support and guidance over the last years. I am grateful to Prof. Dr. Allan Cembella for agreeing to evaluate my thesis and to Dr. Tilmann Harder and Prof. Dr. Kai-Uwe Hinrichs for being examiners for my PhD defense.

I would like to thank the members of my PhD committee Dr. Bernd Krock, Dr. Walter Geibert, Prof. Dr. Tilmann Harder, Dr. Florian Koch, Prof. Dr. Scarlett Trimborn, Dr. Tim Leefmann, and Dr. Jan Tebben for your time and the interesting and constructive discussions.

Many thanks to the angels of the lab Claudia Burau, Ruth Alheit, and Valeria Adrian, for all your practical help and support. I would furthermore like to thank the members of the EcoTrace group, Scarlett Trimborn, Florian Koch, Tina Brenneis, Christian Völkner, Marianne Camoying, Franziska Pausch, and Sebastian Böckmann, for your hospitality and help. I am very grateful to Tina Brenneis and Christian Völkner for their great support in the lab.

I thank the marine chemistry work group, namely Martin Graeve, Kai-Uwe Ludwichowski, Claudia Burau, Valeria Adrian, Erik Stein, Xianyu Kong, Sinah Müller, Matthias Woll, Kerstin Ksionzek, Tim Leefmann, Heiner Baumgarten, Dieter Janssen, Ruth Alheit, Gerhard Kattner, Lauris Boissonnot, and Doreen Kohlbach. I was happy to be a member of this group.

I want to express my gratitude towards my fellow PhD-colleagues of the AWI DokTeam 2017/2018, and all Helmholtz Juniors, particularly Daphnie Galvez. It was a pleasure to work with all of you!

Thanks to my lovely C-218 office mates and to all people who made Markus special: Heiner Baumgarten, Frederik Bussmann, Michael Rudolph, Erin Kunisch, Lauris Boissonnot, Tim Leefmann, Ruth Alheit, Valeria Adrian, Erik Stein, and Sinah Müller.

Many thanks to all my wonderful friends in and outside of AWI and last but not least my family for your encouragements, open ears, motivational words, reading parts of this thesis and for taking me out of myself. I greatly appreciate your help and unconditional support.

“I'd take the awe of understanding over the awe of ignorance any day.”

Douglas Adams (The Salmon of Doubt)

Table of contents

Preface

The manuscripts that are part of this doctoral thesis are listed below. Chapters 3 to 5 are reprints of independent research papers of one published manuscript (Manuscripts I), one submitted manuscript (Manuscript III, under review) and one manuscript in preparation (Manuscript II). Manuscript I was published in an international peer-review journal. The content is unchanged and the labeling of figures and tables is adapted to the general format of this thesis.

Chapter 3: Manuscript I

Quantification, extractability and stability of dissolved domoic acid within marine dissolved organic matter

Jana K. Geuer, Bernd Krock, Tim Leefmann, Boris P. Koch

This manuscript has been published in Marine Chemistry, Vol. 215, 103669 (doi: 10.1016/j.marchem.2019.103669)

I performed dissolved domoic acid analysis and data evaluation and wrote the manuscript with input from all co-authors.

The supplemental dataset to this manuscript was published on PANGAEA:

Geuer, Jana K; Krock, Bernd; Leefmann, Tim; Koch, Boris P (2018): Dissolved domoic acid in the East Atlantic (doi: 10.1594/PANGAEA.896584)

Chapter 4: Manuscript II

Sources and distribution of dissolved domoic acid and molecular fingerprints in Arctic fjord systems at different states of glaciation

Jana K. Geuer, Frederik Bussmann, Sylke Wohlrab, Claudia Burau, Mourad Harir, Philippe Schmitt-Kopplin, Tim Leefmann, Urban Wünsch, Bernd Krock, Uwe John, Nancy Kühne, Boris P. Koch

This manuscript is in preparation for submission to Polar Biology.

I sampled and processed most of the samples, conducted parts of dissolved domoic acid and dissolved organic matter analysis and performed data evaluation. I wrote the manuscript with input from all co-authors.

Chapter 5: Manuscript III

Does dissolved domoic acid improve growth rates and iron content in low iron *Pseudo-nitzschia subcurvata*?

Jana K. Geuer, Scarlett Trimborn, Florian Koch, Tina Brenneis, Bernd Krock, Boris P. Koch

This manuscript was submitted to Frontiers in Marine Science

I participated in experimental design, conducted most of the experiment, performed most of the data acquisition and analysis and wrote the manuscript with contribution from all co-authors.

List of Abbreviations

A:V	Surface to volume
ANOSIM	Analysis of similarities
ASP	Amnesic shellfish poisoning
ASV	Amplicon sequence variants
AW	Atlantic water
BW	Bottom water
C	Carbon number
C:N	Carbon to nitrogen ratio
CAW	Cold Atlantic water
CTD	Conductivity, temperature, depth
DA	Domoic acid
DAb	Domoic acid biosynthesis
dDA	Dissolved domoic acid
DIC	Dissolved inorganic carbon
DBE	Double bond equivalents
DBE/C	Double bond equivalents per carbon
DBE/O	Double bond equivalents per oxygen
DOC	Dissolved organic carbon
DOM	Dissolved organic matter
DON	Dissolved organic nitrogen
EDTA	Ethylenediaminetetraacetic acid
EGC	East Greenland Current
ELISA	Enzyme-linked immunosorbent assay
Fe	Iron
FT-ICR-MS	Fourier transform ion cyclotron resonance mass spectrometry
GF/F	Glass microfiber filters
GMW	Glacial meltwater
GSDW	Greenland Sea Deep water
H/C	Hydrogen to carbon ratio
HCl	Hydrochloric acid
HLB	Hydrophilic-lipophilic balance
HNLC	High-nutrient, low-chlorophyll
HPLC	High-performance liquid chromatography
ICP-MS	Inductively coupled plasma mass spectrometry
IW	Intermediate water

LOD	Limit of detection
LOQ	Limit of quantification
MANOVA	Multivariate analysis of variance
MEP	Methyl-erythritol phosphate
MPW	Modified polar water
MS/MS	Tandem mass spectrometry
MW	Molecular weight
NSW	North Sea water lab standard
O/C	Oxygen to carbon ratio
OTU	Operational taxonomic unit
PC	Polycarbonate
PCA	Principal component analysis
pCO_2	Partial pressure of carbon dioxide
PCR	Polymerase chain reaction
pDA	Particulate domoic acid
PE	Polyethylene
POC	Particulate organic carbon
PON	Particulate organic nitrogen
PPL	Priority PolLutant
PW	Polar water
RP	Reversed phase
SGW	Surface glacial water
SO	Southern Ocean
SPE	Solid-phase extraction
SW	Surface water
TA	Total alkalinity
TAW	Transformed Atlantic water
TDN	Total dissolved nitrogen
UPLC	Ultrahigh performance liquid chromatography
UPW	Ultrapure water
WSC	West Spitzbergen Current

Abstract

Domoic acid (DA) is a well-studied substance produced primarily by the ubiquitous marine diatom genus *Pseudo-nitzschia*. Toxic blooms of this genus can lead to accumulation of DA in organisms of higher trophic levels where it can act as neurotoxin. Especially particulate DA (pDA) has thus been well studied, while dissolved DA (dDA) has not been addressed as much, although it can be released in high amounts into water and can substantially contribute to the total DA of toxic blooms. So far, there are no large-scale quantifications of dDA and it is not yet known how much carbon it contributes to marine dissolved organic matter (DOM). The ecological function of DA has not yet been completely uncovered, particularly its role as a ligand for iron and copper. A recently uncovered gene cluster responsible for the biosynthesis of DA has not yet been detected in situ. The scope of this study was to (i) develop a sensitive method for the extraction of dDA from seawater and its subsequent quantification, (ii) to extend our knowledge on dDA processes by a large-scale assessment of spatial distribution and dDA carbon contribution to marine DOM, and (iii) to further investigate the influence of ecological parameters on release and distribution of dDA, to prove its active biosynthesis in situ and assess its role as an iron ligand.

The highly sensitive quantification method was used to determine dDA concentrations throughout the water column in a transect of the East Atlantic Ocean including parts of the Weddell Sea and Arctic fjord systems. DA's high recovery rate using a standard DOM solid-phase extraction method made it possible to chemically identify and quantify dDA and to calculate how much carbon it contributed to the total inventory of dissolved organic carbon (DA carbon yield). We found that dDA was ubiquitous in the temperate, tropical and polar Atlantic Ocean, occurring throughout the whole water column. Based on almost all marine samples analysed, dDA concentrations uniformly decreased with water depth and correlated with DA carbon yield. Depth gradients, dissolved organic carbon (DOC) radiocarbon dates, and ubiquitous occurrence point to a fairly high persistence of dDA in the ocean, despite the presence of a nitrogen atom, which would have suggested a fast uptake as a reduced nitrogen source.

dDA concentrations in the iron-replete regions of Arctic fjords, which we sampled in July, only weakly correlated with chlorophyll *a* but inversely correlated with phosphate and silicate concentrations, indicating a post-bloom situation. The low availability of phosphate and silicate were presumably responsible for dDA production. The number of potentially DA producing *Pseudo-nitzschia* species determined by microscopy and genomics correlated well with dDA and pDA levels, particularly at the stations with

highest dDA. For the first time, we were also able to verify the in situ presence of genes responsible for DA biosynthesis pointing to an active DA production at these stations. In regions where the water column showed distinct stratification, dDA and DOC concentrations varied significantly between water masses, particularly under strong glacial influence. This was also reflected in the possibility to at least partially chemical distinguish between DOM pools of the different water masses. Higher temperatures and an increased low-nutrient glacial meltwater discharge, which decreases salinity, could potentially increase the share of *Pseudo-nitzschia* species and their toxicity in local blooms. Quantifying dDA might help in assessing these changes in the future.

Since dDA was also found in the Southern Ocean, DA's potential increase of iron bioavailability to *Pseudo-nitzschia* was tested in an experiment. Assessing the ligand function of dDA for the Antarctic species *Pseudo-nitzschia subcurvata*, no enhanced iron or DA uptake could be observed at low iron availability. Since *P. subcurvata* does not produce DA itself, the results furthermore indicate that DA might only yield advantages in terms of iron acquisition for species capable of DA production. However, replete dDA led to higher intracellular copper levels, an observation which needs to be subject of subsequent studies.

The interactions of dDA with its environment, particularly with trace metals are quite complex. dDA, copper and iron interactions should be further investigated, comparing species capable and incapable of DA production. The ubiquitous occurrence of dDA and its persistence might make dDA a good additional parameter to trace toxic blooms even after they have ceased and help in assessing changes in rapidly changing regions such as the polar seas. In this regard, it would prove beneficial to further investigate the mechanisms and speed of its degradation within the water column.

Zusammenfassung

Domoinsäure (domoic acid, DA) ist eine gut untersuchte Substanz, die vornehmlich von der marinen Diatomeengattung *Pseudo-nitzschia* produziert wird. Giftige Algenblüten dieser Gattung können dazu führen, dass DA in Organismen höherer trophischer Ebenen akkumuliert, in denen sie das Nervensystem schädigen kann. Für partikuläre DA (pDA) ist die Studienlage daher besonders gut. Gelöste DA (dDA) hingegen wurde weniger intensiv untersucht, obwohl sie in vergleichbar hohen Mengen ausgeschieden werden kann und erheblich zur Gesamt-DA bei toxischen Blüten beitragen kann. So wurden zum Beispiel keine groß angelegten Quantifizierungen von dDA im Meer durchgeführt. Ferner ist noch unbekannt, wie hoch ihr Kohlenstoffbeitrag zu marinem gelöstem organischem Material (dissolved organic material, DOM) ist. Die genaue ökologische Funktion von DA ist ebenfalls noch nicht bekannt, besonders ihre Rolle als Ligand für Eisen und Kupfer. Ein kürzlich entdecktes Gen-Cluster, welches für die Biosynthese von DA verantwortlich ist, wurde noch nicht im Feld nachgewiesen. Ziel dieser Arbeit war (i) die Entwicklung einer sensiblen Methode zur Extraktion und Quantifizierung von dDA aus Seewasser, (ii) das Wissen über dDA und damit zusammenhängende Prozesse durch eine groß angelegte Bestimmung der räumlichen Verteilung von dDA und ihr Kohlenstoffbeitrag zu marinem DOM zu erweitern, und (iii) näher zu untersuchen, wie ökologische Parameter die Abgabe und Verteilung von dDA bestimmen, ihre aktive Biosynthese im Feld nachzuweisen und ihre Rolle als Eisenligand zu testen.

Die hochsensible Methode der Quantifizierung ermöglichte eine Bestimmung der dDA-Konzentrationen in der gesamten Wassersäule eines Transekts durch den Ostatlantik, einschließlich des antarktischen Weddellmeers und arktischen Fjorden. Die hohe Wiederfindungsrate unter Benutzung der DOM-Festphasenextraktion ermöglichte eine chemische Identifizierung und Quantifizierung von dDA und seines Kohlenstoffbeitrags zur Gesamtheit des DOM (DA-Kohlenstoffanteil). Wir konnten herausfinden, dass dDA im gemäßigten, tropischen und polaren Atlantischen Ozean allgegenwärtig war und in der gesamten Wassersäule vorkam. Nahezu aller analysierter Meeresproben zufolge nahmen dDA Konzentrationen gleichförmig mit zunehmender Tiefe ab und korrelierten mit dem DA-Kohlenstoffanteil. Tiefenprofile, das Radiokarbonalter von gelöstem organischen Kohlenstoff (DOC) und das allgegenwärtige Vorkommen deuten auf eine vergleichsweise hohe Langlebigkeit von dDA im Ozean hin, obwohl es ein Stickstoffatom enthält, welches als reduzierte Stickstoffquelle eine schnelle Aufnahme begünstigen sollte.

dDA Konzentrationen in dem eisenreichen Gebiet Arktischer Fjorde, welche im Juli beprobt wurden, korrelierten nur schwach mit Chlorophyll *a* aber invers mit Phosphat- und Silikatkonzentrationen, was auf Bedingungen hinweist, welche nach einer Algenblüte herrschen. Die geringe Verfügbarkeit von Phosphat und Silikat waren dabei vermutlich für Produktion und Abgabe von dDA verantwortlich. Die potentiell DA-produzierenden, durch Lichtmikroskopie und Genomik bestimmten *Pseudo-nitzschia* Spezies korrelierten gut mit dDA- und pDA-Werten, besonders dort, wo deren Konzentration am höchsten war. Dort konnten wir außerdem zum ersten Mal Gene der DA-Biosynthese vor Ort nachweisen, welche auf eine aktive DA-Produktion hindeuten. In Regionen mit deutlicher Stratifizierung unterschieden sich dDA- und DOC-Konzentrationen signifikant zwischen den Wassermassen, besonders unter Einfluss von Gletscherschmelzwasser. Dies zeigte sich auch in der Möglichkeit, zumindest teilweise den DOM-Pool der einzelnen Wassermassen zu unterscheiden. Höhere Temperaturen und ein erhöhter, nährstoffarmer Schmelzwassereinfluss des Gletschers, könnten durch Verringerung der Salinität zu einer Zunahme an *Pseudo-nitzschia* Spezies und deren Toxizität während Algenblüten führen. Die Quantifizierung von dDA könnte helfen, diese Veränderungen in Zukunft besser zu verfolgen.

Dadurch, dass dDA auch im Südpolarmeer vorkam, wurde ihre potentielle Fähigkeit zur Erhöhung von Eisenbioverfügbarkeit experimentell getestet. Bei näherer Betrachtung der Ligandenfunktion von dDA für die antarktische Spezies *Pseudo-nitzschia subcurvata* konnte keine erhöhte Eisenaufnahme bei geringer Eisenkonzentration festgestellt werden. Da *P. subcurvata* selbst nicht in der Lage ist DA zu produzieren, deuten die Resultate ferner darauf hin, dass DA lediglich für die Spezies vorteilhaft ist, welche auch in der Lage sind, die Substanz eigens herzustellen. Allerdings führte das Vorhandensein von dDA zu höheren intrazellularen Kupfer-Werten; eine Beobachtung, die Gegenstand weiterer Studien sein sollte.

Die Interaktion zwischen dDA und ihrer Umwelt, insbesondere mit Spurenmetallen, ist sehr komplex. Das Zusammenspiel zwischen dDA, Eisen und Kupfer sollte näher untersucht werden. Dabei wäre ein Vergleich von Produzenten und Spezies, die DA nicht synthetisieren können, sinnvoll. Das allgegenwärtige Vorkommen und die Langlebigkeit von dDA könnten es zu einem wertvollen, zusätzlichen Parameter zur Nachverfolgung toxischer Blüten machen, auch wenn diese bereits vorbei sind. Dies wiederum könnte hilfreich bei der Betrachtung sich schnell verändernder Regionen sein, wie der polaren Meere. Diesbezüglich wäre es ferner nützlich, die Mechanismen und Geschwindigkeit des Abbaus von dDA in der Wassersäule näher zu untersuchen.

1 Introduction

Domoic acid (DA), a polar tricarboxylate amino acid, is a well-studied substance produced by marine organisms. Particularly the toxicity of DA has been of interest in the years after the discovery of DA as cause for amnesic shellfish poisoning (ASP) in 1987 (Bates et al., 1989). Many studies of blooms of *Pseudo-nitzschia*, a ubiquitous diatom of which several species produce DA, have been performed (e.g. Kudela et al., 2015; Subba Rao et al., 1988; Trainer et al., 2009b). Furthermore, the production and levels of DA have been studied extensively. Often, DA levels are reported as particulate DA (pDA), which is the amount of DA quantified in the filter cake of filtered seawater or culture, while dissolved DA (dDA) is the DA quantified in the filtrate. The focus of many studies was, however, on pDA since it reaches higher trophic levels and is thus relevant in terms of DA's toxicity (e.g. Bates et al., 1989; McCabe et al., 2016; Work et al., 1993). Only few studies have focused on dDA so far even though it can be released in relatively high amounts and is comparatively persistent in the water column (Umhau et al., 2018). Moreover, DA in its dissolved form has the potential to act as ligand for iron and copper (Rue and Bruland, 2001), but there are still major knowledge gaps concerning this potential function.

1.1 A brief history of domoic acid

DA was first detected in the seaweed *Chondria armata.* The name "domoic" is derived from the Japanese name "Domoi" for this red algae (Takemoto and Daigo, 1958). The molecular formula of DA is $C_{15}H_{21}NO_6$ and its actual structure ({2S-[2a,3b,4b (1Z,3E,5R)]}-2-Carboxy-4-(5-carboxy-1-methyl-1,3-hexadienyl)-3-pyrrolidineacetic acid (IUPAC), Fig.1) was determined after synthesis (Ohfune and Tomita, 1982). DA as a zwitterion is water-soluble, particularly in its anionic and cationic forms and least at its isoelectric point (Falk et al., 1991).

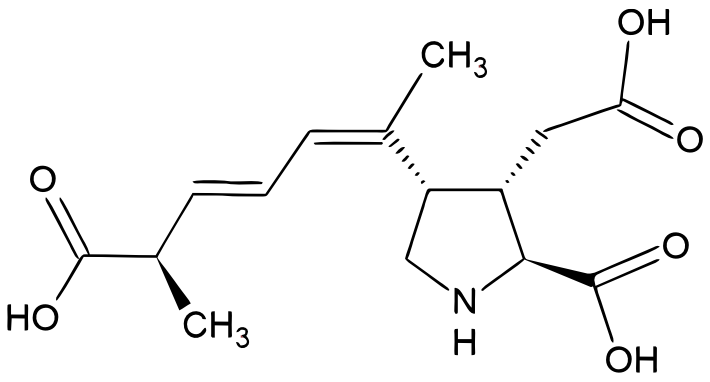

Figure 1: structural formula of domoic acid

DA is moderately thermostable and is photodegraded when exposed to UV light (Bouillon et al., 2006, 2008). Three structural closely related amino acids, isodomoic acid A-C, were later discovered in the same red algae (Maeda et al., 1986). Later on, isodomoic acid D-F were isolated in the same species (Wright et al., 1990), followed by the discovery of isodomoic acid G-H (Zaman et al., 1997). Diene geometrical and regioisomers make up the isodomoic acid family (Clayden et al., 2005). When DA is photodegraded, it is decomposed to some of these isomers (Bouillon et al., 2008).

After its discovery, DA was found to have anthelmintic effects as it can effectively expel parasitic worms (Daigo, 1959). Subsequently, it was also used as an insecticide (Maeda et al., 1984, 1986). In 1987, during an outbreak of shellfish poisoning, DA was found responsible for the contamination of blue mussels and could be traced back to the DA producing diatom species *Pseudo-nitzschia multiseries* (Bates et al., 1989). Symptoms of this poisoning event included vomiting and diarrhoea but primarily neurological symptoms such as disorientation, confusion and memory loss, which led to the name ASP events (Quilliam and Wright, 1989; Wright et al., 1989). DA is structurally similar to the excitatory neurotransmitter glutamate and binds to its receptors, thereby inducing excessive stimulation of nerve cells and thus neuronal damage in the hippocampus (Cendes et al., 1995). Apart from mussels, DA was later also found in razor clams (Wekell et al., 1994). For this reason, safety measures such as sampling plans and state regulatory levels were implemented to counteract such ASP events (Wekell et al., 2002). Toxic *Pseudo-nitzschia* blooms and the resulting transport of DA to higher trophic levels such as fish (Busse et al., 2006) can also poison marine mammals e.g. seals and whales, leading to disorientation and stranding (Scholin et al., 2000; McCabe et al., 2016; Nash et al., 2017). Birds can also be affected by DA poisoning with the same neurological symptoms (Work et al., 1993).

1.2 Domoic acid production: amount, mechanism and influential factors

Apart from red algae, the diatom genera *Pseudo-nitzschia* and *Nitzschia* are mostly known for DA production. These diatoms are of particular interest as they belong to the basis of the food web and the toxin accumulates in organisms of higher trophic levels after consumption of DA producing diatoms (Bates et al., 1989; Work et al., 1993; McCabe et al., 2016).

1.2.1 *Pseudo-nitzschia* species and domoic acid production around the globe

The genus *Pseudo-nitzschia* has a cosmopolitan distribution (Bates et al., 2018; Hasle, 2002; Trainer et al., 2012, Fig. 2). Of a total of 54 known species, 26 are known to express DA at least in some strains and five species have not been tested for DA production yet (reviewed in Bates et al., 2019, 2018; Lelong et al., 2012). For many species, the production of DA and its isomers was only tested on a limited number of strains, thus using matching conditions and genomic tools might unravel production in species previously not known to produce DA (Bates et al., 2018).

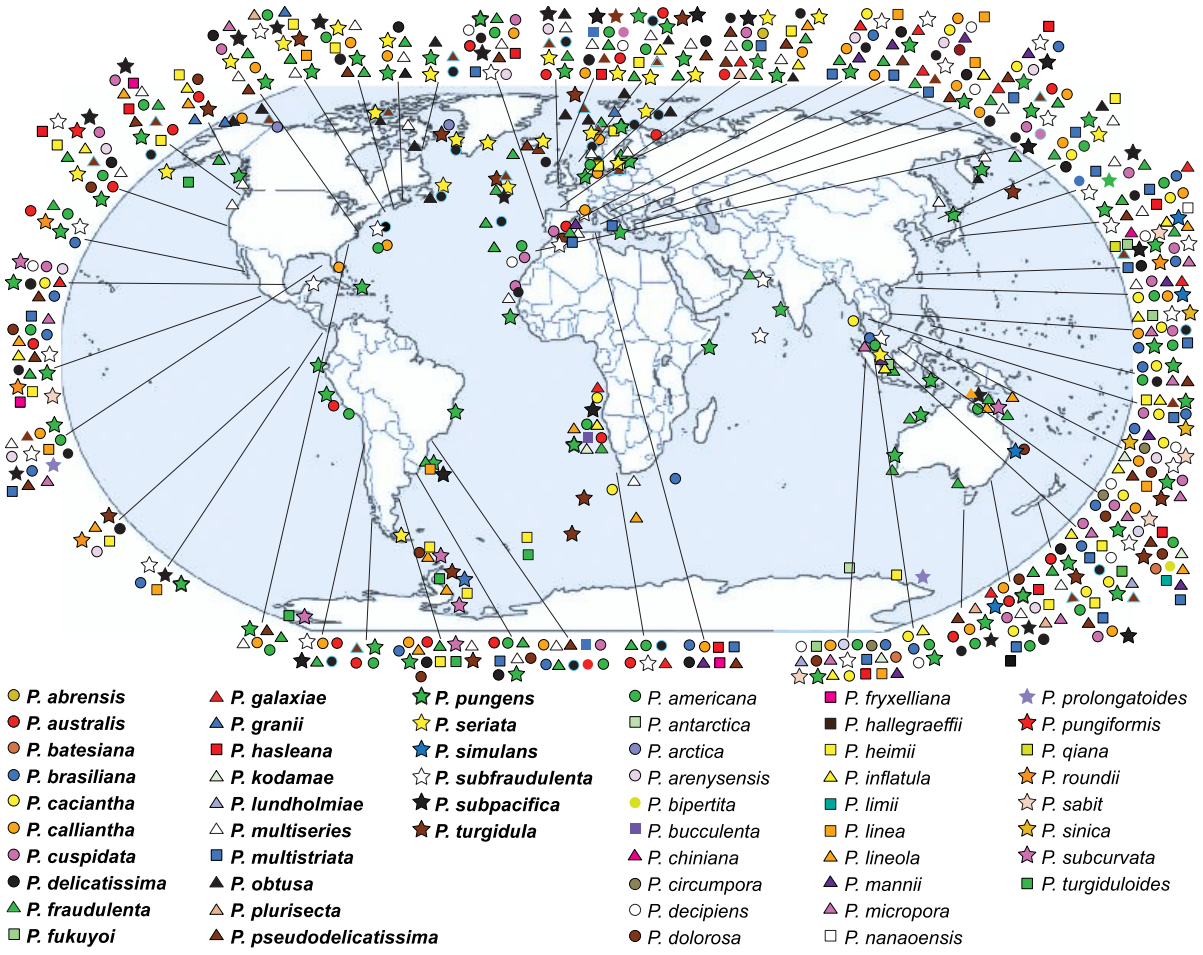

Figure 2: World distribution of the known *Pseudo-nitzschia* species. For the species in bold, some strains were tested positive for domoic acid production, while there are no records of domoic acid production for the other species so far (modified from Bates et al., 2019 complemented with information from Bates et al., 2018; Huang et al., 2019).

Up to today, new *Pseudo-nitzschia* species are still discovered and combining morphological and molecular data has greatly facilitated species distinction (Huang et al., 2019). Only two *Nitzschia* species are so far known to produce DA. Isomers of DA were detected within these two DA producing *Nitzschia* species *N. navis-varingica* and *N. bizertensis* (Romero et al., 2012; Smida et al., 2014; Bates et al., 2018). DA isomers

also occur in few species of *Pseudo-nitzschia*, such as *P. australis* (Rhodes et al., 2004), *P. seriata*, *P. multiseries* (Hansen et al., 2011) and *P.* cf. *delicatissima* (Kotaki, 2008).

Additionally, it might turn out that some of the species not known for DA production so far could still produce the substance and its isomers under the right toxin-inducing conditions or that the amounts produced were below limit of detection (LOD) in the respective studies (Bates et al., 2019).

1.2.2 Differences in the amount of domoic acid production

The amount of DA produced can differ greatly between different *Pseudo-nitzschia* species and even between strains. One of the lowest pDA values ($1.12\ 10^{-7}$ pmol cell^{-1}) was reported for the species *P. galaxiae* (Cerino et al., 2005). *P. australis* can produce more pDA (0.014 to 0.25 pmol cell^{-1}) (Walz et al., 1994; Trainer et al., 2000; Cusack et al., 2002) and is described as a relatively toxic species, e.g. compared to *P. delicatissima*, which only shows 1% of *P. australis'* toxicity (Baugh et al., 2006). *P. multiseries* also often produces comparatively much pDA (e.g. 0.21 pmol cell^{-1}) (Bates et al., 1999). Other species like *P. brasiliana* (0.0014 – 0.0018 pmol cell^{-1}) or *P. fraudulenta* ($6.4\ 10^{-6}$ – $3.8\ 10^{-4}$ pmol cell^{-1}) show a much lower concentration. After sexual reproduction, parent *P. multiseries* have a decreased ability to produce DA and the variability of DA production in sibling offspring clones is high (Bates et al., 1999). Apart from that, DA production can vary in different growth phases of its producers. Many of the DA producing species show a rapid production in their stationary growth phase (Lelong et al., 2012). DA production in the exponential growth phase has also been proven for e.g. *P. australis*, *P. seriata* and *P. cuspidata* (Auro and Cochlan, 2013; Thorel et al., 2014; Harðardottir et al., 2015).

1.2.3 Metabolic pathway of domoic acid production

Recently, N-geranyl-l-glutamic acid was suggested to be a precursor of DA and six compounds potentially participating in the condensation of geranyl pyrophosphate and L-glutamate were identified (Maeno et al., 2018).

Consequently, a model for DA biosynthesis was constructed (Fig. 3). Four genes that encode DA-biosynthesis enzymes (DAb) in *P. multiseries* were unravelled (Brunson et al., 2018). The suggested DA-biosynthetic pathway starts with a geranylation of L-glutamate to N-geranyl-l-glutamic acid using geranyl pyrophosphate, catalysed by DAbA. Next, DAbD performs three successive oxidations leading to 7'-carboxy-N-gernaly-l-glutamic acid.

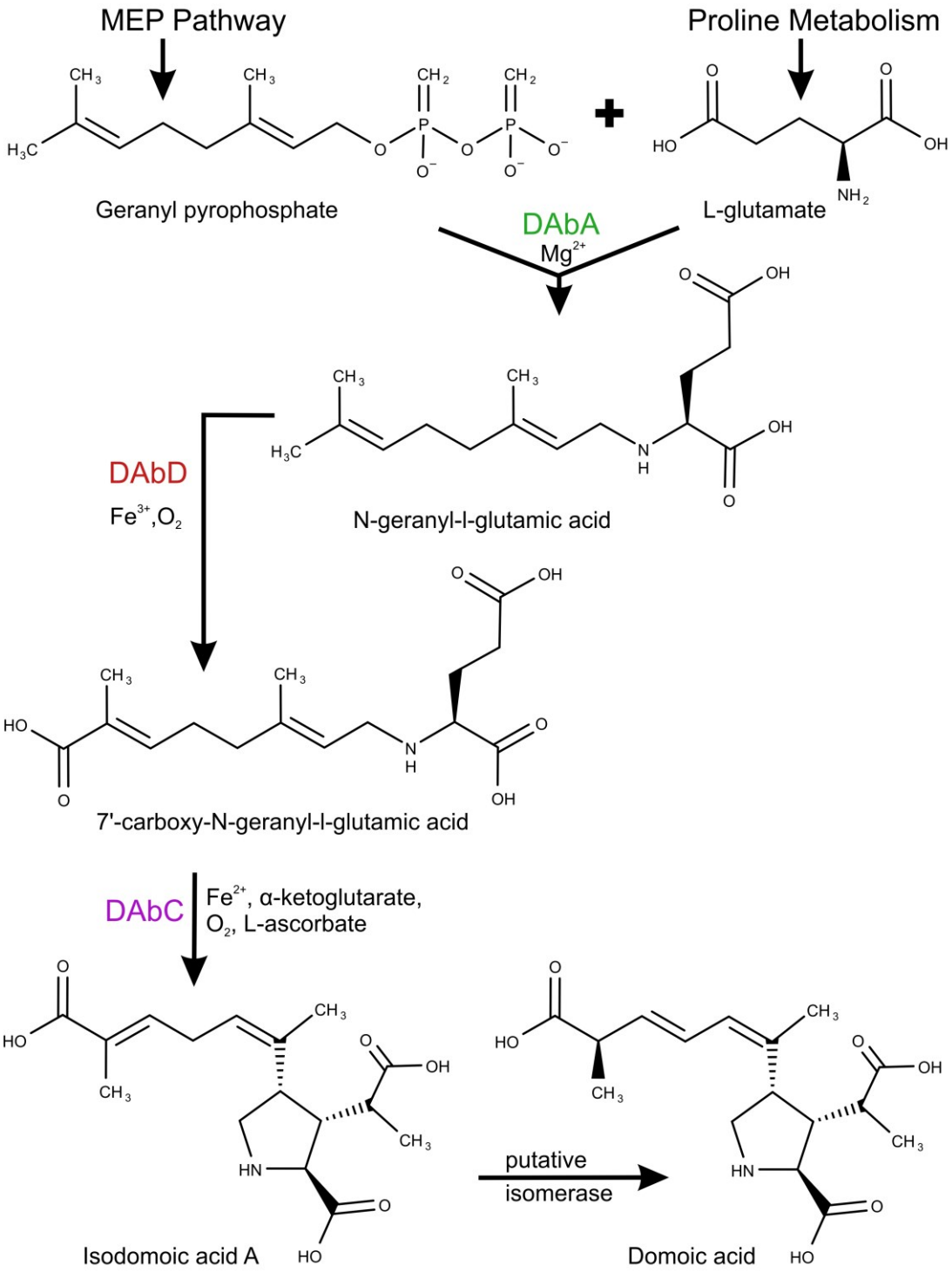

Figure 3: Proposed metabolic pathway of domoic acid biosynthesis. The two precursor molecules are produced in the proline and methylerythritol phosphate metabolic (MEP) pathway. Three domoic acid biosynthetic (DAb) enzyme genes are involved in the biosynthetic pathway, with DAbA catalysing the N-geranylation of L-glutamate, and DAbD and DAbC performing subsequent oxidative reactions and cyclisation of the molecule. (after Brunson et al., 2018 and Harðardóttir et al., 2019)

Subsequently, DAbC catalyses the cyclisation to form isodomoic acid A. As a last step, a putative isomerase likely transforms isodomoic acid A to domoic acid. The DAbB gene encodes a hypothetical protein and could not be linked to isomerase activity (Brunson et al., 2018). Subsequently, the regulating genes with the matching metabolic pathway for the production of the DA precursor geranyl pyrophosphate were also recently unravelled in the toxigenic species *P. seriata*, which is produced in the cells' plastid in the methylerythritol phosphate metabolic (MEP) pathway (Harðardóttir et al., 2019). The authors also suggested that the precursor for L-glutamate was proline.

These genes only have been uncovered recently and have, until now, not been detected in field samples where toxic *Pseudo-nitzschia* occurred.

1.2.4 Environmental conditions influencing domoic acid production

Whether and to which extent *Pseudo-nitzschia* species produce domoic acid also depends on their environment. Various external causes have been described to trigger or enhance the DA production.

1.2.4.1 Presence of predatory organisms

Among others, DA has been suggested to be produced as part of a grazing defence mechanism. In the presence of predatory copepods, DA production is distinctively increased in *P. seriata* (Harðardottir et al., 2015; Tammilehto et al., 2015; Lundholm et al., 2018). Furthermore, reduced escape response rates have been observed in planktonic copepods upon feeding on DA producing *Pseudo-nitzschia* species (Harðardóttir et al., 2018). The presence of grazers can, however, also induce DA production in *P. obtusa*, which were previously not known to produce DA (Harðardottir et al., 2015). The increase of DA production is chemically mediated and happens also without physical contact between *Pseudo-nitzschia* cells and their grazers (Tammilehto et al., 2015). Different herbivorous copepods and some of their exudates can increase DA production levels, while carnivorous grazers cannot (Lundholm et al., 2018). In addition to copepods, brine shrimps increase DA production in several *Pseudo-nitzschia* species (Huang et al., 2019).

1.2.4.2 Bacteria

Bacteria have been shown to influence DA production, mostly by increasing its production (Douglas et al., 1993; Lelong et al., 2012; Bates et al., 2018). Increased DA levels in non-axenic cultures stem from the diatoms, since bacteria associated with *Pseudo-nitzschia* are incapable of producing DA independently (Bates et al., 2004).

The presence of bacteria is furthermore not required for *Pseudo-nitzschia* to produce DA as the latter also produce it in axenic cultures (Douglas and Bates, 1992). However, DA production is distinctively higher in non-axenic cultures than in axenic ones (Douglas et al., 1993). Upon reintroduction of different *Pseudo-nitzschia* associated bacterial species to axenic *P. multiseries* cultures, they increase DA production up to 95-fold compared to axenic cultures. Even bacteria associated with other diatom genera increase DA production (Bates et al., 1995). In addition, *Nitzschia navis-varingica* also produces more DA in non-axenic compared to axenic cultures (Kotaki, 2008). The diversity and abundance of bacterial genera associated with *Pseudo-nitzschia* might furthermore be responsible for the variability in the DA production of different clones of the same strain (Kaczmarska et al., 2005). Apart from DA production being enhanced by bacterial presence, DA presence in turn is suggested to structure the bacterial community and might limit bacterial diversity (Sison-Mangus et al., 2016).

1.2.4.3 Ecological parameters

A variety of ecological parameters can influence DA production. Temperature has an effect on the production of DA, which, however, depends on the respective species tolerance and thus differs between different species and sites. *P. seriata* shows an enhanced production of DA with decreasing temperatures (Lundholm et al., 1994), while DA production in *P. australis* increases with temperature and also irradiance (Thorel et al., 2014). Excessively high temperatures may even inhibit DA production as shown for different *P. multiseries* strains (Amato et al., 2010).

The surrounding pH range can also influence DA production. The species *P. multiseries* has been shown to produce DA when pH is elevated (Lundholm et al., 2004). DA content usually increases with increasing salinity (Doucette et al., 2008). Osmotic stress at low salinities can cause a sudden release of DA into the medium due to cell lysis. Cellular DA contents are highest at a salinity of 30 – 35, with one strain showing enhanced production at high salinities of 40 (Ayache et al., 2019).

1.2.4.4 Domoic acid production as a response to macronutrient limitation

Phosphate limitation can trigger DA production (Pan et al., 1996a; Lema et al., 2017) and increases DA levels in both medium and *Pseudo-nitzschia* cells (Pan et al., 1996a). Furthermore, silicate limitation also increases DA production in *Pseudo-nitzschia* (Pan et al., 1996b; Fehling et al., 2004). *P. seriata* produces DA under both phosphate and silicate limitation. Under phosphate limitation, a higher

amount of DA is released to the medium compared to non-limiting conditions, presumably because of an improper formation of the cell wall due to the phosphate limitation (Pan et al., 1996a). More DA is produced under silicate limitation than phosphate limitation and the amount of DA released from the cells is higher under silicate limitation compared to phosphate limitation (Fehling et al., 2004).

DA synthesis requires nitrogen and the source of nitrogen influences DA production (Bates et al., 1991, 1993; Ryan et al., 2017). High ammonium concentrations, which are toxic to the cell, promote DA production (Bates et al., 1993). Additionally, nitrogen from ammonium is energetically cheaper than nitrate for the DA producing cells (Pan et al., 1998). DA production as a consequence of phosphate or silicate limitation is thus only possible if nitrogen is sufficiently available (Bates et al., 1991). This was also observed in field studies, where DA correlated inversely with silicate, phosphate and nitrogen concentrations (Schnetzer et al., 2007). Particularly high cellular DA was observed under low silicate to nitrogen ratios (Ryan et al., 2017). Furthermore, silicate to nitrogen ratios have an influence on the species composition of *Pseudo-nitzschia* in the field (Thorel et al., 2017).

1.2.4.5 Trace metal availability: domoic acid production and its potential chelating ability for iron and copper

DA has the capability to chelate both iron and copper (Rue and Bruland, 2001). Using the low energy minimum, iron is likely bound to the three carboxyl groups of DA when complexed (Bates et al., 2001). Given adequately high concentrations of dDA, the stability constants of the molecule with iron ($K^{cond}_{FeDA,Fe(III)'} = 10^{8.7 \pm 0.5}\ M^{-1}$) and copper ($K^{cond}_{CuDA,Cu(II)'} = 10^{9.0 \pm 0.2}\ M^{-1}$) are high enough to compete with natural ligands in seawater (Rue and Bruland, 2001) and the ability of DA to complex copper is higher than of all other naturally occurring amino acids (Ladizinsky, 2003).

1.2.4.5.1 Iron

Iron has been connected to DA production both in laboratory and field studies (e.g. Maldonado et al., 2002; Silver et al., 2010; Trick et al., 2010; Wells et al., 2005). An increase in iron can lead to enhanced DA production as shown in laboratory studies (Sobrinho et al., 2017) and in the field (Silver et al., 2010). In iron fertilisation experiments, elevated DA concentrations were observed in the induced phytoplankton blooms (Silver et al., 2010; Trick et al., 2010). However, also iron depletion can enhance DA production, supporting the hypothesis that DA might act as a chelator for iron. In other field studies, an increasing DA production was shown to correlate with low

iron concentrations during *Pseudo-nitzschia* blooms (Trainer et al., 2009b, 2009a). In a laboratory experiment, it could be shown that apart from the production of DA its release is enhanced under iron deficiency. Subsequently, DA producing cells could increase their growth rates (Wells et al., 2005). During another study with iron deficient *P. multiseries*, the cells released DA more rapidly into the medium than their non-limited counterparts. Both the intra- and extracellular DA contents are higher when iron is limited (Maldonado et al., 2002). In a co-incubation experiment, DA producing *Pseudo-nitzschia* were shown to have an advantage over other diatoms if iron limited (Prince et al., 2013). Generally, many *Pseudo-nitzschia* species adapt well to low iron concentrations and some species from iron depleted open ocean regions possess iron storage mechanisms and low iron requiring alternative pathways for energy uptake (Marchetti et al., 2006, 2012, 2015).

1.2.4.5.2 Copper

DA might play a role in both copper acquisition and detoxification (Rue and Bruland, 2001; Wells et al., 2005). High DA productions under copper stress have been observed in different laboratory experiments (Maldonado et al., 2002; Ladizinsky, 2003). The suggested defence mechanism against high copper concentrations was also observed in the field, where *P. australis* accumulated DA under toxic copper levels (Ladizinsky, 2003; Rhodes et al., 2004). Apart from the increase in DA under high copper levels, cellular DA levels also increase when copper is limiting (Ladizinsky, 2003; Wells et al., 2005).

Another mechanism was suggested in which DA was supposed to be released as a ligand competing for copper under iron limitation. In this scenario, copper would be necessary for the cells to function as part of a high-affinity iron uptake system, which *Pseudo-nitzschia* might possess to be able to compete for iron against stronger bacterial chelators (Wells et al., 2005). A co-limitation of iron and copper did, however, not induce DA production in a previously non-toxic *P. delicatissima* strain (Lelong et al., 2013).

Up to now, the biological function of DA as ligand for *Pseudo-nitzschia* is still not fully understood and the role of DA production in terms of iron limitation needs further assessment with different species (Sobrinho et al., 2017; Bates et al., 2018). Furthermore, DA needs to be dissolved in the surrounding medium to be able to act as a ligand and thus the interaction between dDA and low iron levels requires further investigation.

1.3 Release of dissolved domoic acid into the ocean

During DA production, DA levels might still remain constant in the cells since DA is also released into its surrounding medium (Bates et al., 1991). The release is facilitated by the high water solubility of DA (Falk et al., 1991). Furthermore, DA is released from decaying cells (Hagström et al., 2007) and from faeces of organisms of higher trophic levels, such as copepods (Tammilehto et al., 2012) or mussels (Hagström et al., 2007).

1.3.1 Triggers and efficacy of domoic acid release from cells

Different *Pseudo-nitzschia* species release different amounts of DA and more toxic *Pseudo-nitzschia* species produce significantly more pDA than dDA (Baugh et al., 2006). The extent of DA released from live cells depends not only on the species but also on the strain of *Pseudo-nitzschia* (Hagström et al., 2007).

Apart from that, a variety of environmental factors influence the release of DA from the cells. As described above, the release of DA depends for example on the surrounding nutrient regime of the cells (Hagström et al., 2007). The release of DA is particularly high under silicate limitation, where up to 67% of total DA is released into the medium, while under phosphate limitation only 23% is released (Fehling et al., 2004). Experiments also showed that iron deficiency can be responsible for an increased release of dDA (Maldonado et al., 2002; Wells et al., 2005). The release of dDA is also connected to surrounding copper concentrations. Higher DA amounts are released, if copper concentrations are both high (Maldonado et al., 2002) or low (Wells et al., 2005), presumably as a reaction to high, toxic copper amounts or deprivation of copper (Ladizinsky, 2003; Wells et al., 2005). Although DA content in the cell usually is higher at high salinities (Doucette et al., 2008; Macintyre et al., 2011), the release of dDA decreases at high salinities and DA is preferably stored intracellularly by the organisms (Van Meerssche and Pinckney, 2017). Subsequently, more dDA can be released due to osmotic stress that the cells experience at low salinities (Ayache et al., 2019).

In the field, pDA/dDA ratios can be quite complex, as they change with species composition. It was shown that in field samples with more *P. delicatissima* than *P. australis*, pDA values are lower than dDA concentrations. If the species are present in equal densities, however, pDA and dDA are also similar (Baugh et al., 2006). In another field study during a *Pseudo-nitzschia* bloom, pDA and dDA concentrations differed greatly between sampling sites, as did pDA/dDA ratios, which can range from 0 to 20 (Trainer et al., 2009b). In contrast, another study showed a strong linear regression of pDA and dDA throughout the water column. The almost equal

pDA/dDA ratios suggest a mixture of toxic and less toxic *Pseudo-nitzschia* species present (Umhau et al., 2018).

1.3.2 Dissolved domoic acid concentrations in the Ocean

The amounts of dDA in the environment can differ greatly. Usually, high concentrations of dDA are connected to very toxic *Pseudo-nitzschia* blooms (Trainer et al., 2009b; Macintyre et al., 2011; Bates et al., 2018). dDA records from different regions reported concentrations of as low as 0.00064 pmol L^{-1} (Gulf of Alaska) up to 707 pmol L^{-1} during iron enrichment experiments in the Southern Ocean (Silver et al., 2010). During a bloom in the North Sea, highest concentrations in the same range (835 pmol L^{-1}) were reported (Delegrange et al., 2018). During a massive bloom off the Washington State coast, concentrations reached up to 4.0 nmol L^{-1} (Trainer et al., 2009b). Even higher concentrations were measured during *Pseudo-nitzschia* blooms in the Gulf of Mexico (10.7 and 25.7 nmol L^{-1}, respectively) (Macintyre et al., 2011; Liefer et al., 2013). Highest dDA values (> 320 nmol L^{-1}) were reported from Monterey Bay (Kudela et al., 2015; Bates et al., 2018).

Until now, dDA has mainly been quantified in laboratory studies and in areas in which *Pseudo-nitzschia* blooms occurred at the same time. There are, however, no large-scale quantifications of DA in the open ocean.

1.3.3 The fate of dissolved domoic acid in the ocean

1.3.3.1 Photodegradation

When radiated in natural seawater one of the sinks for dDA is photochemical degradation, albeit the removal rate depends on irradiance and only takes place in the upper meters of the water column (Bouillon et al., 2006; Fisher et al., 2006). In the UV range (280 – 400 nm) photodegradation is particularly high, with its maximum at 330 nm. Increasing temperature also increases photodegradation (Bouillon et., 2006). Photooxidation of DA is promoted under the presence of Fe(III) ions by forming a complex, which is more likely to undergo photodegradation than DA alone, while phosphate interacts with Fe(III) to an iron phosphate complex that inhibits photooxidation of DA. Dissolved organic matter (DOM) also increases photodegradation of DA, although its role in this mechanism is unknown (Fisher et al., 2006). When DA is broken down by photodegradation, intermediate products are the three geometric isomers isodomoic acid D, E and F (Bouillon et al., 2008).

1.3.3.2 Bacterial degradation

DA can be removed from the water column by bacterial degradation. It was shown that bacteria from a toxic *Pseudo-nitzschia* bloom site degrade DA more rapidly than from other areas (Hagström et al., 2007). The presence of DA furthermore influences the bacterial community compositions (Sison-Mangus et al., 2016). Bacteria capable of degrading DA associated with blue mussels and soft-shell clams have been found (Stewart et al., 1998). While mussels only take up pDA (Silvert and Subba Rao, 1992) they may excrete DA in their pseudofaeces (Hagström et al., 2007). In the same study, a rapid degradation of dDA in the presence of mussel pseudofaeces and bottom sediment, potentially due to associated bacteria or enzymes, was measured. The degradation of dDA decreases at high salinities, potentially leading to higher residence times in the water column (Van Meerssche and Pinckney, 2017).

1.3.3.3 Downward transport of domoic acid

Although some of dDA is degraded at the surface via photodegradation and below via bacterial degradation, significant amounts of dDA remain in the upper water column and have residence times comparable to pDA. This implies that the loss of dDA by degradation and of pDA by sinking are approximately equal (Umhau et al., 2018). dDA contributing to a large range of the water column is plausible, since dDA is relatively hydrophilic and not very particle reactive (Lail et al., 2007).

DA can be transported to significant depths below the euphotic zone by rapid vertical transport of DA containing cells. Its vertical flux can contribute substantially to deep-ocean and benthic food webs (Sekula-Wood et al., 2009). The dominant vector of DA transport to benthic food webs is biological. Once dissolved, DA is more likely to remain dissolved in the water column than to accumulate at particles due to its highly hydrophilic nature. Only some of the dDA might interact with siliceous debris and colloidal organic matter and contribute to particle sinking (Lail et al., 2007).

Still, there are several other processes involved in downward transport of DA. From DA containing faecal pellets dDA can leach as they are transported downwards (Tammilehto et al., 2012). In addition, *Pseudo-nitzschia* derived marine snow contributes to DA flux to depth, as dDA accumulates in these particles (Schnetzer et al., 2017). In the presence of Fe(III), Cu(II) and Al(III), the adsorption of DA to clays and sediments increases, presumably due to the formation of DA-metal complexes, which enable adsorption (Burns and Ferry, 2007). In the same study, it was shown that DA effectively adsorbs to natural sediment, which might in turn serve as reservoir for DA after blooms.

Since dDA can occur throughout the whole water column (Umhau et al., 2018), it is part of DOM. Marine DOM represents one of the largest organic carbon reservoir on earth (Hansell et al., 2009). DOM is a complex mixture of organic compounds and consists of molecules of different sizes and lability (Kirchman et al., 1991; Carlson and Ducklow, 1995). Labile compounds are primarily produced by algae in the ocean's surface (Hopkinson et al., 2002), while in deeper regions refractory DOM is predominant (Carlson et al., 1994). The vertical distribution of DOM depends on physical properties, but generally DOM concentrations are high at the surface of the water column and decrease with depth (Carlson and Ducklow, 1995). Usually the surface contains highest DOM concentrations due to primary production. DOM can e.g. be released during growth of phytoplankton, grazing, viral lysis and the transformation of particulate matter by degradation (Azam et al., 2011).

However, there are no large-scale quantifications of DA covering the whole water column. Furthermore, it has not yet been examined, how much dDA contributes to DOM in the ocean at different depths of the water column.

1.3.4 Environmental effects of dissolved domoic acid

Although DA is mainly known for its toxicity that occurs via trophic transfer, dDA can also have influences on its environment. dDA was proven to be toxic to small marine copepods (*Tigriopus californicus*) at comparatively very high concentrations of 8.62 µmol L^{-1} (Shaw et al., 1997). Moderate toxicity to other copepods at even higher concentrations of 120.45 and 434.59 µmol L^{-1} (*Pseudocalanus acuspes* and *Temora longicornis*, respectively) was shown as well, while in the same study no lethal effect on *Calanus glacialis* (Windust, 1992), which are known grazers for *Pseudo-nitzschia* species (Tammilehto et al., 2012), was observed. Dissolved DA furthermore was found to decrease grazing rates of krill starting from concentrations of 1.28 µmol L^{-1} (Bargu et al., 2006). dDA may also affect the surrounding phytoplankton community. In co-cultures with *Pseudo-nitzschia* under low iron conditions and dDA addition, the growth of another diatom (*Skeletonema marinoi*) was negatively affected (Prince et al., 2013). At extreme salinities, phytoplankton, particularly cryptophytes and diatoms, become more sensitive to dDA, which can inhibit their growth (Van Meerssche and Pinckney, 2017). Moreover, if continuously subjected to 160 nmol L^{-1} dDA, king scallop larvae (*P. maximus*) show compromised growth, development and survival (Liu et al., 2007). If exposed to dDA for 72 h, the cardiovascular development of zebrafish embryos is disrupted. Cardiac malformation started at low dDA concentrations of 3.21 nmol L^{-1}, mortality increased at 32.12 nmol L^{-1} (Hong et al., 2015). During toxic blooms, dDA

concentrations in that range can occur (3.9 – 321.2 nmol L^{-1}) (Trainer et al., 2009b; Bates et al., 2018), while the lethal doses of dDA found for copepods are likely higher than the concentrations occurring even at toxic blooms.

1.4 Quantification of domoic acid

The majority of quantification methods for DA are based on chromatographic approaches or receptor binding assays. After the first approaches were based on chromatography, enzymatic approaches became also popular for the quantification of DA (Van Dolah et al., 1997; Garthwaite et al., 1998).

1.4.1 Liquid chromatography, mass spectrometry and other separation methods

Traditionally, DA was analysed via reversed-phase high-performance liquid chromatography (RP-HPLC) using a diode array detector and detection at 242 nm. Using fast atom bombardment mass spectrometry, the parent ion signal of 312 *m/z* in positive mode and 310 *m/z* in negative mode shows an increase in peak intensity upon purification of DA (Quilliam and Wright, 1989). RP-HPLC was later used as one of the standard methods to quantify DA with a LOD of 50 pmol L^{-1}. In this method, a derivatisation of DA with 9-fluorenylemthylchloroformate was performed, followed by fluorescence detection (Pocklington et al., 1989). Later, HPLC tandem mass spectrometry (MS/MS) was implemented to quantify DA using electrospray with positive ionisation and 312 *m/z* as parent ion and fragments 266 *m/z* and 161 *m/z* for detection (Scholin et al., 2000). Within this method, the fragmentation pathway for DA in positive mode (Fig. 4) was also determined (Furey et al., 2001).

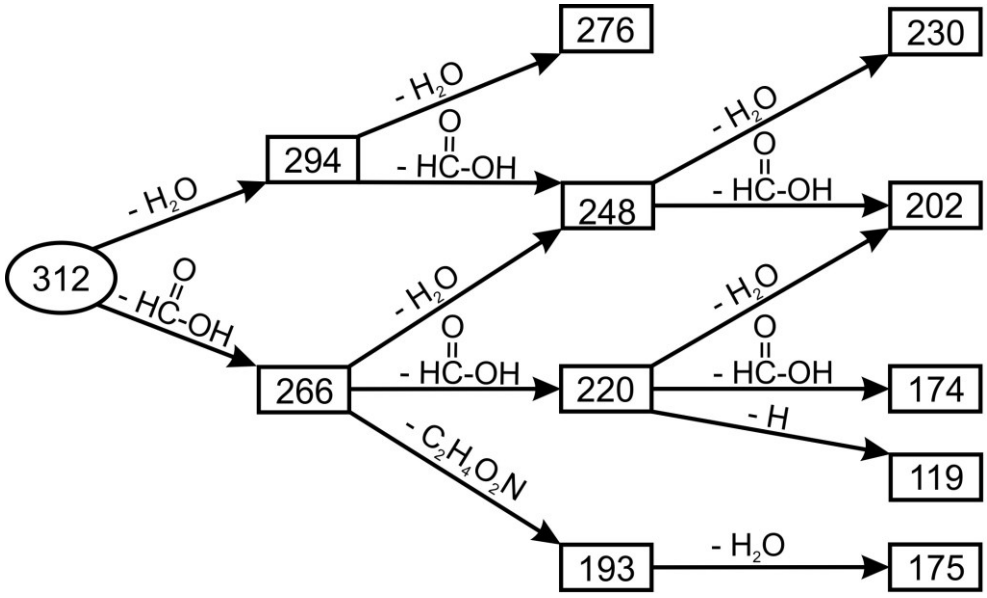

Figure 4: Mass spectrometric fragmentation pattern for domoic acid after positive ionisation. The initial *m/z* ratio of DA after positive ionisation is 312. Values in boxes represent *m/z* ratios after dissociation of functional residues shown on the arrows. (modified from Furey et al., 2001).

Usually, the fragment used for quantification of DA is 266 *m/z*, since it usually yields the largest peaks and highest sensitivity (Scholin et al., 2000; Wang et al., 2007). HPLC-MS/MS has remained a popular method to quantify DA both from particles and seawater up to date (Trainer et al., 2000; Sekula-Wood et al., 2009; Zhang et al., 2016; Umhau et al., 2018). The limit of quantification (LOQ) for this method is usually quite low (e.g. 96 and 16 pmol L^{-1}, respectively) (Barbaro et al., 2013; Zhang et al., 2016). Other methods for the quantification of DA include capillary electrophoresis (Nguyen et al., 1990) and methods that were based on this technique. Being advantageous due to low required sample volumes an advanced quantification method using capillary electrochromatography was developed (Wu et al., 2009). Furthermore, a capillary electrophoresis-based enzyme immunoassay with electrochemical detection has been established (Zhang and Zhang, 2012).

1.4.2 Receptor binding assays

In addition to early HPLC quantification methods, receptor-binding assays were developed for a more rapid quantification of DA. The first high throughput pharmacologic assay for the quantification of DA was also capable of determining its toxic potency. The assay used membrane preparations from frog brains since they contain many kainite/quisqualate receptors with glutamate binding sites that bind DA (Van Dolah et al., 1994). To eliminate the use of experimental animals, a microplate receptor binding assay using a cloned glutamate receptor was later constructed (Van Dolah et al., 1997).

Furthermore, a competitive enzyme linked immunoassay (ELISA) for the quantification of DA in mussel extracts was developed based on a polyclonal serum against an ovalbumin-DA conjugate, which was raised in mice (Smith and Kitts, 1995). Since this method was based on the limited resource of mouse serum, polyclonal antibodies against DA were later raised in sheep. They were used in a robust indirect competitive ELISA highly sensitive for DA with a LOQ of 481 pmol L^{-1} and appropriate for analysis in cultures and seawater (Garthwaite et al., 1998). Modified versions of the latter indirect competitive ELISA method are still frequently used for both pDA and dDA quantification with commercially available kits (e.g. Trainer et al., 2009b; Trick et al., 2018). The LOD obtained using this method is quite low (22 pmol L^{-1}) (Trainer et al., 2009b).

1.4.3 Sample preparation of dissolved domoic acid prior to quantification

To quantify dDA, particularly by HPLC-MS/MS, samples need to be desalted and concentrated. This can be achieved by different methods. A common technique is solid-phase extraction (SPE). Different loadings for the cartridges have been used to extract dDA. C18 cartridges used on acidified samples yield a good recovery of >90% (Wang et al., 2007). Thus, extraction dDA prior to LC-MS on C18 cartridges is a method commonly used (Trainer et al., 2000; Pan et al., 2001). In another study, cartridges were filled with a polymer (based on 2-(trifluoromethyl) acrylic acid monomers), determined by computational modelling and predicted to retain DA well under acidic conditions. The recovery rate for this type of extraction was 95% (Piletska et al., 2008). Furthermore, hydrophilic-lipophilic balance (HLB) cartridges were tested to extract DA from seawater. This material, however, only resulted in recovery rates of 57 to 69% (Barbaro et al., 2013). SPE with magnetic beads to remove salt interferences yields recovery rates of 86-98% (Zhang et al., 2016).

Common for the SPE of DOM from seawater is the use of styrene-divinylbenzene polymer (Priority PolLutant, PPL) cartridges, which are non-polar and extract a high proportion of DOM (Dittmar et al., 2008; Li et al., 2017). An efficient extraction of dDA from seawater with these cartridges should be possible but has not been tested yet.

2 Objectives

The overall motivation of this thesis was to elucidate the ecological and biogeochemical role of dDA in the Atlantic Ocean, with a spatial focus on the Arctic and Antarctic sectors. My aims were (i) to develop a method for dDA quantification, (ii) to determine the broad-scale dDA distribution and dDA's contribution to DOM and (iii) to improve our understanding of dDA's ecological function i.a. by acting as an iron ligand.

The detailed research objectives were:

(i) Method development

DA is usually quantified via receptor binding assays or LC-MS (Scholin et al., 2000). To extract DA for LC-MS analysis, mostly C18 solid-phase extraction cartridges are used (Trainer et al., 2000; Wang et al., 2007). To be able to scale marine dDA concentration to the total DOM, I aimed at developing a quantification pipeline consisting of

a. A sample preparation that can be combined with a standard method used for marine DOM (Dittmar et al., 2008; Li et al., 2017),
b. A separation and quantification method that is reproducible, quantitative, and sensitive.

(ii) Dissolved domoic acid quantity and distribution

Previous studies have quantified dDA concentrations during phytoplankton blooms in the euphotic zone (Trainer et al., 2009b; Trick et al., 2018) and showed that it can represent a significant fraction of the total DA during toxic blooms (Umhau et al., 2018). I aimed at answering the following questions:

a. What is the overall spatial dDA distribution in the East Atlantic Ocean and its polar sectors?
b. How long does dDA persist in different depths?
c. How much does dDA contribute to the inventory of marine DOM?

(iii) Ecological relevance in Polar Regions

Many regions of Antarctica are high-nutrient, low-chlorophyll (HNLC) areas due to low iron bioavailability (Allanson et al., 1981; Martin et al., 1990). DA has previously been suggested to act as a ligand for iron and copper (Rue and Bruland, 2001). dDA could play a part in the efficient iron uptake in *Pseudo-nitzschia* and might thus partially be responsible for their good adaptation and importance to Antarctic primary production (Hoppe et al., 2013). I therefore hypothesize:

a. If dDA functions as an iron ligand, the concentration is higher in HNLC areas where iron is limited.
b. The growth rate of the Antarctic species *Pseudo-nitzschia subcurvata* increases where dissolved DA is available at low iron conditions.
c. The cellular iron content increases if dissolved DA is available because DA increases the bioavailability of iron.

Apart from its assumed ligand function and its occurrence in HNLC regions, dDA also occurs in iron replete regions of the Arctic Ocean. So far, DA has not been studied in the Arctic fjord systems Scoresby Sund (East Greenland) and Arnarfjörður (Iceland). These systems differ strongly in their state of glaciation. To further elucidate the potential ecological function of dDA in this region I addressed the following research question: How is the occurrence of domoic acid linked to different environmental parameters, water masses and the occurrence of producers?

This question was addressed by testing the following hypotheses:

d. dDA correlates with *Pseudo-nitzschia* abundance, cellular pDA content and metatranscriptome reads of the DA biosynthesis gene cluster.
e. Nutrient concentrations inversely correlate with dDA concentration since low silicate and phosphate enhance dDA release.
f. dDA concentration varies with the type of water mass.

3 Manuscript I

Quantification, extractability and stability of dissolved domoic acid within marine dissolved organic matter

Jana K. Geuer*, Bernd Krock, Tim Leefmann, Boris P. Koch

Alfred Wegener Institute Helmholtz Centre for Polar and Marine Research, Am Handelshafen 12, 27570 Bremerhaven, Germany

*Corresponding author mail address: jana.geuer@awi.de

Highlights

- Spatial distribution of dissolved domoic acid concentration in East Atlantic Ocean.
- Quantitative contribution of a single compound to the entire pool of marine DOM.
- Dissolved domoic acid moderately stable in the ocean.
- Concentration of domoic acid decreases with increasing depth.
- Domoic acid quantity helps deduce high structural diversity by direct infusion FTMS.

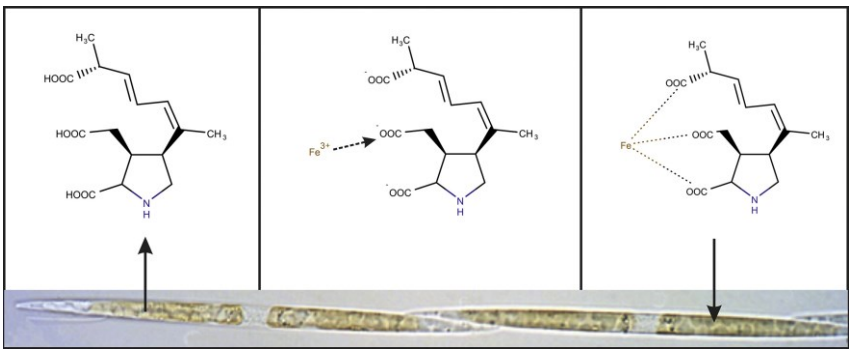

3.1 Abstract

The widespread diatom *Pseudo-nitzschia* can produce domoic acid (DA). DA is a compound with well described neurotoxic effects on vertebrates including humans known as amnesic shellfish poisoning (ASP) syndrome. It has also been suggested to serve as an organic ligand that binds to iron and copper. By binding these trace elements, DA may increase their solubility and bioavailability. In order to serve this function, DA has to be excreted and reabsorbed by the cells. Only few records of dissolved domoic acid (dDA) concentrations in the ocean exist. To accomplish quantification by ultrahigh performance liquid chromatography (UPLC), samples have to be pre-concentrated and desalted using solid-phase extraction, a procedure commonly applied for dissolved organic matter. Our major goals were to quantify dDA in a basin-wide assessment in the East Atlantic Ocean, to determine extraction efficiencies for complexed and uncomplexed dDA, and to assess whether domoic acid is represented by its molecular formula in direct-infusion high resolution mass spectrometry. Our results showed that dDA was extracted almost quantitatively and occurred ubiquitously in the ocean surface but also in deeper (and older) water, indicating surprisingly high stability in seawater. The maximum concentration measured was 173 pmol L^{-1} and the average molar dDA carbon yield was 7.7 ppm. Both carbon yield and dDA concentration decreased with increasing water depth. Providing quantification of dDA in the water column, we seek to improve our understanding of toxic bloom dynamics and the mechanistic understanding of DA production.

3.2 Introduction

Domoic acid (DA) is a non-essential amino acid occurring in the ocean (Wright et al., 1989). It was first described in 1958 as a secondary metabolite of the macroalga *Chondria armata* (Takemoto and Daigo, 1958) and later of other red algae species (Jiang et al., 2014). Almost 30 years after its discovery, DA regained attention when it was identified as the causative compound of a shellfish poisoning incident that was prompted by the consumption of blue mussels (*Mytilus edulis*) on Prince Edward Island, Canada, in 1987. Affected people showed symptoms such as vomiting, diarrhoea, confusion, disorientation, memory loss, coma and death (Quilliam and Wright, 1989; Wright et al., 1989). Due to their neurological symptoms, intoxications caused by seafood contaminated with DA were called amnesic shellfish poisoning (ASP) events (Quilliam and Wright, 1989). After analysing the plankton community at the time of the ASP event, it was suggested that the pennate diatom genus

Pseudo-nitzschia pungens f. multiseries (later renamed as *Pseudo-nitzschia multiseries*) was responsible for contaminating the shellfish with DA and was confirmed as a DA-producer (Bates et al., 1998; Bates et al., 1989). In the following years, it became evident that *Pseudo-nitzschia* species are cosmopolitans and that various species of this genus are capable of DA production (Trainer et al., 2012). If DA enters the food chain in high amounts, its trophic transfer can harm wildlife. High DA levels often occur during *Pseudo-nitzschia* blooms with high cell densities and DA production. Uptake of toxic *Pseudo-nitzschia* can lead to an accumulation of elevated DA values in higher trophic level organisms that can be found long after toxic blooms (Lefebvre et al., 2002; Martin et al., 1990). The uptake of high levels of DA via trophic transfer can cause severe neurological dysfunctions and death in mammals (Scholin et al., 2000; Trainer et al., 2000; Wekell et al., 1994).

Dissolved DA (dDA) is furthermore reported to influence other phytoplankton and the trophic food web (Van Meerssche and Pinckney, 2017; Bargu et al., 2006; Liu et al., 2007). Cardiac malformation increases in zebrafish embryos when subjected to 3.2 pmol L^{-1} dDA. At a concentration of 32 pmol L^{-1} mortality increases and changes in the cardiac development gene expression levels can be observed (Hong et al., 2015). Liu et al. (2007) observed an accumulation of DA in king sea scallops larvae. Growth and survival of the larvae decreased when they were subjected to dDA at a concentration of 96,361 pmol L^{-1}.

In Arctic waters DA-producing *Pseudo-nitzschia* are common elements of the food chain (Tammilehto et al., 2012). Along the Northeast Atlantic more than ten different *Pseudo-nitzschia* species occur, especially in the Irish Sea, at the northwest coast of Spain and off the west coast of Africa (Hasle, 2002; Trainer et al., 2012). Reports of DA-producing *Pseudo-nitzschia* also exist from the Southeast Atlantic at the South African west coast (Pitcher et al., 2014) and the Southwest Atlantic in Argentine coastal waters (Almandoz et al., 2007). Despite the large body of knowledge about the toxicity of DA in mammals, little is known about its ecological function. Even though it is known that DA has an impact on the phytoplankton community and that its production depends on the environmental conditions and the presence of predators (Harðardottir et al., 2015), it is yet to be determined which function DA fulfils for its producers (Prince et al., 2013). Very recently, it has been shown that DA levels increased in *Pseudo-nitzschia* by exudates of predatory copepods (Tammilehto et al., 2015). Furthermore, escape response levels of copepods decrease under a toxic *Pseudo-nitzschia* diet (Harðardottir et al., 2018). This strongly suggests that DA production may be involved in an inducible defence mechanism of at least some

Pseudo-nitzschia species against grazing. Furthermore, nutrient availability can influence DA production e.g. under phosphate limiting conditions (Lema et al., 2017). DA is capable of chelating iron and copper and may thus participate in iron acquisition or copper detoxification (Rue and Bruland, 2001). Enhanced production of DA was observable in iron fertilization experiments with clearly elevated DA concentrations (Silver et al., 2010; Trick et al., 2010) and in laboratory experiments with elevated DA concentrations under copper stress (Maldonado et al., 2002). In addition, the presence of dDA might improve the acquisition of iron for the producing diatoms (Prince et al., 2013). The observation that, in contrast to other eukaryotic phytoplankton, *Pseudo-nitzschia* species were frequently found in high-nutrient, low-chlorophyll (HNLC) areas of the world's oceans resulted in the hypothesis that DA-production might be induced by limitation of bioavailable iron (Fe) and involved in iron utilization of *Pseudo-nitzschia* (Wells et al., 2005). Wells et al. (2005) found that under Fe limitation *Pseudo-nitzschia* actively released DA into the culture medium, which is consistent with its hypothesized function as a compound involved in Fe uptake.

dDA is also part of the complex pool of marine DOM that plays an important role in the interaction between the geosphere and biosphere (Amon and Benner, 1996; Ludwig et al., 1996). Marine organic ligands represent one group of these interacting molecules within bulk DOM, as they have the capability of complexing trace metals (Ahsanullah and Florence, 1984; Gledhill and van den Berg, 1994; Gordon et al., 2000; Skrabal et al., 2000). Ligands can either help reduce toxic trace metals such as copper (Ahsanullah and Florence, 1984) or mediate the transport of essential trace metals such as iron or zinc (Aristilde et al., 2012; Gledhill and van den Berg, 1994). If DA is released by *Pseudo-nitzschia* into the marine environment as Fe activator and given the global distribution of *Pseudo-nitzschia*, dDA should be part of dissolved organic matter (DOM) at least in areas with frequent *Pseudo-nitzschia* proliferations. Marine DOM constitutes the largest proportion of organic carbon in the ocean (Hansell et al., 2009). The photic zone, depending on site and season, contains highest DOM concentrations, as it is released during primary production (Azam et al., 2011; Fischer et al., 2000). Bulk DOM can be categorised into refractory, semi-labile and labile DOM (Amon and Benner, 1996; Carlson and Ducklow, 1995). Marine microorganisms metabolise labile and semi-labile DOM, which is turned over more rapidly (Kirchman et al., 1991).

Fourier transform ion cyclotron resonance mass spectrometry (FT-ICR-MS) enables assessing complex organic mixtures (Kujawinski et al., 2002; Stenson et al., 2002) and, due to its high mass resolution and accuracy, allows the assignment of molecular

formulas and thus molecular elemental ratios (Koch et al., 2005; Stenson et al., 2003). In combination with other approaches, such as bacterial activity monitoring, the transformation of specific molecular formulas in DOM samples can be tracked with FT-ICR-MS (Kamjunke et al., 2017).

Solid-phase extraction is a common method for DOM extraction, enrichment and desalting. Different sorbents were applied in the past, including e.g. the silica based C18 (Aiken et al., 1979; Kim et al., 2003; Louchouam et al., 2000) and the styrene divinyl benzene polymer (PPL, Agilent; Dittmar et al., 2008; Li et al., 2017). dDA samples were desalted and concentrated with solid-phase extraction using magnetic beads of $CuFe_2O_4$ nanospheres (Zhang et al., 2016), on C18 cartridges (Wang et al., 2007) and a 2-(trifluoromethyl)acrylic acid resin (Piletska et al., 2008). Desalting is necessary for subsequent quantification using high-performance liquid chromatography coupled to electrospray tandem mass spectrometry (HPLC-MS/MS) (Furey et al., 2001; Piletska et al., 2008; Wang et al., 2007).

Although particulate DA has been frequently measured in marine samples, only few studies covered dDA (Busse et al., 2006; Trainer et al., 2009; Umhau et al., 2018). Previous dDA quantification in seawater was based on a derivatisation procedure and subsequent quantification via HPLC and fluorescence detection (Pocklington et al., 1990). Enzyme-linked immunosorbent assay (ELISA) has also been applied to quantify both particulate and dDA (Trainer et al., 2009; Trainer et al., 2000). A method of sample preparation for dDA (0.45 µm filter pore size) was described by Guannel et al. (2015). Another method for the quantification of dDA in seawater combined filtration and a C18 solid-phase extraction prior to LC-MS quantification (Pan et al., 2001; Trainer et al., 2000; Wang et al., 2007). Few records of marine dDA quantification exist for the North American West Coast and the French coast of the southern North Sea (Delegrange et al., 2018; Trainer et al., 2009, 2000), but none for the Atlantic Ocean.

So far, the quantification of marine dDA is restricted to smaller regions. In this study, our goal was to (i) determine the extraction efficiency of dDA using PPL solid-phase extraction (ii) quantify the concentration of dDA with a highly sensitive chemical method in seawater on a larger spatial scale in the East Atlantic Ocean, (iii) determine if the molecular formula of DA in high resolution mass spectrometry can represent the substance without chromatographic separation, (iv) determine which proportion of the bulk marine DOC is derived from dDA (carbon yield) and (v) assess the depth profile and stability of dDA.

3.3 Methods

3.3.1 Study area and sample processing

Samples were taken on a transect in the East Atlantic Ocean from 50°N to 70°S (for details see Koch and Kattner, 2012) Water samples were collected during two cruises (ANTXXV/1 and 2 of RV Polarstern) between November 2008 and January 2009. Surface samples (2 m water depth) were taken with a towed fish sampler. Water samples from other depths were collected using Niskin bottles attached to a rosette sampler connected to a CTD. All water samples were filtered through pre-combusted GF/F filters (Whatman, 0.7 µm nominal pore size; combustion: 450 °C, 5 h), not exceeding a pressure of 200 mbar. For DOC and nutrient analysis, aliquots were taken and stored at −20 °C in pre-combusted glass ampoules.

Solid-phase extraction (SPE) was performed as described previously (Flerus et al., 2012). In short, ~5 L of filtered water were acidified to pH 2 (hydrochloric acid, Suprapur, Merck) and extracted using a precleaned styrene-divinylbenzene polymer cartridge (PPL, 1 g, Mega Bond Elut, Varian). After extraction, cartridges were dried and eluted with 5 mL of methanol (LiChrosolv, Merck), equivalent to an enrichment factor of ~1000. Extracted samples were stored in pre-combusted glass ampules at −20 °C to prevent esterification (Flerus et al., 2011).

3.3.2 Assessment of domoic acid extraction yield

The extraction efficiency of dDA was determined for the uncomplexed and the complexed form (DA-iron complex). Sodium chloride (Fisher Chemical) was pre-combusted (500 °C for 6 h) to remove organic material and then dissolved in 500 mL ultrapure water (Milli-Q, Merck) to a final concentration of 35 g L^{-1}. This salt solution was used as reference. For uncomplexed samples, pure DA (Calbiochem, Merck Group) was added to obtain a final concentration of 2 µg L^{-1} (6.4 nmol L^{-1}). In an additional treatment, iron chloride (Fisher Chemical) was added at a final iron concentration of 17.4 µg L^{-1} (64 nmol L^{-1}) to obtain the complexed form of DA. Iron reference samples contained only 17.4 µg L^{-1} (64 nmol L^{-1}) iron without DA. Prior to extraction, cartridges were conditioned with 6 mL methanol, followed by 6 mL ultrapure water acidified to pH 2. All treatments were acidified to pH 2 (hydrochloric acid; Suprapur, Merck) and concentrated by SPE (200 mg PPL, Bond Elut, Agilent). The acidified samples were loaded onto the conditioned cartridges at a flow rate ≤ 40 mL min^{-1}. After loading, remaining salts were washed off the cartridges with acidified ultrapure water. The cartridges were dried under a nitrogen stream. Elution

was performed with 1 mL methanol (LiChrosolv, Merck). The exact volume of eluates was determined by weighing. Each treatment preparation and extraction was performed in triplicate.

3.3.3 Data evaluation

Quantification of dissolved organic carbon (DOC) and its radiocarbon age as well as molecular characterization by Fourier transform ion cyclotron resonance mass spectrometry (FT-ICR-MS) was performed as described previously (Flerus et al., 2012; Ksionzek et al., 2016).

3.3.4 Separation and quantification of dissolved domoic acid

Quantification of dDA was performed using ultrahigh performance liquid chromatography (UPLC, ACQUITY, Waters) coupled to triple quadrupole mass spectrometry (MS/MS, Xevo TQ-S, Waters). Separation was performed on a BEH C18 column (2.1 × 50 mm, 1.7 µm, ACQUITY, Waters) and a pre-column (BEH C18, 1.7 µm, VanGuard™, Waters) at a column temperature of 35 °C. Mobile phase A consisted of an aqueous formate buffer (40 mM, pH 5.8, ammonium formate, Riedel-de Haën; formic acid, Merck), mobile phase B was acetonitrile (LiChrosolv, Merck). Run time was 4.5 min at a flow rate of 0.6 mL min^{-1}. A gradient was run for 3.8 min from 1 to 99% B followed by an isocratic step for 0.2 min. In a linear gradient for 0.3 min eluents were returned to initial conditions and the column was equilibrated for 0.2 min.

The samples were subsequently analysed by UPLC-MS/MS with electrospray ionisation switching between positive and negative mode. Positive ionisation was used to obtain high intensity signals for quantification, while negative ionisation served as quality control. Cone voltage was 30 V for positive and − 30 V for negative ionisation, collision energy was 16 V for positive and 20 V for negative ionisation, respectively. Mass transitions that were used for the detection of DA were *m/z* 312 > 266 and 312 > 193 in positive mode and *m/z* 310 > 222 and *m/z* 310 > 160 in negative mode.

The dDA concentration was measured in the solid-phase extracts. Due to the complex matrix, the mass concentration of dDA in one extract was determined using standard addition (added concentrations: 0.25, 1, 5 10, 15, 50, 100 µg L^{-1}). dDA concentrations in the remaining extracts were assessed via a one-point calibration. From the extract concentration of dDA (pg L^{-1}) its molar concentration in the original water samples [dDA] (pmol L^{-1}) was calculated as follows

$$[\mathrm{dDA}] = \frac{\frac{[\mathrm{dDA}]_{\mathrm{extract}}}{\text{enrichment factor}\cdot M_{\mathrm{DA}}}}{0.91} \quad (1)$$

where $[\mathrm{dDA}]_{\mathrm{extract}}$ is the concentration of dDA (pg L^{-1}) in the extract, M_{DA} is the molar mass of DA (311.33 g mol^{-1}), enrichment factor is the factor by which a seawater sample was concentrated during SPE (~1000) and 0.91 is the average DA extraction efficiency based on the SPE method applied (see below).

DA carbon yield was calculated according to Eq. (2):

$$\text{Domoic acid carbon yield (ppm)} = \frac{[\mathrm{dDA}]\cdot 15}{[\mathrm{DOC}]}\cdot 10^{6} \quad (2)$$

where [DOC] and [dDA] are the DOC and dDA concentrations in original seawater, respectively, and 15 is the number of carbon atoms in a DA molecule.

The limits of detection and quantification (LOD and LOQ, respectively) for seawater extracts were assessed via standard addition. Different concentrations of DA were added to a sample in which no dDA was detected. A total of 10 different DA concentrations (0.1, 0.25, 0.5, 1, 2.5, 5, 10, 50, 100, 1000 µg L^{-1}) were measured 10 times. Calculations of LOD and LOQ were based on the standard deviation of response and the slope, based on a calibration curve. The limit of detection was defined as

$$\mathrm{LOD} = \frac{3.3\cdot\sigma}{\text{slope}} \quad (3)$$

where σ was the standard deviation of y-intercepts of the linear regression (concentrations 0, 0.1, 0.25, 0.5, 1, 2.5, 5 µg L^{-1}) close to the LOD and slope was the average slope of a calibration curve with all measured concentrations (n = 10). Limit of quantification was calculated analogously using the following formula:

$$\mathrm{LOQ} = \frac{10\cdot\sigma}{\text{slope}} \quad (4)$$

Due to the matrix underlying the DA peak, other methods to evaluate LOD and LOQ such as using blank deviation or signal-to-noise were inapplicable. Thus, a deep-water sample from the Southern Ocean showing no quantifiable signal at the target mass transition having an assumable very small concentration was picked for the determination of LOQ and LOD. For the method used, LOD was 3 µg L^{-1} and LOQ was 8 µg L^{-1}, equivalent to an LOD of ~10 pmol dDA L^{-1} and LOQ of ~26 pmol dDA L^{-1}, considering the enrichment factor of ~1000 for solid-phase extraction. The dataset of this study is available online on the PANGAEA™ database (https://doi.pangaea.de/10.1594/PANGAEA.896584).

3.3.5 Carbon-weighted relative summed peak intensity in FT-ICR-MS

To compare the DA carbon yield determined by MS/MS with relative peak intensities obtained by FT-ICR-MS, we calculated carbon-weighted relative summed peak intensities (Cw.r.s.i) according to Eq. (5):

$$Cw.r.s.i = \frac{r.i._{DA} \cdot C_{DA}}{\sum r.i._{all} \cdot C_{all}} \quad (5)$$

where r.i. is the respective relative intensity of either DA or all formulae in the sample and C is the respective number of carbon atoms.

3.3.6 Statistical analysis and sample distinction

All samples were assigned to two groups: the first group consisted of samples from the epipelagic zone (≤ 200 m water depth); the second group of all samples derived from deeper layers. The samples were furthermore grouped into a northern and southern area at a longitudinal split at 12°S based on bio-optical provinces by Taylor et al. (2011). The authors performed a pigment-based study and bio-optical characterization during the same cruise. They defined bio-optical provinces based on phytoplankton community structure by their bio-optical features with cluster analysis of hyperspectral data and simultaneous pigment analysis. Linear regression models were used to test for correlation between pairwise variables. Differences between group averages were assessed by one-sided Wilcoxon rank sum tests and results were considered significant if the calculated probability was below 0.05.

3.4 Results

3.4.1 Extraction and quantification of dissolved domoic acid

The extraction efficiency of uncomplexed dDA using PPL cartridges in saline water was 91 ± 3% ($n = 3$) and significantly higher ($p < 0.05$) compared to Fe(III)-spiked dDA treatments (78 ± 3%). Only the uncomplexed form of dDA was quantified in the extracts.

The retention time for DA in the UPLC method used was 0.60 ± 0.01 min ($n = 43$; Fig. 2a). Different mass transitions were recorded simultaneously. Of the four mass transitions that were measured for pure DA, mass transitions in positive ionisation mode resulted in larger peak areas compared to negative ionisation. Mass transition *m/z* 312 > 266 in positive mode yielded highest peak areas compared to all other transitions. Channel *m/z* 312 > 193 in positive mode was used as a qualitative check for DA, as were the negative mode mass transitions *m/z* 310 > 222 and 310 > 160.

Mass transition peak areas used for quantification showed a significant linear correlation ($p < 0.05$) with increasing dDA concentration both in water and in dDA-spiked extracts with high coefficients of determination (0.99). Although the base line of the quantification trace showed high noise due to the underlying complex organic matrix, the respective DA peaks were reliably distinguished by manual integration. Furthermore, a standard addition experiment confirmed that methanol extracts spiked with dDA showed a higher response and also a linear ion enhancement compared to dDA in aqueous solution with the same concentrations (Fig. 1).

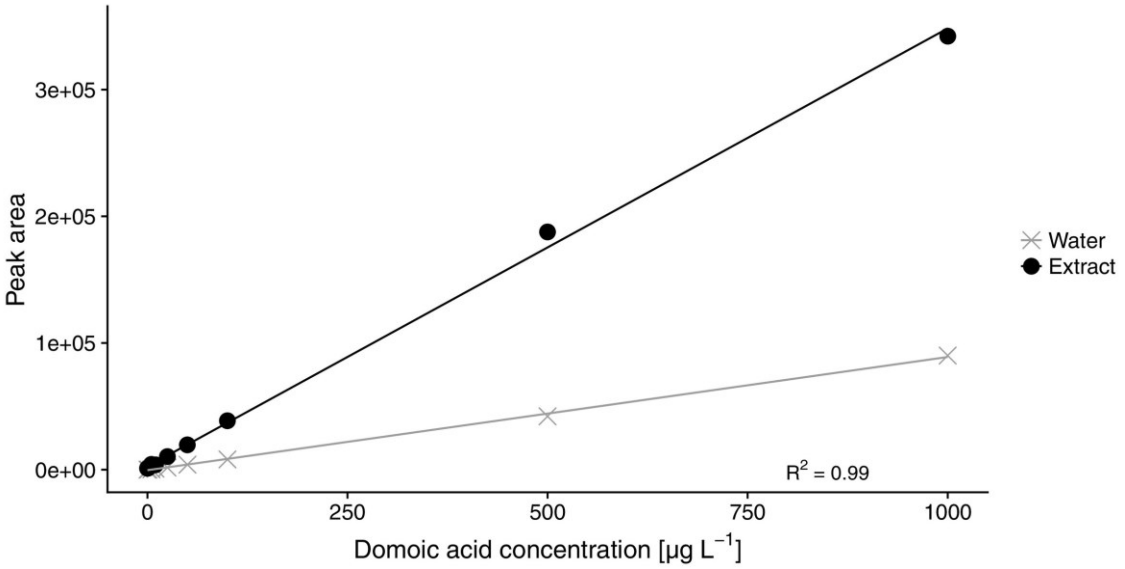

Fig. 1. Linear regression of dDA concentration and the peak area of mass transition *m/z* 312 > 266 in positive mode as measured for aqueous DA standards and spiked methanol extracts. Grey crosses represent water samples, black dots spiked extracts. For both linear regressions, R^2 was 0.99.

Since dDA quantification was challenged by a strong background matrix, we performed a standard addition for the sample with the largest DA peak area (station 1043 at 2 m water depth, Fig. 2a). The procedure yielded a linear regression curve (Fig. 2b) with a high coefficient of determination ($R^2 = 0.99$) and small standard errors for y-intercept (4%) and slope (5%, n = 10). Considering the extraction efficiency of 91%, the concentration of dDA was 173 pmol L^{-1} in original seawater.

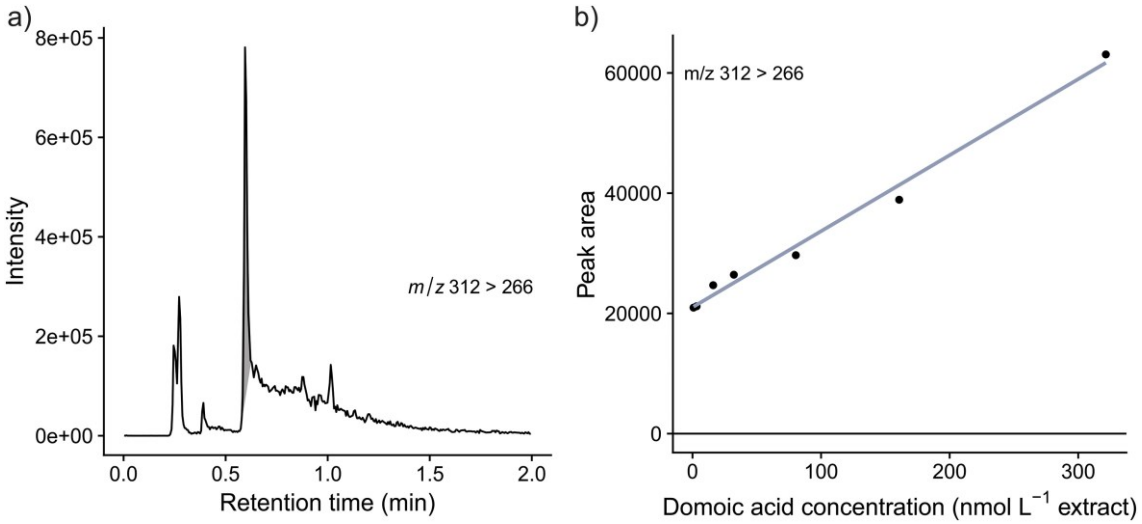

Fig. 2. dDA quantification using standard addition experiments. a) UPLC extracted ion chromatogram in positive mode (*m/z* 312 > 266) of a seawater extract containing dDA (shaded grey). b) Standard addition: the regression line drawn was calculated by least squares linear regression. Extrapolated x-intercept = 167 nmol L^{-1}, y-intercept = 21024, slope = 1.31, R^2 = 0.99.

Based on the linear regression and the high coefficient of determination we applied a one-point calibration to calculate the concentrations of all other samples. For our calculation of dDA concentrations in the water column, we accounted for the standard recovery of the uncomplexed molecule (91%) assuming that the equilibrium in the ocean shifts towards uncomplexed dDA. With this quantification strategy, dDA was detected (LOD = 10 pmol L^{-1}) in 81% of all samples analysed (n = 216).

3.4.2 Mass and structure: is domoic acid represented by its molecular formula in high resolution mass spectrometry without chromatographic separation?

Direct infusion FT-ICR-MS-spectra of the DOM extracts on average yielded 2718 ± 803 different molecular formulas (excl. isotopologues; Fig. 3a). In negative electrospray ionisation, the *m/z* value of 310.13765 represented the singly charged molecular mass of the neutral formula $C_{15}H_{21}NO_6$ that is also the molecular formula of DA (Fig. 3a). The DA standard used for quantification showed the same peak.

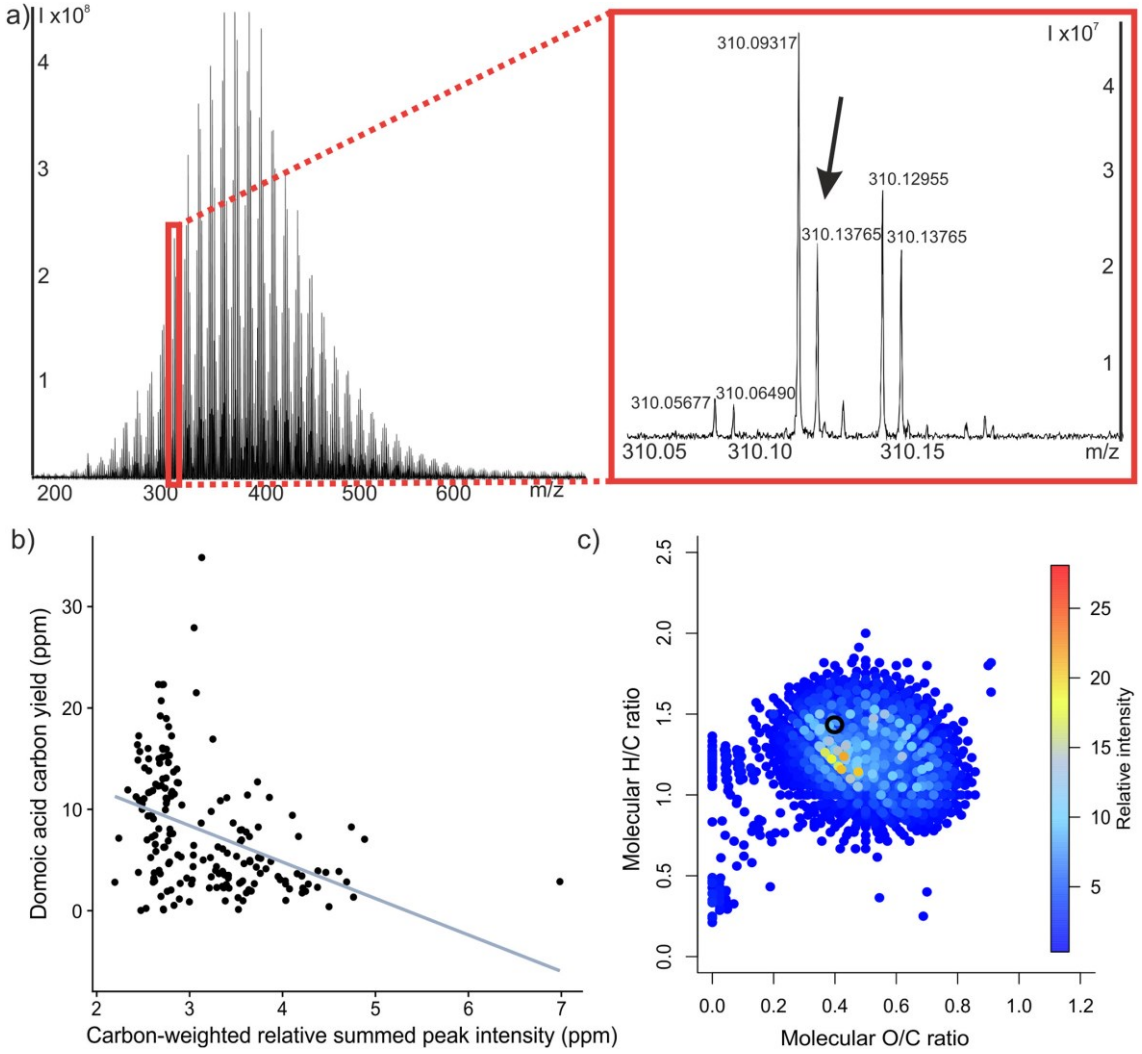

Fig. 3. a) FT-ICR mass spectrum of the DOM extract containing the highest concentration of dDA. The red rectangle encases the *m/z* ratios, in which the DA molecular formula can be found (enlarged in right panel). The arrow marks the peak representing the molecular formula, which matches DA. b) Molar carbon yield of DA plotted against relative peak magnitude of the formula representing DA, $R^2 = 0.15$. c) Van Krevelen plot of the same sample: the molecular ratios of oxygen to carbon (O/C) and hydrogen to carbon (H/C) of the molecular formulas calculated from *m/z* ratios of the sample were plotted. Colours represent relative summed, median projected intensities of the molecules. The location of DA's molecular formula is marked with a black circle. (For interpretation of the references to colour in this figure legend, the reader is referred to the web version of this article.)

The molecular formula $C_{15}H_{21}NO_6$ was detected in the DA standard and in all samples measured by FT-ICR-MS ($n = 204$; Fig. 3a) and its respective relative peak magnitude contributed between 0.023 and 0.051% of the summed peak magnitude in each spectrum. However, there was no correlation of the carbon-weighted relative summed peak intensity of the formula and the DA carbon yield (Fig. 3b).

DA has a molecular ratio of hydrogen to carbon (H/C = 1.4) and oxygen to carbon (O/C = 0.4) that is close to the average ratio of all calculated molecular formulas in a PPL-extracted marine DOM sample (average H/C ratio: 1.25, average O/C ratio: 0.49; Fig. 3c). A data base query in the open database PubChem (National Center for

Biotechnology Information) was carried out to explore other potential known structures for the formula $C_{15}H_{21}NO_6$ and its respective molecular mass. The search (as of December 2017) yielded 1193 known chemical structures for the molecular formula of DA.

3.4.3 Distribution of dissolved domoic acid in the Eastern Atlantic

The distribution of dDA in the water column differed along the study area. Our highest concentration measured was 173 pmol L^{-1} in surface water close to the equator (Fig. 4a). The overall average concentration of dDA was 32 pmol L^{-1}. In general, dDA concentrations were highest at the surface and decreased exponentially with increasing depth (Fig. 4b). Significantly higher dDA concentrations were found in the epipelagic zone compared to other water depths below 200 m where concentrations never exceeded 37 pmol L^{-1}. We observed significantly higher dDA concentrations in the northern East Atlantic (North of 12°S) compared to the southern section ($p < 0.05$; Fig. 4a).

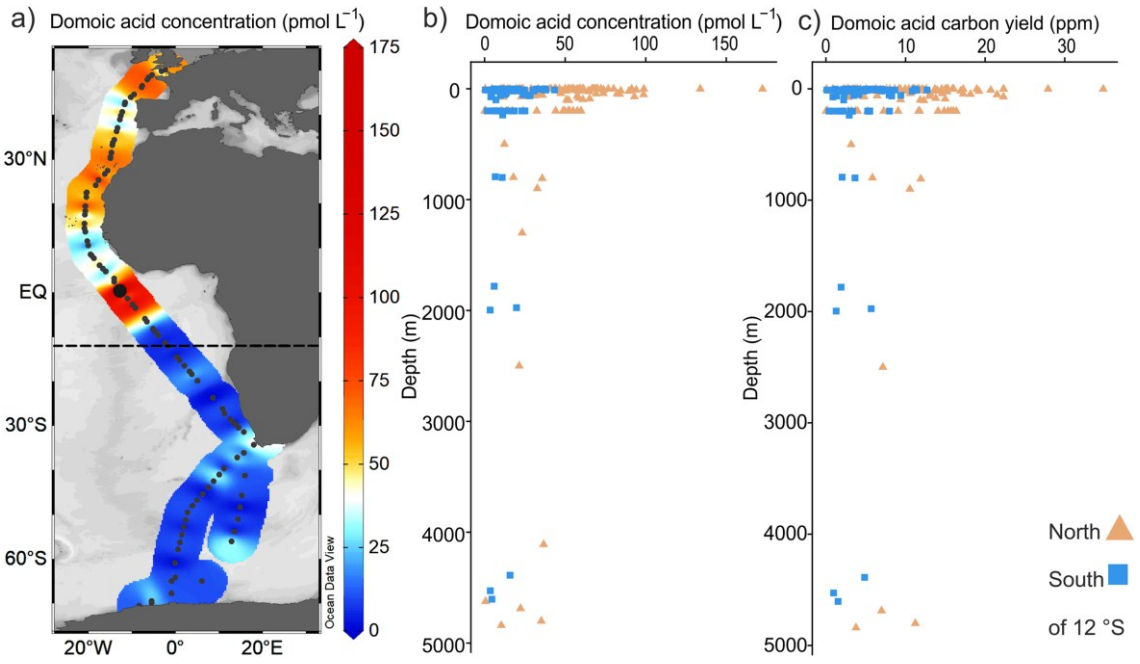

Fig. 4. dDA concentration in the East Atlantic Ocean (RV Polarstern cruises ANTXXV/I and II, 2008/2009): a) Surface concentrations (pmol L^{-1}; represented by colour code); larger black dot: highest dDA concentration in the dataset, dashed line: separation of samples into two groups, North and South of 12°S. b) dDA concentration versus water depth and c) molar proportion of carbon contributed by dDA to total DOC (DA carbon yield) versus depth. Northern samples are represented as yellow triangles and southern samples as blue squares. (For interpretation of the references to colour in this figure legend, the reader is referred to the web version of this article.)

The average molar contribution of dDA-derived carbon to total DOC (DA carbon yield) was 7.7 ppm and showed the same depth distribution as the dDA concentration: the maximum value was 35 ppm coinciding with the highest dDA concentration (Fig. 4).

Similar to dDA concentration, DA carbon yield was significantly higher in the euphotic zone compared to deeper water ($p < 0.05$) and significantly higher in the northern compared to the southern section ($p < 0.05$) (Fig. 4c). High surface concentrations were observed at the French coast, the northern African coast and in open waters close to the equator.

We carried out multiple linear regressions of dDA concentration with a range of environmental variables that were available from the Eastern Atlantic cruise (Flerus et al., 2012; Lechtenfeld et al., 2014; Taylor et al., 2011). However, no significant correlation with oceanographic parameters or nutrient, amino acid, pigment or iron and copper concentrations could be found.

3.5 Discussion

3.5.1 Extraction of dissolved domoic acid from seawater

An efficient dDA extraction is important, because it allows assessing the contribution of dDA to bulk marine DOM that is frequently extracted by the same method (Dittmar et al., 2008; Li et al., 2017). The average recovery of dDA in artificial seawater was reproducible, almost quantitative (91 ± 3%), and clearly exceeded the extraction efficiency of bulk marine DOC (42%; Flerus et al., 2012; Li et al., 2017). Such high dDA recovery is in agreement with results obtained by Wang et al. (2007) who investigated the extractability of dDA in seawater using C18 SPE cartridges and also found a recovery of >90%. The authors emphasised that DA is highly hydrophilic and that acidification, leading to protonation of carboxyl groups, is essential to achieve good retention on C18 cartridges. Compared to C18, PPL is capable to retain more hydrophilic components, which qualifies PPL for the extraction of dDA as part of the bulk marine DOM.

Differences in the extraction efficiency of complexed and uncomplexed dDA were revealed by the addition of iron chloride to dDA in artificial seawater, which led to a 13% drop in extraction recovery of dDA compared to the unspiked dDA treatment. Several competing effects contribute to this change in the recovery: (i) the high ionic strength of the medium, (ii) the impact of sample acidification prior to extraction, and (iii) the stability constant of the Fe-DA complex. Since both treatments were acidified before extraction and the amount of iron chloride added was small compared to the ionic strength of the artificial seawater medium (3.3 ppm change), it is likely that the decrease in recovery was primarily due to the complexation of iron with DA. The extraction was performed at pH 2, where dDA occurs as a zwitterion and thus

nominally neutral (Walter et al., 1992), which is an important precondition for a successful extraction using a moderately nonpolar solid phase. DA metal complex formation is favoured when DA is deprotonated (Fisher et al., 2006). Due to the acidic environment prior to extraction, DA is protonated and thus, the equilibrium shifts to the uncomplexed form of DA. DA is a tricarboxylate amino acid and structurally resembles some terrestrial phytosiderophores, which form tridentate complexes (Rue and Bruland, 2001). Compared to the neutral protonated form of DA, the ionic complex has a higher polarity, which can explain the decrease in extractability. In the spiking experiment, the amount of Fe(III) added (final concentration in water: 64 nmol L^{-1}) exceeded the dDA concentration (6.4 nmol L^{-1}) by a factor of ten, suggesting a high proportion of complexed dDA molecules. Although the decrease of extraction efficiency by 13% for the complexed dDA was significant, the loss was lower than expected, most likely due to a competitive reaction between complexation with iron and protonation as a result of sample acidification.

3.5.2 Quantification of dissolved domoic acid

The mass transition *m/z* 312 > 266 in positive mode was chosen for quantification, since it yielded highest peak areas, which is in agreement with previous LC-MS/MS DA quantifications (Scholin et al., 2000; Wang et al., 2007). Since the existing FT-ICR-MS spectra were acquired using negative ionisation (Lechtenfeld et al., 2014), we also applied negative mode mass transitions for quantification and confirmed the presence of dDA in the samples.

We observed high noise in the base line of the quantification trace. Ciminiello et al. (2005) tested a method for the quantification of DA in extracts of tissue. They observed ion suppression for positive and slight ion enhancement for negative ionisation. Comparing calibration curves of DA standards in water and in spiked extracts for the positive mass transition revealed that our quantification was subject to a matrix effect. Ciminiello et al. (2005) suggested to use matrix matched standards for quantification to counteract the matrix effects. Thus, we applied a standard addition to quantify the samples. Based on the linear regression and the high coefficient of determination ($R^2 = 0.99$), we applied a one-point calibration to calculate the concentration of the other samples.

Using the standard recovery of 91% to calculate dDA concentrations assumes that the equilibrium in the ocean shifts towards uncomplexed dDA. This is supported by the finding that DA is a weak ligand for iron and copper (Wells et al., 2005) and that its

concentration in the Eastern Atlantic (max. 173 pmol L^{-1} in this study) is well below the concentration of free dissolved iron (Klunder et al., 2011).

We detected dDA in 81% of our samples implying that the molecule was ubiquitously produced and relatively persistent. It has been previously shown that DA is mainly produced by the marine diatom *Pseudo-nitzschia* spp. (Bates et al., 1998; Bates et al., 1989), many species of which are cosmopolitans (Casteleyn et al., 2008; Hasle et al., 1996) and capable of producing DA (Hasle, 2002). However, the production of DA is not only dependent on species but on growth conditions and environmental factors (Bates et al., 1998).

Although most of the DA remains in the cell, it is also released into the surrounding seawater, for example under copper stress (Maldonado et al., 2002; Wang et al., 2007). Few previous studies have measured dDA in seawater, most of which were performed along the West Coast of North America (Trainer et al., 2009; Trick et al., 2018; Umhau et al., 2018) or focused on method development (Busse et al., 2006; Guannel et al., 2015; Pocklington et al., 1990).

In the recent past, different methods have been used to quantify dDA in seawater. Wang et al. (2007) quantified dDA by LC-MS with an LOD of 96 pmol L^{-1}, while Trainer et al. (2009) and Guannel et al. (2015) used a direct competitive ELISA for quantification. The LOD for the two methods was 22 pmol L^{-1} (Trainer et al., 2009) and 32 pmol L^{-1} (Guannel et al., 2015) compared to an LOD of 10 pmol DA L^{-1} in our study. Most field studies quantified dDA using ELISA (Delegrange et al., 2018; Trainer et al., 2009; Trick et al., 2018) whereas LC-MS has only been used sporadically for quantification (Trainer et al., 2000; Umhau et al., 2018). The UPLC-MS/MS method developed here allowed fast quantification and a comprehensive spatial assessment of dDA.

Particulate DA (amount of DA in the filter residue for a defined volume of seawater) can reach quite high levels: During a massive coast-wide *Pseudo-nitzschia* bloom at the North American West Coast high particulate DA values up to 64,241 pmol L^{-1} were found (McCabe et al., 2016). Smith et al. (2018) also reported up to 86,817 pmol L^{-1} particulate DA during *Pseudo-nitzschia* blooms at the Californian coast. Guannel et al. (2015) measured a maximum of 592 pmol L^{-1} particulate DA in the South Atlantic Ocean during austral spring 2007, exceeding our maximum dDA concentration by a factor of three. Based on the results of Guannel et al. (2015), it was to be expected that the concentrations of dDA measured in this study were well below the value of the particulate phase. Wang et al. (2007) found that the dDA concentration in the medium

surrounding the cell was approximately 11% of the intracellular DA levels. In a time series study in the southern North Sea, dDA contributed around 83% of the total measured DA (Delegrange et al., 2018). During a toxic bloom of *Pseudo-nitzschia*, dDA should thus be released into the surrounding water in amounts well quantifiable by the method used in this study.

DA has been suggested to improve trace metal acquisition for its producers (Rue and Bruland, 2001; Prince et al., 2013; Maldonado et al., 2002). Due to its widespread spatial distribution, dDA does not only have the potential to change available trace metal concentrations for *Pseudo-nitzschia*, but for other protists as well. A negative effect of dDA on the growth of the diatom *Skeletonema marinoi* likely connected to iron availability could be observed in an experiment (Prince et al., 2013). The release of dDA might also decrease cupric ion concentrations and thereby enhance the growth of co-occurring *Eutreptiella* spp. in the field (Trick et al., 2018). Additionally, growth inhibition of other phytoplankton with dDA was previously observed at high salinities (Van Meerssche and Pinckney, 2017). Furthermore, dDA can also affect higher trophic level organisms: the survival and growth of king sea scallops larvae has been shown to decrease under dDA exposure of 96,361 pmol L^{-1} (Liu et al., 2007) and increasing dDA levels can supress krill grazing rates (Bargu et al., 2006). In zebrafish embryos, dDA was shown to disrupt normal cardiac development from concentrations of 3.2 pmol L^{-1} dDA and embryo mortality rates increased when subjected to dDA concentrations of 32 pmol L^{-1} (Hong et al., 2015). Thus, our method of quantifying dDA could serve as useful tool to detect such low concentrations that can already affect the surrounding organisms.

3.5.3 Mass and structure: is domoic acid represented by its molecular formula in high resolution mass spectrometry without chromatographic separation?

The molecular formula of DA is $C_{15}H_{21}NO_6$, represented by the deprotonated molecular ion of 310.13765 *m/z*. This mass was detected in the negative ionisation FT-ICR mass spectra of each sample with an average relative magnitude of 0.033% of the summed peak magnitudes. DA carries three carboxyl groups and a secondary amine group facilitating ionisation in positive and negative electrospray mode (Ciminiello et al., 2005). Ionisation in general has a large impact on selectivity and oxygenated molecules tend to ionise better in negative mode (Hertkorn et al., 2013; Hertkorn et al., 2008).

Since dDA was almost quantitatively extracted by SPE, it is worthwhile to compare its molecular size, elemental composition, and relative peak magnitude of its mass signal to the peak-magnitude weighted average values of the entire pool of molecular formulas in each DOM sample. Compared to the average *m/z* ratio of bulk DOM (417 Da) (Flerus et al., 2012), the molecular weight of DA was comparatively small, whereas its molecular ratio (H/C = 1.4 and O/C = 0.4) was close to the average ratio of all calculated molecular formulas (average H/C ratio: 1.25, average O/C ratio: 0.49), which makes DA a generic molecule for marine DOM.

The average composition of marine DOM in our study was $C_{19.0}H_{23.8}N_{0.6}O_{9.4}$. Based on an average surface bulk DOC concentration of 64 µmol L^{-1}, an average of 19 carbon atoms per molecule and 2438 molecular formulas calculated per surface sample, the average DOM compound could contribute a maximum of 1382 pmol L^{-1} at the surface. For dDA, the calculated maximum concentration was 173 pmol L^{-1}. This average maximum concentration can be considered as a conservative upper limit because it does not consider structural isomers (isobars). However, our dDA concentration only differs by a factor of ten from the maximum value for a naturally occurring single marine DOM compound.

Comparing dDA carbon yield with the respective carbon weighted summed peak intensities should show if the contribution of dDA could explain the magnitude of the signal of the molecular formula $C_{15}H_{21}NO_6$ and if this could be estimated by its carbon yield. Therefore it is worthwhile to explore if the relative peak intensities of the DA mass signal (310.13765 *m/z*) correlate with the dDA carbon yield (Fig. 3a). The lack of correlation demonstrated that the structural diversity that is projected on the molecular ion 310.13765 *m/z* was high and concealed the quantitative contribution of dDA.

Although dDA was almost quantitatively extracted, the peak magnitude of its respective formula is dominated by one or many structural isomers with the same molecular formula that are present in higher concentration and/or ionise more efficiently (Cheng et al., 1995). Structural isomers that can contribute to the DA mass peak signal were not covered by our selective DA quantification method (Hertkorn et al., 2013). However, a query in the PubChem database yielded 1193 known chemical structures for the molecular formula $C_{15}H_{21}NO_6$. Most of these compounds are unlikely to occur in marine environments and only some are thus likely to account for the imbalance between DA concentration and peak magnitude. However, the database result demonstrates the potentially high chemical diversity that has an important influence on the relative peak magnitudes and therefore prevents quantitative conclusions about

molecular compounds in direct infusion analyses of marine DOM using high-resolution mass spectrometry. This is especially true for larger molecules, since the number of structural isomers increases with molecular mass.

3.5.4 Spatial distribution of dissolved domoic acid in the Eastern Atlantic

On average, we observed higher dDA concentrations in the northern part of our sampling transect. High surface concentrations occurred along the French coast, the northern African coast and in open waters close to the equator. Probable sources of dDA are blooms of toxigenic *Pseudo-nitzschia* species. Hasle (2002) and Trainer et al. (2012) summarised the global occurrence of toxic *Pseudo-nitzschia* species and listed reports of different toxic species along the East Atlantic towards South Africa. Several species were observed in the English Channel, the coast of Spain and the North West African coast, where also comparatively high dDA concentrations occurred at the surface (Fig. 4a). North of the English Channel, dDA concentrations were recorded for the year 2012 and varied distinctively between months. In November 2012, dDA concentrations of around 160 pmol L^{-1} were recorded (Delegrange et al., 2018). The dDA concentrations for the same area in the same month of 2008 measured in our study were around 80 pmol L^{-1}, which is likely due to interannual variability. At least one clade of the species *Pseudo-nitzschia pungens* and the species *Pseudo-nitzschia multiseries* have been reported to be cosmopolitan (Casteleyn et al., 2008; Hasle, 2002). Both species have been found in the equatorial West Atlantic (Hasle, 2002; Trainer et al., 2012). *Pseudo-nitzschia pungens* has been reported to be capable of expressing DA in small levels (e.g. Bates et al., 1998; Rhodes et al., 1996; Trainer et al., 1998), whereas *Pseudo-nitzschia multiseries* is known as toxic species (e.g. Bates et al., 1998; Bates et al., 1989; Fryxell et al., 1990; Subba Rao et al., 1988) and could potentially contribute to high dDA concentrations observed close to the equator.

Average dDA concentrations south of 12°S were 33% lower compared to the northern locations. For the southern part of the transect, highest dDA concentrations occurred at the tip of South Africa, where the existence of toxic species and a large richness of *Pseudo-nitzschia* species in the northern Benguela upwelling zone has been reported (Hasle, 2002; Trainer et al., 2012). This zone is prone to toxigenic *Pseudo-nitzschia* blooms that can impact offshore organisms (Guannel et al., 2015). Taking into consideration that 11% to 88% of the total DA can be released as dDA in the medium surrounding *Pseudo-nitzschia* (Wang et al., 2007; Pan et al., 2001; Umhau et al., 2018), the maximum dDA concentrations measured in this study could stem from particulate DA levels similar to those detected in toxic blooms (Scholin et al., 2000;

Trainer et al., 2000). Despite high chlorophyll concentrations in the Southern Ocean, we found relatively low concentrations of dDA (Fig. 4a). Different areas of the Southern Ocean show great variability in plankton diversity (Almandoz et al., 2008; Hasle, 2002; Trainer et al., 2012). Several *Pseudo-nitzschia* species have been reported to contribute to local diatom communities (Almandoz et al., 2008; Hegseth and Von Quillfeldt, 2002), however, only *P. turgidula* showed low toxicity (Rhodes et al., 2013). Potential sources of dDA in the Southern Ocean are thus scarce, which matches low dDA concentrations determined in our study.

Although our cruise took place in austral summer and chlorophyll was high at some stations, there was no correlation between chlorophyll and dDA concentration ($R^2 = 0.007$). Taylor et al. (2011) quantified mean values of marine phytoplankton chlorophyll concentrations during the first part of the same cruise via remote sensing. They found two phytoplankton blooms at ~22°N and ~15°N and also analysed the phytoplankton composition. Stations with the highest diatom yield were outside of these blooms (Taylor et al., 2011) and our surface dDA concentrations at diatom-dominated stations were relatively low (between 50 and 100 pmol L^{-1}). This can be explained by the fact that *Pseudo-nitzschia* species were likely not dominant within the blooms (Taylor et al., 2011) and that cells with low DA levels excrete less dDA than highly toxic cells (Wang et al., 2007). Furthermore, blooms of *Pseudo-nitzschia* do not necessarily have to be associated with high DA concentrations (Smith et al., 1990). It is also possible that the occurrence of toxigenic *Pseudo-nitzschia* cells and dDA concentration are time-decoupled.

3.5.5 Depth profiles and stability of dissolved domoic acid

dDA concentrations were significantly higher in the epipelagic zone in comparison to water depths below 200 m, which is in accordance with the observation of high concentrations of dDA off the North American West coast (Trainer et al., 2009; Trick et al., 2018). dDA concentrations were generally decreasing with increasing depth, which is likely related to the production by *Pseudo-nitzschia* at the sea surface and the deep chlorophyll maximum, microbial removal and mixing with deep water below the photic zone (Malviya et al., 2016).

The molar proportion of carbon contributed by dDA to total DOC (DA carbon yield) was decreasing similar to the dDA concentration profile (Fig. 4b, c). Bulk DOC concentrations decrease with increasing depth, with the proportion of refractory DOC increasing with depth (Carlson and Ducklow, 1995). The decrease of DA carbon yield with increasing depth implies that dDA is degraded faster than DOC (Fig. 4c).

A potential sink for dDA at the surface is photooxidation. Both DOM and Fe(III) accelerate DA photooxidation, while the presence of phosphate can slow it down (Fisher et al., 2006). Although dDA is degraded within a few days of sunlight exposure (Bouillon et al., 2006), it is only affected within approximately the upper two meters, thus limiting photooxidation as dDA sink (Bouillon et al., 2008). Considering that DA carbon yield decreased with depth in the same pattern as dDA concentration, it is not likely that photodegradation was an important dDA sink in our study.

We also found dDA in deeper water at lower concentrations, likely due to vertical flux (Scharek et al., 1999) and subsequent release of dDA from phytoplankton cells e.g. by sloppy feeding (Møller et al., 2003). Furthermore, DA is rapidly transported downward by vertical particle flux in coastal waters and many cells that are transported downward stay intact (Sekula-Wood et al., 2009). Particulate DA decreases with increasing depth (Sekula-Wood et al., 2009). This could be explained with degradation but also leaching of dDA, resulting in the pattern we observed in our study (Fig. 4b). Recently, Umhau et al. (2018) measured both particulate and dDA in sediment traps at different depths. Both DA pools were almost equal and both were decreasing with depth while their ratio remained unchanged, confirming dDA as important contributor to total DA levels in the ocean. Overall, the widespread occurrence of dDA even in deep Atlantic water suggests that dDA is relatively resistant to degradation. Previous studies have shown that nitrogen, phosphorus and sulfur containing DOM compounds tend to degrade faster due to selective microbial removal (Hopkinson et al., 2002; Hopkinson and Vallino, 2005; Koch et al., 2014; Ksionzek et al., 2016). Since DA is carbon rich and contains only one nitrogen atom but no phosphorus or sulfur, it should be less attractive for microbial consumption. This is in accordance with the previous finding that only few bacterial strains related to shellfish tissue were capable of degrading DA (Stewart et al., 1998).

We found dDA in up to 5000 m water depth. dDA accumulation in the surface and export flux require a relatively high stability of DA. Although the toxin can be degraded and is removed from the water column faster than average DOC, a transport downwards in intact *Pseudo-nitzschia* cells and accumulation in higher trophic levels could still serve as a preservation process for DA (Sekula-Wood et al., 2009; Costa et al., 2005). The DOC in our study showed, in accordance with previous other studies, a high radiocarbon age (Lechtenfeld et al., 2014), implying that substances at depth are relatively resistant to degradation. Carbon derived from dDA contributed to this DOC and might even be stabilized within the complex DOM matrix.

3.6 Conclusions

DA has been studied for decades due to its dual role as a marine toxin and organic iron-binding ligand. Our study shows that dDA is well extractable, quantifiable and ionisable in negative electrospray mode using tandem mass spectrometry. The high recovery rate is an ideal premise for its characterization within the entirety of marine DOM.

The molecular formula that matches DA was identified in our FT-ICR-MS analyses. Molecular mass, O/C and H/C ratios are close to the average of this study's DOC, which suggests that dDA is a representative contributor to solid-phase extractable DOM. However, as a result of structural diversity, the relative peak magnitude did not correspond to the DA quantity, emphasizing the limits of structural interpretations of non-targeted, direct infusion analyses of highly complex DOM samples using FT-ICR-MS.

The sensitivity of DA quantification using UPLC-MS/MS was high enough to allow for quantification in most samples of our study area, probably due to the ubiquitous occurrence of its primary producing organisms. Generally, dDA quantification could serve as a useful additional tool to monitor the occurrence of DA apart from the quantification in phytoplankton or the contaminated tissue. The widespread occurrence of dDA, also in deep Atlantic Ocean waters, suggests that DA is relatively resistant to degradation.

Quantification of dDA in the water column, as a consequence of enhanced intracellular DA production, supports our future understanding of toxic bloom dynamics, the role of dDA for its producers and assists the development of approaches to chemically characterize marine DOM.

Acknowledgements

We sincerely thank Claudia Burau for performing solid-phase extraction tests. We would like to acknowledge the crew and the master of the research vessel *Polarstern* for their support during the cruises Ant 25/1 and 25/2. We are grateful for the support by Wolfgang Drebing and Thomas Max with domoic acid analysis. We furthermore want to express our thanks to Svenja Hoppe, Claudia Burau and Theresa Grunwald for proofreading.

Funding

This study was financially supported by the strategy fund of the Alfred Wegener Institute Helmholtz Centre for Polar and Marine Research in the framework of the project “Inorganics in organics: Chemical and biological controls on micronutrient and carbon fluxes in the polar ocean” (Koch; IP76010001). Sampling was possible by the support of the Deutsche Forschungsgemeinschaft (DFG) in the framework of the priority programme “Antarctic Research with comparative investigations in Arctic ice areas” (Grant KO 2164/8-1+2).

References

Ahsanullah, M., Florence, T.M., 1984. Toxicity of copper to the marine amphipod *Allorchestes compressa* in the presence of water- and lipid-soluble ligands. *Mar. Biol.* 84, 41–45.

Aiken, G.R., Thurman, E.M., Malcom, R.L., Walton, H.F., 1979. Comparison of XAD macroporous resins for the concentration of fulvic acid from aqueous solution. *Anal. Chem.* 51, 1799–1803.

Almandoz, G.O., Ferrario, M.E., Ferreyra, G.A., Schloss, I.R., Esteves, J.L., Paparazzo, F.E., 2007. The genus *Pseudo-nitzschia* (Bacillariophyceae) in continental shelf waters of Argentina (Southwestern Atlantic Ocean, 38–55°S). *Harmful Algae* 6, 93–103.

Almandoz, G.O., Ferreyra, G.A., Schloss, I.R., Dogliotti, A.I., Rupolo, V., Paparazzo, F.E., Esteves, J.L., Ferrario, M.E., 2008. Distribution and ecology of *Pseudo-nitzschia* species (Bacillariophyceae) in surface waters of the Weddell Sea (Antarctica). *Polar Biol.* 31, 429–442.

Amon, R.M.W., Benner, R., 1996. Bacterial utilization of different size classes of dissolved organic matter. *Limnol. Oceanogr.* 41, 41–51.

Aristilde, L., Xu, Y., Morel, F.M.M., 2012. Weak organic ligands enhance zinc uptake in marine phytoplankton. *Environ. Sci. Technol.* 46, 5438–5445.

Azam, F., Jiao, N., Sanders, S., Stone, R., Ogawa, H., Amagai, Y., Koike, I., Kaiser, K., Benner, R., Paulinski, J.D., McCarthy, M., Hedges, J.I., Hatcher, P.G., Worden, A.Z., Aristeguí, J., Duarte, C.M., Agustí, S., Doval, M., Álvarez-Salgado, X.A., Hansell, D.A., 2011. Microbial Carbon Pump in the Ocean. *AAAS Science.* The American Associeation for the Advancement of Science.

Bargu, S., Lefebvre, K.A., Silver, M.W., 2006. Effect of dissolved domoic acid on the grazing rate of krill *Euphausia pacifica*. *Mar. Ecol. Prog. Ser.* 312, 169–175.

Bates, S.S., Bird, C.J., de Freitas, A.S.W., Foxall, R., Gilgan, M., Hanic, L.A., Johnson, G.R., McCulloch, A.W., Odense, P., Pocklington, R., Quilliam, M.A., Sim, P.G., Smith, J.C., Subba Rao, D.V., Todd, E.C.D., Walter, J.A., Wright, J.L.C., 1989. Pennate diatom *Nitzschia pungens* as the primary source of domoic acid, a toxin in shellfish from eastern Prince Edward Island, Canada. *Can. J. Fish. Aquat. Sci.* 46, 1203–1215.

Bates, S.S., Garrison, D.L., Horner, R.A., 1998. Bloom dynamics and physiology domoic acid-producing *Pseudo-nitzschia* species. In: Anderson, D.M., Cembella, A.D., Hallegraeff, G.M. (Eds.), *Physiological Ecology Harmful Algal Blooms.* Springer Verlag, Heidelberg, pp. 267–292.

Bouillon, R.-C., Knierim, T.L., Kieber, R.J., Skrabal, S.A., Wright, J.L.C., 2006. Photodegradation of the algal toxin domoic acid in natural water matrices. *Limnol. Oceanogr.* 51, 321–330.

Bouillon, R.-C., Kieber, R.J., Skrabal, S.A., Wright, J.L.C., 2008. Photochemistry and identification of photodegradation products of the marine toxin domoic acid. *Mar. Chem.* 110, 18–27.

Busse, L.B., Venrick, E.L., Antrobus, R., Miller, P.E., Vigilant, V., Silver, M.W., Mengelt, C., Mydlarz, L., Prezelin, B.B., 2006. Domoic acid in phytoplankton and fish in San Diego, CA, USA. *Harmful Algae* 5, 91–101.

Carlson, C.A., Ducklow, H.W., 1995. Dissolved organic carbon in the upper ocean of the central equatorial Pacific Ocean, 1992: daily and finescale vertical variations. *Deep Sea Res. II Top. Stud. Oceanogr.* 42, 639–656.

Casteleyn, G., Chepurnov, V.A., Leliaert, F., Mann, D.G., Bates, S.S., Lundholm, N., Rhodes, L., Sabbe, K., Vyverman, W., 2008. *Pseudo-nitzschia pungens* (Bacillariophyceae): A cosmopolitan diatom species? *Harmful Algae* 7, 241–257.

Cheng, X., Chen, R., Bruce, J.E., Schwartz, B.L., Anderson, G.A., Hofstadler, S.A., Gale, D.C., Smith, R.D., Gao, J., Sigal, G.B., Mammen, M., Whitesides, G.M., 1995. Using electrospray ionization FTICR mass spectrometry to study competitive binding of inhibitors to carbonic anhydrase. *J. Am. Chem. Soc.* 117, 8859–8860.

Ciminiello, P., Dell'Aversano, C., Fattorusso, E., Forino, M., Magno, G.S., Tartaglione, L., Quilliam, M.A., Tubaro, A., Poletti, R., 2005. Hydrophilic interaction liquid chromatography/mass spectrometry for determination of domoic acid in Adriatic shellfish. *Rapid Commun. Mass Spectrom.* 19, 2030–2038.

Costa, P.R., Rosa, R., Duarte-Silva, A., Brotas, V., Sampayo, M.A.M., 2005. Accumulation, transformation and tissue distribution of domoic acid, the amnesic shellfish poisoning toxin, in the common cuttlefish, *Sepia officinalis*. *Aquat. Toxicol.* 74, 82–91.

Delegrange, A., Lefebvre, A., Gohin, F., Courcot, L., Vincent, D., 2018. *Pseudo-nitzschia* sp. diversity and seasonality in the southern North Sea, domoic acid levels and associated phytoplankton communities. *Estuar. Coast*. *Shelf Sci.* 214, 194–206.

Dittmar, T., Koch, B.P., Hertkorn, N., Kattner, G., 2008. A simple and efficient method for the solid-phase extraction of dissolved organic matter (SPE-DOM) from seawater. *Limnol. Oceanogr. Methods* 6, 230–235.

Fischer, G., Ratmeyer, V., Wefer, G., 2000. Organic carbon fluxes in the Atlantic and the Southern Ocean: relationship to primary production compiled from satellite radio- meter data. *Deep Sea Res. II Top. Stud. Oceanogr.* 47, 1961–1997.

Fisher, J.M., Reese, J.G., Pellechia, P.J., Moeller, P.L., Ferry, J.L., 2006. Role of Fe(III), phosphate, dissolved organic matter, and nitrate during the photodegradation of domoic acid in the marine environment. *Environ. Sci. Technol.* 40, 2200–2205.

Flerus, R., Koch, B.P., Schmitt-Kopplin, P., Witt, M., Kattner, G., 2011. Molecular level investigation of reactions between dissolved organic matter and extraction solvents using FT-ICR MS. *Mar. Chem.* 124, 100–107.

Flerus, R., Lechtenfeld, O.J., Koch, B.P., McCallister, S.L., Schmitt-Kopplin, P., Benner, R., Kaiser, K., Kattner, G., 2012. A molecular perspective on the ageing of marine dissolved organic matter. *Biogeosciences* 9, 1935–1955.

Fryxell, G.A., Reap, M.E., Valencic, R.L., 1990. *Nitzschia pungens* Grunow *f. multiseries* Hasle: observations of a known neurotoxic diatom. *Nov. Hedwigia Beih* 100, 171–188.

Furey, A., Lehane, M., Gillman, M., James, K.J., Fernandez-Puente, P., James, K.J., 2001. Determination of domoic acid in shellfish by liquid chromatography with electro- spray ionization and multiple tandem mass spectrometry. *J. Chromatogr.* A 938, 167–174.

Gledhill, M., van den Berg, C.M.G., 1994. Determination of complexation of iron(III) with natural organic complexing ligands in seawater using cathodic stripping voltammetry. *Mar. Chem.* 47, 41–54.

Gordon, A.S., Donat, J.R., Kango, R.A., Dyer, B.J., Stuart, L.M., 2000. Dissolved copper- complexing ligands in cultures of marine bacteria and estuarine water. *Mar. Chem.* 70, 149–160.

Guannel, M.L., Haring, D., Twiner, M.J., Wang, Z., Noble, A.E., Lee, P.A., Saito, M.A., Rocap, G., 2015. Toxigenicity and biogeography of the diatom *Pseudo-nitzschia* across distinct environmental regimes in the South Atlantic Ocean. *Mar. Ecol. Prog. Ser*. 526, 67–87.

Hansell, D., Carlson, C.A., Repeta, D.J., Schlitzer, R., 2009. Dissolved organic matter in the ocean: a controversy stimulates new insights. *Oceanography* 22, 202–211.

Harðardottir, S., Pančic, M., Tammilehto, A., Krock, B., Møller, E.F., Nielsen, T.G., Lundholm, N., 2015. Dangerous relations in the Arctic marine food web: interactions between toxin producing *Pseudo-nitzschia* diatoms and *Calanus* Copepodites. *Mar. Drugs* 13, 3809–3835.

Harðardottir, S., Krock, B., Wohlrab, S., John, U., Gissel, T., Lundholm, N., 2018. Can domoic acid affect escape response in copepods? *Harmful Algae* 79, 50–52.

Hasle, G.R., 2002. Are most of the domoic acid-producing species of the diatom genus *Pseudo-nitzschia* cosmopolites? *Harmful Algae* 1, 137–146.

Hasle, G.R., Lange, C.B., Syvertsen, E.E., 1996. A review of *Pseudo-nitzschia*, with special reference to the Skagerrak, North Atlantic, and adjacent waters. *Helgolaender Meeresun.* 50, 131–175.

Hegseth, E.N., Von Quillfeldt, C.H., 2002. Low phytoplankton biomass and ice algal blooms in the Weddell Sea during the ice-filled summer of 1997. *Antarct. Sci.* 14, 231–243.

Hertkorn, N., Frommberger, M., Witt, M., Koch, B.P., Schmitt-Kopplin, P., Perdue, E.M., 2008. Natural organic matter and the event horizon of mass spectrometry. *Anal. Chem.* 80, 8908–8919.

Hertkorn, N., Harir, M., Koch, B.P., Michalke, B., Schmitt-Kopplin, P., 2013. High-field NMR spectroscopy and FTICR mass spectrometry: powerful discovery tools for the molecular level characterization of marine dissolved organic matter. *Biogeosciences* 10, 1583–1624.

Hong, Z., Zhang, Y., Zou, Z., Zhu, R., Gao, Y., 2015. Influences of Domoic acid exposure on cardiac development and the expression of cardiovascular relative genes in zebrafish (*Daniorerio*) embryos. *J. Biochem. Mol. Toxicol.* 29, 246–260.

Hopkinson, C.S., Vallino, J.J., 2005. Efficient export of carbon to the deep ocean through dissolved organic matter. *Nature* 433, 715–717.

Hopkinson, C.S., Vallino, J.J., Nolin, A., 2002. Decomposition of dissolved organic matter from the continental margin. *Deep Sea Res. II Top. Stud. Oceanogr.* 49, 4461–4478.

Jiang, S., Kuwano, K., Ishikawa, N., Yano, M., Takatani, T., Arakawa, O., 2014. Production of domoic acid by laboratory culture of the red alga *Chondria armata*. *Toxicon* 92, 1–5.

Kamjunke, N., von Tümpling, W., Hertkorn, N., Harir, M., Schmitt-Kopplin, P., Norf, H., Weitere, M., Herzsprung, P., 2017. A new approach for evaluating transformations of dissolved organic matter (DOM) via high-resolution mass spectrometry and relating it to bacterial activity. *Water Res.* 123, 513–523.

Kim, S., Kramer, R.W., Hatcher, P.G., 2003. Graphical method for analysis of ultrahigh-resolution broadband mass spectra of natural organic matter, the van Krevelen diagram. *Anal. Chem.* 75, 5336–5344.

Kirchman, D.L., Suzuki, Y., Garside, C., Ducklow, H.W., 1991. High turnover rates of dissolved organic carbon during a spring phytoplankton bloom. *Lett. Nat.* 352, 612–614.

Klunder, M.B., Laan, P., Middag, R., De Baar, H.J.W., van Ooijen, J.C., 2011. Dissolved iron in the Southern Ocean (Atlantic sector). *Deep. Res. Part II Top. Stud. Oceanogr.* 58, 2678–2694.

Koch, B.P., Kattner, G., 2012. Sources and rapid biogeochemical transformation of dissolved organic matter in the Atlantic surface ocean. *Biogeosciences* 9, 2597–2602.

Koch, B.P., Witt, M., Engbrodt, R., Dittmar, T., Kattner, G., 2005. Molecular formulae of marine and terrigenous dissolved organic matter detected by electrospray ionization Fourier transform ion cyclotron resonance mass spectrometry. *Geochim. Cosmochim. Acta* 69, 3299–3308.

Koch, B.P., Kattner, G., Witt, M., Passow, U., 2014. Molecular insights into the microbial formation of marine dissolved organic matter: recalcitrant or labile? *Biogeosciences* 11, 4173–4190.

Ksionzek, K.B., Lechtenfeld, O.J., McCallister, S.L., Schmitt-Kopplin, P., Geuer, J.K., Geibert, W., Koch, B.P., 2016. Dissolved organic sulfur in the ocean: biogeochemistry of a petagram inventory. *Science* 354, 456–459.

Kujawinski, E.B., Hatcher, P.G., Freitas, M.A., 2002. High-resolution fourier transform ion cyclotron resonance mass spectrometry of humic and fulvic acids: improvements and comparisons. *Anal. Chem.* 74, 413–419.

Lechtenfeld, O.J., Kattner, G., Flerus, R., McCallister, S.L., Schmitt-Kopplin, P., Koch, B.P., 2014. Molecular transformation and degradation of refractory dissolved organic matter in the Atlantic and Southern Ocean. *Geochim. Cosmochim. Acta* 126, 321–337.

Lefebvre, K.A., Silver, M.W., Coale, S.L., Tjeerdema, R.S., 2002. Domoic acid in planktivorous fish in relation to toxic *Pseudo-nitzschia* cell densities. *Mar. Biol.* 140, 625–631.

Lema, K.A., Latimier, M., Nézan, É., Fauchot, J., Le Gac, M., 2017. Inter and intra-specific growth and domoic acid production in relation to nutrient ratios and concentrations in *Pseudo-nitzschia*: phosphate an important factor. *Harmful Algae* 64, 11–19.

Li, Y., Harir, M., Uhl, J., Kanawati, B., Lucio, M., Smirnov, K.S., Koch, B.P., Schmitt-Kopplin, P., Hertkorn, N., 2017. How representative are dissolved organic matter (DOM) extracts? A comprehensive study of sorbent selectivity for DOM isolation. *Water Res.* 116, 316–323.

Liu, H., Kelly, M.S., Campbell, D.A., Dong, S.L., Zhu, J.X., Wang, S.F., 2007. Exposure to domoic acid affects larval development of king scallop *Pecten maximus* (Linnaeus, 1758). *Aquat. Toxicol.* 81, 152–158.

Louchouam, P., Opsahl, S., Benner, R., 2000. Isolation and quantification of dissolved lignin from natural waters using solid-phase extraction and GC/MS. *Anal. Chem.* 72, 2780–2787.

Ludwig, W., Probst, J.-L., Kempe, S., 1996. Predicting the oceanic input of organic carbon by continental erosion. *Glob. Biogeochem. Cycles* 10, 23–41.

Maldonado, M.T., Hughes, M.P., Rue, E.L., Wells, M.L., 2002. The effect of Fe and Cu on growth and domoic acid production by *Pseudo-nitzschia multiseries* and *Pseudo-nitzschia australis*. *Limnol. Oceanogr.* 47, 515–526.

Malviya, S., Scalco, E., Audic, S., Vincent, F., Veluchamy, A., Poulain, J., Wincker, P., Iudicone, D., de Vargas, C., Bittner, L., Zingone, A., Bowler, C., 2016. Insights into global diatom distribution and diversity in the world's ocean. *Proc. Natl. Acad. Sci.* 113, E1516–E1525.

Martin, J.L., Haya, K., Burridge, L.E., Wildish, D.J., 1990. *Nitzschia pseudodelicatissima* – a source of domoic acid in the Bay of Fundy, eastern Canada. *Mar. Ecol. Prog. Ser.* 67, 177–182.

McCabe, R.M., Hickey, B.M., Kudela, R.M., Lefebvre, K.A., Adams, N.G., Bill, B.D., Gulland, F.M.D., Thomson, R.E., Cochlan, W.P., Trainer, V.L., 2016. An unprecedented coastwide toxic algal bloom linked to anomalous ocean conditions. *Geophys. Res. Lett.* 43, 10,366–10,376.

Møller, E.F., Thor, P., Nielsen, T.G., 2003. Production of DOC by *Calanus finmarchicus*, *C. glacialis* and *C. hyperboreus* through sloppy feeding and leakage from fecal pellets. *Mar. Ecol. Prog. Ser.* 262, 185–191.

Pan, Y., Parsons, M.L., Busman, M., Moeller, P.D.R., Dortch, Q., Powell, C.L., Doucette, G.J., 2001. *Pseudo-nitzschia* sp. cf. *pseudodelicatissima* – a confirmed producer of domoic acid from the northern Gulf of Mexico. *Mar. Ecol. Prog. Ser*. 220, 83–92.

Piletska, E.V., Villoslada, F.N., Chianella, I., Bossi, A., Karim, K., Whitcombe, M.J., Piletsky, S.A., Doucette, G.J., Ramsdell, J.S., 2008. Extraction of domoic acid from seawater and urine using a resin based on 2-(trifluoromethyl)acrylic acid. *Anal. Chim. Acta* 610, 35–43.

Pitcher, G.C., Cembella, A.D., Krock, B., Macey, B.M., Mansfield, L., Probyn, T.A., 2014. Identification of the marine diatom *Pseudo-nitzschia multiseries* (Bacillariophyceae) as a source of the toxin domoic acid in Algoa Bay, South Africa. *African J. Mar. Sci.* 36, 523–528.

Pocklington, R., Milley, J.E., Bates, S.S., Bird, C.J., de Freitas, A.S.W., Quilliam, M.A., 1990. Trace determination of domoic acid in seawater and phytoplankton by high-performance liquid chromatography of the fluorenylmethoxycarbonyl (FMOC) derivative. *Int. J. Environ. Anal. Chem.* 38, 351–368.

Prince, E.K., Irmer, F., Pohnert, G., 2013. Domoic acid improves the competitive ability of *pseudo-nitzschia delicatissima* against the diatom *skeletonema marinoi*. *Mar. Drugs* 11, 2398–2412.

Quilliam, M.A., Wright, J.L.C., 1989. The amnesic shellfish poisoning mystery. *Anal. Chem.* 61, 1053A–1060A.

Rhodes, L., White, D., Shyre, M., Atkinson, M., 1996. *Pseudo-nitzschia* species isolated from New Zealand coastal waters: domoic acid production in vitro and links with shellfish toxicity. In: Yasumoto, T., Oshima, Y., Fukuyo, M. (Eds.), *Harmful and Toxic Algal Blooms.* Intergovernmental Oceanographic Commission of UNESCO, Paris, pp. 155–158.

Rhodes, L., Jiang, W., Knight, J., Adamson, K., Smith, V., Langi, V., Edgar, M., 2013. The genus *Pseudo-nitzschia* (Bacillariophyceae) in New Zealand: analysis of the last decade's monitoring data. N. Z. J. *Mar. Freshw. Res.* 47, 490–503.

Rue, E., Bruland, K., 2001. Domoic acid binds iron and copper: a possible role for the toxin produced by the marine diatom *Pseudo-nitzschia*. *Mar. Chem.* 76, 127–134.

Scharek, R., Tupas, L.M., Karl, D.M., 1999. Diatom fluxes to the deep sea in the oligo-trophic North Pacific gyre at Station ALOHA. *Mar. Ecol. Prog. Ser.* 182, 55–67.

Scholin, C.A., Gulland, F., Doucette, G.J., Benson, S., Busman, M., Chavez, F.P., Cordaro, J., DeLong, R., De Vogelaere, A., Harvey, J., Haulena, M., Lefebvre, K.A., Lipscomb, T., Loscutoff, S., Lowenstine, L.J., Marin, R., Miller, P.E., McLellan, W.A., Moeller, P.D.R., Powell, C.L., Rowles, T., Silvagni, P., Silver, M., Spraker, T., Trainer, V., Van Dolah, F.M., 2000. Mortality of sea lions along the central California coast linked to a toxic diatom bloom. *Nature* 403, 80–84.

Sekula-Wood, E., Schnetzer, A., Benitez-Nelson, C.R., Anderson, C., Berelson, W.M., Brzezinski, M.A., Burns, J.M., Caron, D.A., Cetinic, I., Ferry, J.L., Fitzpatrick, E., Jones, B.H., Miller, P.E., Morton, S.L., Schaffner, R.A., Siegel, D.A., Thunell, R., 2009. Rapid downward transport of the neurotoxin domoic acid in coastal waters. *Nat. Geosci.* 2, 272–275.

Silver, M.W., Bargu, S., Coale, S.L., Benitez-Nelson, C.R., Garcia, A.C., Roberts, K.J., Sekula-Wood, E., Bruland, K.W., Coale, K.H., 2010. Toxic diatoms and domoic acid in natural and iron enriched waters of the oceanic Pacific. *Proc. Natl. Acad. Sci.* 107, 20762–20767.

Skrabal, S.A., Donat, J.R., Burdige, D.J., 2000. Pore water distributions of dissolved copper and copper-complexing ligands in estuarine and coastal marine sediments. *Geochim. Cosmochim. Acta* 64, 1843–1857.

Smith, J.C., Odense, P., Angus, R., Bates, S.S., Bird, C.J., Cormier, P., de Freitas, A.S.W., Léger, C., O'Neil, D., Pauley, K., Worms, J., 1990. Variation in domoic acid levels in *Nitzschia* species: implications for monitoring programs. *Bull. Aquac. Assoc. Can.* 90, 27–31.

Smith, J., Gellene, A.G., Hubbard, K.A., Bowers, H.A., Kudela, R.M., Hayashi, K., Caron, D.A., 2018. *Pseudo-nitzschia* species composition varies concurrently with domoic acid concentrations during two different bloom events in the Southern California bight. *J. Plankton Res.* 40, 1–17.

Stenson, A.C., Landing, W.M., Marshall, A.G., Cooper, W.T., 2002. Ionization and fragmentation of humic substances in electrospray ionization Fourier transform- ion cyclotron resonance mass spectrometry. *Anal. Chem.* 74, 4397–4409.

Stenson, A.C., Marshall, A.G., Cooper, W.T., 2003. Exact masses and chemical formulas of individual Suwannee River fulvic acids from ultrahigh resolution electrospray ionization Fourier transform ion cyclotron resonance mass spectra. *Anal. Chem.* 75, 1275–1284.

Stewart, J.E., Marks, L.J., Gilgan, M.W., Pfeiffer, E., Zwicker, B.M., 1998. Microbial utilization of the neurotoxin domoic acid: blue mussels (*Mytilus edulis*) and soft shell clams (*Mya arenaria*) as sources of the microorganisms. *Can. J. Microbiol.* 44, 456–464.

Subba Rao, D.V., Quilliam, M.A., Pocklington, R., 1988. Domoic acid – a neurotoxic amino acid produced by the marine diatom *Nitzschia pungens* in culture. *Can. J. Fish. Aquat. Sci.* 45, 2076–2079.

Takemoto, T., Daigo, K., 1958. Constituents of *Chondria armata*. *Chem. Pharm. Bull.* 6, 578–580.

Tammilehto, A., Nielsen, T.G., Krock, B., Møller, E.F., Lundholm, N., 2012. *Calanus* spp.- vectors for the biotoxin, domoic acid, in the Arctic marine ecosystem? *Harmful Algae* 20, 165–174.

Tammilehto, A., Nielsen, T.G., Krock, B., Møller, E.F., Lundholm, N., 2015. Induction of domoic acid production in the toxic diatom *Pseudo-nitzschia seriata* by calanoid copepods. *Aquat. Toxicol.* 159, 52–61.

Taylor, B.B., Torrecilla, E., Bernhardt, A., Taylor, M.H., Peeken, I., Röttgers, R., Piera, J., Bracher, A., 2011. Bio-optical provinces in the eastern Atlantic Ocean and their biogeographical relevance. *Biogeosciences* 8, 3609–3629.

Trainer, V.L., Adams, N.G., Bill, B.D., Anulacion, B.F., Wekell, J.C., 1998. Concentration and dispersal of a *Pseudo-nitzschia* bloom in Penn Cove, Washington, USA. *Nat. Toxins* 6, 113–126.

Trainer, V.L., Adams, N.G., Bill, B.D., Stehr, C.M., Wekell, J.C., Moeller, P., Busman, M., Woodruff, D., 2000. Domoic acid production near California coastal upwelling zones, June (1998). *Limnol. Oceanogr.* 45, 1818–1833.

Trainer, V.L., Wells, M.L., Cochlan, W.P., Trick, C.G., Bill, B.D., Batgh, K.A., Beall, B.F., Herndon, J., Lundholm, N., 2009. An ecological study of a massive bloom of toxigenic *Pseudo-nitzschia cuspidata* off the Washington State coast. *Limnol. Oceanogr*. 54, 1461–1474.

Trainer, V.L., Bates, S.S., Lundholm, N., Thessen, A.E., Cochlan, W.P., Adams, N.G., Trick, C.G., 2012. *Pseudo-nitzschia* physiological ecology, phylogeny, toxicity, monitoring and impacts on ecosystem health. *Harmful Algae* 14, 271–300.

Trick, C.G., Bill, B.D., Cochlan, W.P., Wells, M.L., Trainer, V.L., Pickell, L.D., 2010. Iron enrichment stimulates toxic diatom production in high-nitrate, low-chlorophyll areas. *Proc. Natl. Acad. Sci.* 107, 5887–5892.

Trick, C.G., Trainer, V.L., Cochlan, W.P., Wells, M.L., Beall, B.F., 2018. The successional formation and release of domoic acid in a *Pseudo-nitzschia* bloom in the Juan de Fuca Eddy: a drifter study. *Harmful Algae* 79, 105–114.

Umhau, B.P., Benitez-Nelson, C.R., Anderson, C.R., McCabe, K., Burrell, C., 2018. A time series of water column distributions and sinking particle flux of *Pseudo-Nitzschia* and domoic acid in the Santa Barbara Basin, California. *Toxins* 10, 480.

Van Meerssche, E., Pinckney, J.L., 2017. The influence of salinity in the domoic acid effect on estuarine phytoplankton communities. *Harmful Algae* 69, 65–74.

Walter, J.A., Leek, D.M., Falk, M., 1992. NMR study of the protonation of domoic acid. *Can. J. Chem.* 70, 1156–1161.

Wang, Z., King, K.L., Ramsdell, J.S., Doucette, G.J., 2007. Determination of domoic acid in seawater and phytoplankton by liquid chromatography-tandem mass spectrometry. *J. Chromatogr. A* 1163, 169–176.

Wekell, J.C., Gauglitz, E.J., Bamett, H.J., Hatfield, C.L., Simons, D., Ayres, D., 1994. Occurrence of domoic acid in Washington State razor clams (*Siliqua patula*) during 1991–1993. *Nat. Toxins* 2, 197–205.

Wells, M.L., Trick, C.G., Cochlan, W.P., Hughes, M.P., Trainer, V.L., 2005. Domoic acid: the synergy of iron, copper, and the toxicity of diatoms. Limnol. Oceanogr. 50, 1908–1917.

Wright, J.L.C., Boyd, R.K., de Freitas, A.S.W., Falk, M., Foxall, R.A., Jamieson, W.D., Laycock, M.V., McCulloch, A.W., McInnes, A.G., Odense, P., Pathak, V.P., Quilliam, M.A., Ragan, M.A., Sim, P.G., Thibault, P., Walter, J.A., Gilgan, M., Richard, D.J.A., Dewar, D., 1989. Identification of domoic acid, a neuroexcitatory amino acid, in toxic mussels from eastern Prince Edward Island. *Can. J. Chem.* 67, 481–490.

Zhang, W., Lin, M., Tong, P., Lu, Q., Zhang, L., 2016. Ferrite nanospheres-based magnetic solid-phase extraction for determination of domoic acid in seawater samples using high-performance liquid chromatography with tandem mass spectrometry. *J. Chromatogr. A* 1443, 54–61.

4 Manuscript II

Sources and distribution of dissolved domoic acid and molecular fingerprints in Arctic fjord systems at different states of glaciation

Jana K. Geuer[*1], Frederik Bussmann[1], Sylke Wohlrab[1,2], Claudia Burau[1,3], Mourad Harir[4], Philippe Schmitt-Kopplin[4], Tim Leefmann[1,‡5], Urban Wünsch[6, ‡7], Bernd Krock[1], Uwe John[1,2], Nancy Kühne[1], Boris P. Koch[1,3]

[1]Alfred Wegener Institute Helmholtz Centre for Polar- and Marine Research, Bremerhaven, Germany

[2]Helmholtz Institute for Functional Marine Biodiversity, University of Oldenburg, Germany

[3]Department of Technology, University of Applied Sciences Bremerhaven, Bremerhaven, Germany

[4]Helmholtz Zentrum München, German Research Center for Environmental Health, Germany

[5]Helmholtz Zentrum Geesthacht, Centre for Materials and Coastal Research, Germany

[6]Technical University of Denmark

[7]Chalmers University of Technology, Sweden

*Corresponding author: jana.geuer@awi.de, ‡Currently at

Keywords:

- *Pseudo-nitzschia*
- water masses
- FT-ICR-MS
- dissolved organic matter
- toxin
- glacier
- stratification
- *Nitzschia*
- DNA
- RNA

4.1 Abstract

The production and release of domoic acid (DA), a neurotoxic amino acid, produced primarily by different species of the diatom *Pseudo-nitzschia*, depends on environmental factors. *Pseudo-nitzschia* species are known to occur all over the Arctic Ocean and contribute to local phytoplankton blooms. Arctic water influences Arctic fjords to different extents depending on their morphology in summer, once the sea ice starts melting. Dissolved domoic acid (dDA) seems to be a comparatively persistent molecule that contributes to the pool of marine dissolved organic matter (DOM) and was ubiquitously detected in the Eastern Atlantic and the Southern Ocean. So far, dDA has not been assessed in Arctic fjord systems. This study aimed at (i) determining the connection between dDA, the abundance of *Pseudo-nitzschia*, chlorophyll *a* and macronutrient availability, (ii) testing whether the amount of dDA, pDA and *Pseudo-nitzschia* correlate, (iii) comparing species determination and counts by light microscopy and DNA barcoding and (iv) detecting the DA biosynthesis gene cluster. Moreover, we tested whether dDA as a contributor to DOM and chemical fingerprints differed by water mass in the studied fjord systems. dDA occurred throughout the study area and matched well with pDA, microscopic *Pseudo-nitzschia* cell counts and genetic identifications, particularly where dDA concentrations were high. Low phosphate and silicate concentrations are likely connected to high dDA concentrations. Due to limited resolution within the *Pseudo-nitzschia* species complex in the reference database, it was not possible to exactly resolve species composition with the genomic data. However, we could show that DA was actively produced where its concentrations were particularly high, as we found gene activity involved in DA biosynthesis. In highly stratified water columns, DOM can be chemically distinguished, particularly if glacial discharge was high. Our results suggest that warming might influence *Pseudo-nitzschia* blooms and the release of dDA in the future.

4.2 Introduction

The neurotoxic tricarboxylic amino acid domoic acid (DA) is known as main cause for amnesic shellfish poisoning and is primarily produced by the diatom genera *Pseudo-nitzschia* and *Nitzschia* (Bates et al., 1989). Particulate DA (pDA) accumulates in higher trophic levels and is thus an important measure for the toxicity of DA (Silvert and Subba Rao, 1992). During toxic blooms, however, dissolved DA (dDA) is also an important contributor to total DA levels (Umhau et al., 2018) and we previously found dDA in throughout the Eastern Atlantic Ocean (Geuer et al., 2019). Production and release of DA are dependent on different environmental parameters such as salinity,

macronutrient and trace metal availability and exudates of predatory organisms (Ayache et al., 2019; Maldonado et al., 2002; Pan et al., 1996a; Tammilehto et al., 2015). While the ecological function of DA is not fully understood, dDA is known to have an impact on its environment by reducing grazing rates of predators (Bargu et al., 2006) and inhibiting growth of other phytoplankton in combination with low iron concentrations and extreme salinities (Prince et al., 2013; Van Meerssche and Pinckney, 2017).

4.2.1 *Pseudo-nitzschia, Nitzschia* and domoic acid production in the Arctic Ocean

Algae of the genus *Pseudo-nitzschia* are mostly euryhaline (Ayache et al., 2019) and occur ubiquitously in the global ocean, including the Arctic Ocean and its marginal regions. For example, *P. delicatissima, P. pungens, P. pseudodelicatissima, P. seriata,* and *P. granii* have been found in the Chukchi Sea (Von Quillfeldt et al., 2003) and *P. obtusa, P. arctica,* and *P. delicatissima* were discovered in Disko Bay (west Greenland) (Harðardottir et al., 2015; Lundholm et al., 2018). Species of the genus *Nitzschia* also occur in the Arctic (Johnsen et al., 2018; Kauko et al., 2018; Leu et al., 2015) with the species *N. frigida* being distributed broadest (Leu et al., 2015). Other species include *N. arctica*, *N. polaris*, *N. promare*, *N. pellucida*, *N. neofrigida*, *N. longissima*, *N. laevissima* (Melnikov, 2018; Melnikov et al., 2002). However, among these Arctic *Nitzschia* species, to the best of our knowledge, there are no records of DA production.

Whether *Pseudo-nitzschia* produces DA depends on the species, strains and regional biogeochemical setup and grazing pressure. *P. seriata* at the Greenland west coast was found to produce pDA in amounts of up to 0.0062 pg cell^{-1} and may thus cause amnesic shellfish poisoning (Hansen et al., 2011). DA production increases in the presence of grazers (Lundholm et al., 2018; Tammilehto et al., 2015) as shown for the species *P. obtusa* (Harðardottir et al., 2015). In addition, DA production varies regionally: *P. arctica* and *P. delicatissima* from Disko Bay did not produce DA (Lundholm et al., 2018) but *P. delicatissima* were reported to express DA at the US West Coast (Fuentes and Wikfors, 2013).

Recently the metabolic pathway leading to the precursor molecules necessary for DA synthesis was uncovered (Harðardóttir et al., 2019). Furthermore, a cluster of four genes encoding enzymes that are involved in DA biosynthesis (DAb) was unravelled. Three of the enzymes DAbA, C and D were shown to be involved in the formation of DA. They perform oxidations and cyclisation, while DAbB encodes a hypothetical

protein (Brunson et al., 2018). The responsible gene cluster has, however, not yet been detected in the field.

4.2.2 Arctic fjords: Primary productivity, water masses and chemical fingerprints

Arctic fjord systems are subject to global warming due to increased freshwater discharge. In the Eurasian Arctic, the Svalbard archipelago is one of the main fjordic regions. In addition, the entire coastline of Greenland is dominated by fjords due to glaciological action (Cottier et al., 2010). In our study, we compared three different fjord systems (Kongsfjorden on the west coast of Spitzbergen, Scoresby Sund on the east coast of Greenland and Arnarfjörður in the northwest of Iceland) differing in size, glacier volume and freshwater input (Koch et al., 2017) and which undergo drastic seasonal changes. In summer months, the West Spitzbergen Current (WSC) flows northwards on the eastern side of the Fram Strait, transporting comparatively warm water (Haugan, 1999). On the western side, the East Greenland Current (EGC), which is cold and low in salinity, flows southward (Aagaard and Coachman, 1968). Kongsfjorden is dominated by Arctic water in winter, which changes to Atlantic dominance in summer by advection of Atlantic water (AW) across the shelf (Svendsen et al., 2002). The inflow of AW is closely related to onset of spring blooms and seems to be the main controlling factor (Hegseth and Tverberg, 2013). With its vulnerability to climate changes and the large number of scientific studies, Kongsfjorden is an important Arctic monitoring site (Hop et al., 2002; Svendsen et al., 2002). The Scoresby Sund and its northernmost branch called Nordvestfjord constitute the longest fjord in the world that is heavily influenced by iceberg formation and glacial meltwater. Icebergs are particularly released by the Daugaard-Jensen Glacier that terminates at the head of Nordvestfjord (Dowdeswell et al., 1992). The Icelandic Arnarfjörður in contrast is much smaller and only about 100 m deep. Around June, summer stratification occurs in the fjord, when early spring coastal current and cold fjord water meet (Jónsdóttir, 2015). Cysts from the toxic phytoplankton *Alexandrium* occur in both Greenland and Iceland. Conditions found in fjords like Arnarfjörður are favourable for this diatom and may be for other toxic phytoplankton species as well (Richlen et al., 2016).

Dissolved organic carbon (DOC) concentration in the Arctic Ocean strongly varies between different water masses (Bussmann and Kattner, 2000). Beyond bulk analyses, Fourier Transform Ion Cyclotron Mass Spectrometry (FT-ICR-MS) has been applied to distinguish molecular patterns of marine dissolved organic matter (DOM) from different

sources (Hertkorn and Kettrup, 2005; Koch et al., 2005). In different layers of a water column (upper 2000 m of Mariana Trench), the molecular composition of DOM was highly stratified (Li et al., 2019). Although DOM composition from Svalbard fjords differs significantly from Pacific DOM, it was suggested that DOM from local blooms in Arctic fjords turns over quickly, without leaving a seasonal imprint on the molecular DOM composition (Osterholz et al., 2014).

4.2.3 Objectives

In a recent study, we found that dissolved domoic acid ubiquitously occurs in the Eastern Atlantic and in the iron depleted Atlantic Sector of the Southern Ocean (Geuer et al., 2019) but so far, there are no records on dDA in Arctic fjords. In Kongsfjorden, *Pseudo-nitzschia* spp. have been found before (Hegseth et al., 2019; Rytter Hasle and Riddervold Heimdal, 1998) but there are no records of DA producing *Pseudo-nitzschia* species in Scoresby Sund and the inside of Arnarfjörður, even though they are broadly distributed in the Arctic Ocean, can contribute to local phytoplankton blooms and occur at the south and west of Iceland in warmer waters (Jiang et al., 2001; Lundholm et al., 2003). Moreover, we hypothesize that (i) dDA concentrations correlate with the cell abundance of *Pseudo-nitzschia* species and chlorophyll *a* concentrations and inversely with macronutrients in the study area, (ii) pDA is highest where dDA and *Pseudo-nitzschia* cell abundances are highest and that (iii) microscopic cell counts match DNA barcodes for *Pseudo-nitzschia* species at the respective stations. Moreover, we aimed at detecting the DA biosynthesis gene cluster (iv). dDA is a comparatively persistent contributor to DOM (Geuer et al., 2019) and thus leaves an imprint in the chemical signature of the water. This led us to test if biogeochemical processes in general leave chemical fingerprints that are suitable to differentiate fjords and their water masses.

4.3 Materials and Methods

4.3.1 Study area

Samples were collected during a cruise (MSM56, July 2016 on RV Maria S. Merian) to three Arctic fjords: Kongsfjorden at the west coast of Spitzbergen, Scoresby Sund at the eastern coast of Greenland and Arnarfjörður in the northwest of Iceland (Fig. 1).

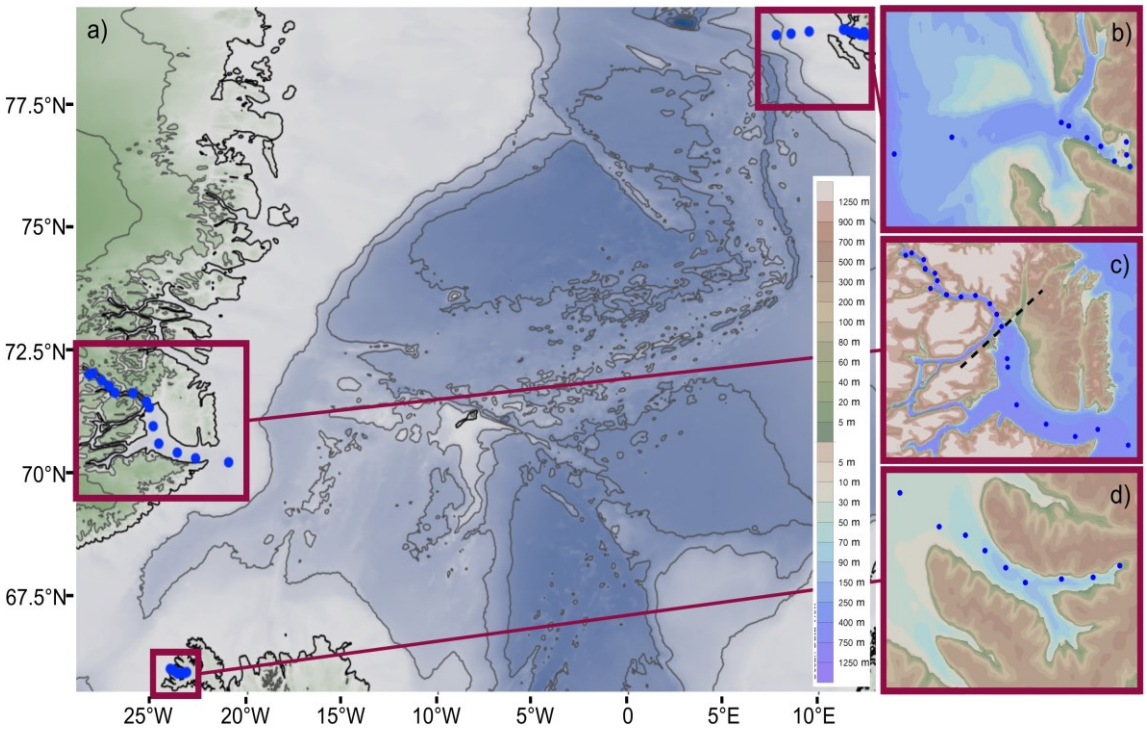

Figure 1: a) Sampling area of MSM 56. Three different Arctic fjords were sampled. The fjords sampled were b) Kongsfjorden (Spitzbergen), c) Scoresby Sund (east Greenland), with divided into outer Scoresby Sund and the inner branch Nordvestfjord (divided by dotted black line) and d) Arnarfjörður (northwest of Iceland). Blue dots represent stations. The colour scale shows the fjord's bathymetry.

4.3.1.1 Kongsfjorden

In the inner Kongsfjorden (Fig. 1b), glacial outflow leads to an increase of zooplankton mortality and a reduction of primary production. These glacial effects, however, diminish close to the outer fjord (Hop et al., 2002). The fjord has steep physical gradients and is subject to seasonal environmental changes, tides, glacial run-off and local winds (Svendsen et al., 2002). Spring blooms start with breakup of the ice and are either dominated by diatoms or by *Phaeocystis* in Arctic or Atlantic water, respectively. In 2012, the bloom was first diatom dominated and later *Phaeocystis* dominated. In the post bloom stage, nutrients, primary production and phytoplankton biomass are low (Hodal et al., 2012).

Relative warm and saline AW from the WSC flows into Kongsfjorden during late summer at intermediate depth (Tverberg et al., 2019, Table 1). The relatively warm surface of the WSC is dependent on season and can reach up to 7 °C, while in deep regions of 800 m temperature is below 2 °C with a salinity of ~35 (Aagaard and Coachman, 1968).

4.3.1.2 Scoresby Sund

The EGC flows from north southwards along the east Greenland coast and consists of three water masses. Polar water (PW) (around 0 °C) can reach salinities below 30 in the surface and up to 34 at the bottom. Atlantic Intermediate Water (warmer than 0 °C, salinities of up to 35), which is usually found below PW, reaches into depths of up to 800 m. Below 800 m, Deep Water of below 0 °C with salinities between 34.9 and 35.0 can be found (Aagaard and Coachman, 1968).

The Scoresby Sund is a fjord system located on the east coast of Greenland. From the outer fjord the inner fjord branches off into several smaller fjords (Fig. 1c). Water depths of the outer fjord range between 200 and 650 m, while the deeper inner fjord is 800 to 1600 m deep. The Daugaard-Jensen Glacier within Nordvestfjord has been described as one of the most productive outlet glaciers of the Greenland ice sheet and one of the most important sources of icebergs in Scoresby Sund (Dowdeswell et al., 1992; Reeh and Olesen, 1986). Location and distribution of icebergs are influenced by their source as well as topography and bathymetry of the fjord system and their density decreases with increasing distance from the Daugaard-Jensen Glacier (Dowdeswell et al., 1992). The ice velocity of the glacier remained constant between 1996 to 2005 (Rignot and Kanagaratnam, 2006). The biogeochemical regimes differ between outer Scoresby Sund and Nordvestfjord: In the outer fjord, productivity is high due to the input of nutrient from AW and PW from the shelf and the less pronounced surface meltwater influence. The inner Nordvestfjord is greatly influenced by the drainage of glaciers, which supplies silicate (but no other macronutrients) and forms a freshwater layer at the surface of the fjord (Table 1).

4.3.1.3 Arnarfjörður

From the south of Iceland, AW flows north around Iceland and mixes with PW (Marine and Malmberg, 1999). Cold and low salinity PW is derived from Greenland and Arctic water from the northeast of Iceland, where both mix with warm saline AW to form Icelandic coastal water (Stefánsson and Ólafsson, 1991).

The water column in Arnarfjörður is strongly stratified in summer, with a 40 m thick layer of 7-8 °C and a salinity of 34.35 – 34.45 at the surface and 3 °C with a salinity of 34.5 at the bottom (Table 1) while in September to October surface waters cool down, start to sink and cause mixing of the fjords water column. This subsequently leads to increased productivity since the water is oxygenated and nutrient-rich (Jónsdóttir, 2015). Temperatures between 2-12 °C in Arnarfjörður were previously observed in July

(Richlen et al., 2016). Within Arnarfjörður, aquaculture farms for salmonids are located (Karbowski et al., 2019).

4.3.2 Water and dissolved organic matter sampling

Water samples were taken with a water rosette equipped with Niskin bottles, a CTD (conductivity, temperature, depth) sensor (SBE11plus Deck Unit with SBE9 sensors, Sea-Bird Scientific, Germany), and a chlorophyll *a* fluorescence sensor (ECO- AFL/FL, WET Labs, Sea-Bird Scientific). Water samples were collected at the water surface, in the chlorophyll maximum and at depths of 20, 40, 100, 200, 1000 m, and ~ 10 m above bottom depth.

For each DOM sample, 1 L seawater was collected in borosilicate bottles (Schott AG, Germany). Samples were filtered through combusted glass fibre filters (Whatman GF/F, 0.7 µm, Sigma-Aldrich, Germany). Samples for DOC were either taken from this filtrate or filtered via syringe filters if no solid phase extraction (SPE) was performed for the respective sample. In that case, a pre-cleaned syringe with a syringe filter (Whatman, GF/F, 0.7 µm, Sigma-Aldrich) was used and 50 mL sample passed the filter for conditioning before the actual samples were filtered. Until analysis, the samples were stored at -20 °C in 50 mL high-density polyethylene bottles (VWR, Germany) that were pre-cleaned in an acid bath and subsequently rinsed thoroughly with ultrapure water (UPW, MilliQ, Merck Millipore, Merck KGaA, Germany).

The remaining filtrate was acidified to pH 2 using hydrochloric acid (HCl, Suprapur®, Sigma-Aldrich). For SPE (Dittmar et al., 2008), cartridges filled with a styrene-divinylbenzene polymer (PPL, 200 mg, Agilent Technologies GmbH, Germany) were first conditioned with 6 mL of methanol (LiChrosolv, Merck KGaA) and 6 mL of acidified (pH 2) UPW. 500 mL of the sample were extracted at a flow rate of < 4 mL min^{-1}. Subsequently, the cartridges were washed with 6 mL of acidified UPW to remove salts. The cartridges were dried under a stream of nitrogen gas and stored in combusted aluminium foil at -20 °C until further processing. Before elution, empty combusted screw top vials (Agilent Technologies GmbH) were weighed. Then 500 µL of methanol were used to elute the samples from the cartridge into the vials. When the 500 µL were soaked up by the cartridge matrix, another 500 µL were added on top. Nitrogen gas was used to apply a slight pressure to ensure a collection of most of the methanol used for elution. Samples were stored at -20 °C to prevent esterification by methanol (Flerus et al., 2011).

High-temperature catalytic oxidation and subsequent non-dispersive infrared spectroscopy and chemiluminescence detection (TOC-$L_{CPH/CPN}$, Shimadzu, Germany)

was used to determine concentrations of DOC and total dissolved nitrogen (TDN) in the water samples. On each day of analysis, samples were thawed and subsequently homogenised thoroughly. In the autosampler, 6.5 mL per sample were acidified with 1 M HCl (Suprapur®, Sigma-Aldrich) and sparged with oxygen to remove inorganic carbon. 50 µL of sample was injected on the catalyst (680 °C) in triplicate yielding average concentrations. Additional injections were performed if the standard variation or the coefficient of variation exceeded 1%, respectively. A potassium hydrogen phthalate standard, UPW and a deep-sea reference sample (Hansell Laboratory, University of Miami, USA) were measured after every batch of six samples. The limit of quantification (LOQ) was 7 µM for DOC and 11 µM for TDN and the accuracy of the method was ± 5%.

DOC and TDN were also determined in the extracted samples (DOC_{SPE}). 130 µL were evaporated under a stream of nitrogen gas and subsequently dissolved in 6.5 mL UPW and sonicated for 15 min. Quantification was equal to water samples. DOC_{SPE} was calculated using the enrichment factor (EF) and volume of extract used (V_E) and the volume of UPW used for redissolving the sample (V_{UPW}):

$$DOC_{SPE} = DOC \Big/ \frac{EF}{V_{UPW}/V_E} \quad (1)$$

4.3.3 Nutrients

From the CTD rosette, inorganic nutrient samples were collected in 50 mL low-density polyethylene (PE) bottles (VWR) and stored at -20 °C until further analysis. Nitrate, phosphate and silicate concentrations were determined by a spectrophotometric autoanalyzer (QuAAtro39, SEAL Analytical, Germany) using standard methods (Kattner and Becker, 1991) applied and modified by the manufacturer (coefficient of variation = 0,3%). Limit of detection (LOD) was 0.01 µM for phosphate, 0.02 µM for silicate and 0.03 µM for nitric oxides. Concentrations were calibrated against certified reference material (NMIJ CRM 7602-a, National Metrology Institute of Japan).

4.3.4 Water mass determination

Salinity and temperature were measured using the CTD sensor and used to assign different water masses in our study area (Table 1). To verify the water masses identified, the potential temperature (θ) was calculated according to Fofonoff and Millard (1983) as well as the potential density (σ_θ) (package “oce”, R).

Table 1: Water masses in the different fjords including their abbreviations. The ranges of temperature (T) and salinity for each water mass are shown. Water masses with no reference have been assigned in this study.

Origin	Name	Abbr.	T (°C)	Salinity	Reference
Kongs-fjorden	Surface water	SW	1.0 - 7.0	30.0 - 34.0	(Tverberg et al., 2019)
	Intermediate water	IW	1.0 - 7.0	34.0 - 34.7	(Tverberg et al., 2019)
	Transformed Atlantic water	TAW	1.0 - 7.0	34.7 - 34.9	(Tverberg et al., 2019)
	Atlantic water	AW	3.0 - 7.0	34.9 - 35.2	(Tverberg et al., 2019)
	Cold Atlantic water	CAW	< 3.0	> 34.9	(Tverberg et al., 2019)
Scoresby Sund	Glacial meltwater	GMW		< 20	
	Surface glacial water	SGW		25.0 - 33.0	(Seifert et al., 2019)
	Modified polar water	MPW	-1 - 1	33.0 - 34.7	(Seifert et al., 2019)
	Polar water	PW	< -1	33.0 - 34.2	(Seifert et al., 2019)
	Atlantic water	AW	> 1	> 34.6	(Seifert et al., 2019)
	Greenland Sea deep water	GSDW	< 1	> 34.8	(Seifert et al., 2019)
Arnar-fjörður	Surface water	SW	> 7.0	33.5 - 34.6	(Jónsdóttir, 2015)
	Intermediate water	IW	5.0 - 7.0	34.4 - 34.5	
	Bottom water	BW	< 3	~ 34.5	(Jónsdóttir, 2015)

4.3.5 Domoic acid

dDA was quantified as described previously (Geuer et al., 2019). Reversed phase ultrahigh performance liquid chromatography (RP-UPLC, ACQUITY, Waters GmbH, Germany) with tandem mass spectrometry (MS/MS, Xevo TQ-XS, Waters) using electrospray ionisation in positive mode was used. Mobile phases were 20 mmol L^{-1} ammonium formate (Riedel-de Haën AG, Germany) buffer at 5.8 pH (formic acid, Merck KGaA) as mobile phase A and 100% acetonitrile as mobile phase B (LiChrosolv, Merck KGaA). A gradient was run from 0 to 3.5 min changing from 99% to 5% mobile phase A. From 3.5 to 4.3 min, mobile phase A increased to 99% which was subsequently kept until 4.5 min. Quantification of dDA was performed with mass transitions m/z 312 > 266 for quantification and m/z 312 > 193 as quality control. LOD and LOQ were determined by standard addition using a sample containing no DA and final concentrations of 0.25, 0.5, 1.0, 5.0, 10.0 µg DA L^{-1} (performed in quintuplets). Considering the average enrichment factor of 776, the resulting LOD and LOQ was 6 pmol DA L^{-1} and 18 pmol DA L^{-1}, respectively. LOD, LOQ, DA carbon yield and the carbon weighed relative summed peak intensities for the molecular formula of DA was calculated according to Geuer et al. (2019).

pDA was quantified as described in Wohlrab et al. (2019) from integrated plankton net hauls from 30 to 0 m water depth. Contents of the plankton net hauls were collected and diluted with sterile filtered seawater to a volume of 2 L. The sample was filtered over a gaze gravity filter tower with a sequence of meshes (200 µm – 20 µm). The collected particles were back flushed with 45 mL sterile filtered seawater from which a subset of 15 mL was used for the analysis of lipophilic phycotoxins. After centrifuging, the supernatant was removed, the pellet was resuspended in 500 µL methanol, homogenized by reciprocal shaking with ceramic beads (Lysing Beads Matrix D, MP Biomedicals, USA), and filtered by centrifugation with spin filters (0.45 µm pore size, Millipore, Merck KGaA). Samples were analysed via liquid chromatography (LC 1100 Agilent) coupled to a Sciex API 4000QTrap hybrid triple quadrupole-linear ion trap mass spectrometer (AB Sciex Germany GmbH, Germany). A C8 phase (50 × 2 mm, 3 µm Hypersil BDS 120 Å (Phenomenex, Germany)) at 20 °C was used for separation. A gradient elution was performed using an aqueous buffer A and a mixture of acetonitrile/water (95:5 v/v) with 2.0 mM ammonium formate and 50 mM formic acid in both solvents. DA was detected in positive mode with a detection limit of 2248 pg μL^{-1} in extract.

4.3.6 Phytoplankton counts and species identification

Plankton community samples for species identification and counting were taken from the upper five CTD depths within the upper 30 m of the water column. The samples were preserved using a glutardialdehyde/formaldehyde solution for later analysis. Light microscopy was used to analyse and count fixed samples by the Institute of Oceanology of the Polish Academy of Sciences, Sopot, Poland.

Samples for RNA and DNA extraction were taken from distinct size classes, i.e. 20-50 µm and 3-20 µm. Samples for the size class 20-50 µm were integratively sampled from the surface (1 to 30 m) through a hose connected to a shipboard membrane pump (QBY-25- SS; AGB-Pumpen, Germany). In total, 60 L of seawater per depth and sampling station were passed over a sequential filter tower with progressively decreasing nylon mesh-sizes (200, 50, and 20 µm) to obtain the distinct plankton size-fractions. RNA and DNA samples for the size class of 3-20 µm were taken at distinct depths (3 m, 30 m, and the depth corresponding to the deep chlorophyll maximum) during CTD casts. Water samples were mixed (18 L), pre-filtered (20 µm) and then 15 L were passed over a 3 µm polycarbonate membrane filter (TSTP with a diameter of 142 mm, Millipore, USA) using a peristaltic pump. Retentates from

the filter tower were backwashed into centrifuge tubes with 0.2 µm-filtered seawater, adjusted to a total volume of 45 mL and split into three 15 mL aliquots.

Cell suspensions were centrifuged for 15 min at 3,600 x g at 4 °C, pellets for DNA analysis were resuspended in 700 µL SL1 lysis buffer (Macherey-Nagel, Germany), whereas pellets for RNA analysis were resuspended in Tri Reagent (Sigma Aldrich). Each sample was transferred to a microcentrifuge vial with 0.2 µm glass beads (Sigma Aldrich). Vials were shock-frozen in liquid nitrogen and kept at -20 °C (for DNA) or -80 °C (for RNA) until further processing. Polycarbonate filters were separated into quarters and one quarter was used for each DNA and RNA sample. Retentates from the polycarbonate filter were direct flushed into a 50 mL collection tube with 700 µL SL1 lysis buffer or 1 mL Tri Reagent for DNA or RNA analysis respectively, Resuspended filter retentates were transferred into microcentrifuge vial with 0.2 µm glass beads, shock-frozen in liquid nitrogen and kept at -20 °C (for DNA) or -80 °C (for RNA).

RNA was isolated after thawing the samples on ice. The cells were lysed in a homogeniser (MagNa Lyser, Roche, Germany), then chloroform was added to the samples, which were subsequently vortexed for 20 s. After 5 min incubation at room temperature, the samples were transferred into down spun Phase Lock tubes (2 mL heavy gel, Eppendorf, Germany) and incubated for another 5 min before centrifugation for 15 min at 12,000 x g. The upper aqueous phase was mixed well with 2 µL of 5 M linear acrylamide and 1:10 volume of 3 M sodium acetate (pH 5.2 - 5.5) before 1 volume of isopropanol (100%) was added and the samples incubated for 90 min at -20 °C. An RNA pellet was obtained by 20 min centrifugation at 12,000 x g. Then, the supernatant was removed from the pellet, and 1 mL of ethanol (70%) was added to wash the pellet by vortexing. After centrifugation (10 min, 12,000 x g) the liquid was removed and the pellet washed again with 1 mL of ethanol (96-99%) repeating the subsequent steps. The pellet was then air dried and resuspended in 10-30 µL of RNAse-free water.

A NanoDrop spectrophotometer (Thermo Fisher Scientific, Germany) was used to quantify RNA in the samples. Subsequently, its quality was assessed on a Bioanalyzer 2100 (Agilent Technologies GmbH). High quality RNA was used to generate cDNA libraries according to the manual provided with the TruSeq Stranded mRNA LibraryPrep Kit (Illumina GmbH, Germany). Briefly, the polyA containing mRNA was purified, fragmented and primed before first strand cDNA was synthesized. Then, the RNA template was degraded. For synthesis of the second cDNA strand, dUTP

nucleotides were used. The 3' ends were adenylated to prepare cDNA for adapter ligation, which possess single thymine nucleotides on the 3' end. These enabled ligation to the fragment. After ligation, dUTPs were enzymatically removed. Polymerase chain reaction (PCR) was used to amplify cDNA. The cDNA library produced was validated quantitatively (by Quantus Flourometer, Promega, Germany) and qualitatively (by DNA 7500 Chip assay with 2100 Bioanalyzer, Agilent Technologies GmbH). The samples were paired end sequenced by next-generation sequencing on an Illumina NextSeq 500 platform (Illumina Inc, San Diego, CA, USA). Raw reads were de-multiplexed and converted into FASTQ files with the bcl2fastq conversion software v2.20 (Illumina Inc). Reads were imported into the CLC Genomics Workbench v12 (Qiagen, Germany) and reads per station were aligned to the DA biosynthetic gene cluster from *Pseudo-nitzschia multiseries* isolate 15091C3 available at GenBank (accession MH202990) (Brunson et al., 2018).

DNA was extracted with the Genomic DNA from soil Kit (Macherey-Nagel) according to the manufactures protocol. DNA extracts were diluted to 5 ng mL^{-1} with 10 nM Tris pH 8.5 and the 18S rRNA gene V4 region was amplified in triplicates per sample with primers and PCR conditions published by Xiao et al. (2017). Metabarcoding libraries were prepared from pooled triplicated PCR products per sample according to the 16S Metagenomic Sequencing Library Preparation protocol by Illumina (Illumina Inc). The samples were sequenced on a 2 x 301 bp run on the Illumina MiSeq (Illumina Inc) with the 600 cycle Miseq® Reagent Kit v3 (Illumina Inc). Raw reads were de-multiplexed and converted into FASTQ files with the bcl2fastq conversion software v2.20 (Illumina Inc). Raw reads were assembled into *amplicon sequence variants* (ASV), high-resolution analogues to traditional operational taxonomic units (OTUs) with the R package Dada2 (Callahan et al., 2016). Primers were removed from the reads with Cutadapt (Martin, 2011) and ASVs were constructed, cleaned from chimera and taxonomically annotated following the guidelines of the Dada2 online tutorial (https://benjjneb.github.io/dada2/tutorial.html). ASVs resolve individual sequences without clustering and allow a high-resolution taxonomic assignment to them. The PR^2 database was used as reference for taxonomic assignment (del Campo et al., 2018). ASVs were filtered for taxonomic annotations belonging to *Pseudo-nitzschia* spp. and *Nitzschia* spp. The ASV sequences were used to construct a phylogenetic tree with the CLCGenomicsWorkbench v12 (Qiagen) with *Navicula* spp. as outgroup. ASV abundances of both size fractions (20 – 200 µm and 3 – 20 µm) were pooled, as the target species could be present in both. ASV abundances were normalized based on library size factors with the R package GMPR (Chen et al., 2018). Normalized counts

were graphically mapped to the phylogenetic tree with the R package phyloseq (McMurdie and Holmes, 2013).

4.3.7 Ultrahigh resolution mass spectrometry analysis and evaluation

Fourier-transform ion cyclotron resonance mass spectra (FT-ICR-MS) were analysed on a 12 T Bruker Solarix mass spectrometer (Bruker Daltonics GmbH, Germany) as described in Wünsch et al. (2018). A North Sea water lab standard (NSW) and UPW was measured after every tenth sample.

Data evaluation was based on the open-access software UltraMassExplorer (www.awi.de/en/ume; Leefmann et al., 2019). Molecular formulas were calculated in the range of 200 to 650 *m/z* with a mass accuracy threshold of ≤ ± 0.2 ppm for the formula assignment. For formula assignment, the elemental combinations $^{12}C_{0-\infty}$, $^{13}C_{0-1}$, $^{1}H_{0-\infty}$, $^{16}O_{0-\infty}$, $^{14}N_{0-2}$, $^{32}S_{0-1}$, and double bond equivalents (DBE) ≤ 20 were allowed. Formulas detected in the process blank (extracted UPW) and which were part of a list of potential surfactants (Lechtenfeld et al., 2013; Leefmann et al., 2019) were removed from the data set. Furthermore, formulas with a ^{13}C isotope not corresponding to a parent ^{12}C formula were also removed.

4.3.8 Statistical analyses

The software application RStudio® with the programming language R was used for all statistical tests. To test for normal distribution, the Shapiro-Wilk test was used. (Multiple) linear regression models were applied to test for linear correlations between two or more variables if the data was normally distributed. Kendall correlation was used to test for correlations between different non-normally distributed variables. If $p \leq 0.05$, significance was assumed. Differences between group means were assessed by analysis of variance. Alternatively, Wilcoxon signed-rank test was used if the data were not normally distributed.

To assess differences in DOM by water mass, bulk molecular parameters were calculated per sample based on the assigned formulas. These parameters comprised oxygen and hydrogen to carbon ratios, DBE, DBE per carbon and oxygen, molecular weight, and carbon number (O/C_w, H/C_w, DBE_w, DBE/C_w, DBE/O_w, MW_w, $\#C_w$) and were calculated intensity weighted as described previously (Koch et al., 2008; Sleighter and Hatcher, 2008). Bulk parameters were analysed with principal component (PC) analysis (PCA) (Li et al., 2019; Sleighter et al., 2010). Statistically significant differences between water masses were assessed by multivariate analysis of

variance (MANOVA) and analysis of similarities (ANOSIM) using the packages stats, vegan and ggbiplot.

4.4 Results

4.4.1 Morphology and physical oceanography

Both Kongsfjorden (26 km length, 350 m depth, 6 – 14 km width) and Arnarfjörður (30 km length, 100 m depth, 5 – 10 km width) were comparatively small in relation to Scoresby Sund, which is ~350 km long, 29 km wide at its mouth, and up to 1450 m deep. The spatial sampling resolution differed for each fjord and was highest in Kongsfjorden, followed by Arnarfjörður and Scoresby Sund (0.3, 0.2, and 0.1 stations/km, respectively).

In inner Kongsfjorden, the salinity showed a gradient from surface to bottom. Surface salinity was < 34 and strongly influenced by inflowing warm AW, which gradually mixed with the colder glacial influenced inner fjord water (Fig. 2a). At the deepest parts of the fjord (> 300 m), the water was cold and dense (T < 3 °C, sal > 34.9). Glacial influences were most prominent in Scoresby Sund. At the glacier's tongue in Nordvestfjord, salinity in the upper GMW was lowest in the cruise area (10 - 20). Nordvestfjord is narrower and deeper than the Outer Scoresby Sund and the glacial influence is higher on the surface water whereas AW dominates deep areas. Number of icebergs and surface salinity decrease closer to the fjord's mouth in Outer Scoresby Sund (Bach, 2016). AW, GSDW, and PW enter from the fjords mouth and can be found throughout the Outer Scoresby Sund (Fig. 2b). Arnarfjörður, in contrast, was completely ice-free and showed the warmest surface temperatures with up to 12 °C in the strongly stratified SW (Fig. 2c). In the inner fjord, salinity was only slightly lower (< 34) at the surface (< 20 m).

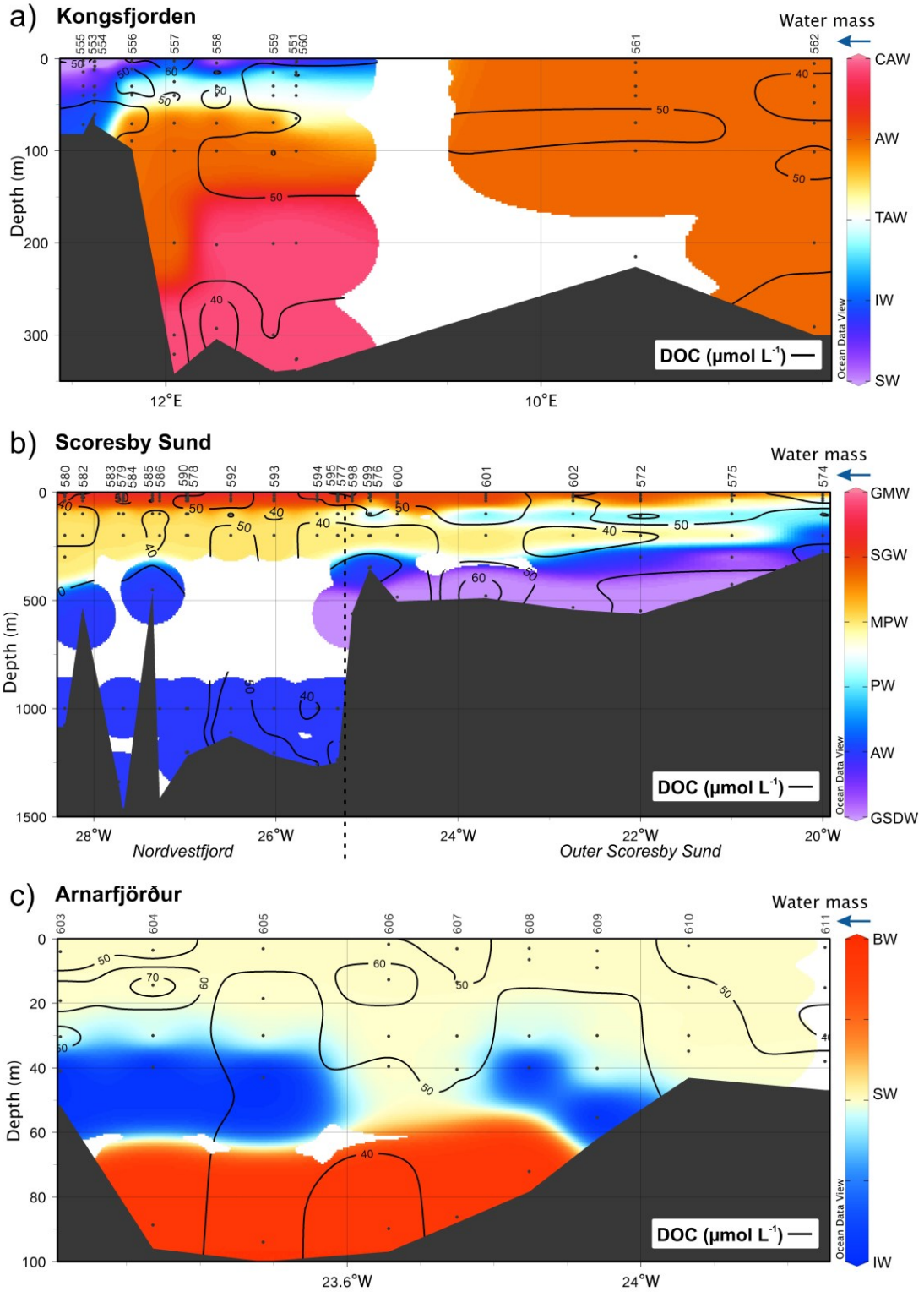

Figure 2: Water masses definitions (c.f. Table 1; depicted as colours) and distribution of dissolved organic carbon (DOC; contours) in the three different fjords. DOC sampling depths depicted as black dots. a) Kongsfjorden: Surface water (SW; violet), Intermediate water (IW, blue), Transformed Atlantic water (TAW; white), Atlantic water (AW; orange), Cold Atlantic water (CAW; red). b) Scoresby Sund: Greenland Sea Deep water (GSDW; violet), Atlantic water (AW; blue), Polar water (PW; turquoise), Modified polar water (MPW; yellow), Surface glacial water (SGW; red), Glacial meltwater (GMW; pink) originating from the Daugaard-Jensen glacier (left). c) Arnarfjörður: Surface water (SW; yellow) reaching up to the fjords mouth (left), Intermediate water (IW; blue), Bottom water (BW; red). Blue arrows on the upper right corner mark the fjords' mouth. The dotted line in Scoresby Sund divides Nordvestfjord and Outer Scoresby Sund.

4.4.2 Dissolved organic carbon and inorganic nutrients

4.4.2.1 Dissolved organic carbon distribution

Inside Kongsfjorden, DOC concentrations were high (up to 67 µmol L^{-1}) within the uppermost 70 m (Fig. 2a). At 200 m depth in CAW, concentrations were between 55 and 60 µmol L^{-1}. In the AW offshore and inflowing at 100 m depth, DOC concentration was approximately 50 µmol L^{-1}.

Within Nordvestfjord in Scoresby Sund, surface concentrations of DOC in the upper 3 m (GMW) were comparatively low, at around 30 µmol L^{-1} and as low as 13 µmol L^{-1} near the mouth of the glacier (Fig. 2b). However, in the water layer below, DOC concentrations were higher and reached up to 90 µmol L^{-1}, while in both layers below (MPW and AW) they were lower (~40 - 50 µmol L^{-1}). At the mouth of the fjord, SGW had high DOC concentrations of up to 84 µmol L^{-1}. Within the PW entering the fjord at 100 m depth, DOC concentrations ranged between 40 and 68 µmol L^{-1} in the outer fjord. Below, DOC concentration was mostly ~40 µmol L^{-1}. Inside Arnarfjörður, DOC was comparatively high throughout the water column with concentrations of around 70 µmol L^{-1} at a depth of 15 m and bottom DOC concentrations of approximately 60 µmol L^{-1} (Fig. 2c). DOC concentrations were up to 50 µmol L^{-1} in the upper 40 m of the remaining fjord and slightly lower at the bottom of the fjord and at the fjord's mouth.

4.4.2.2 Dissolved organic matter distribution and molecular variations in the different water masses

Some of the water masses defined in this study differed significantly in DOC concentrations ($p < 0.05$). In Arnarfjörður, DOC concentrations were different between SW and BW and in Scoresby Sund and SGW contained significantly more DOC than AW, GMW, and GSDW ($p < 0.01$). There were no statistical differences in DOC concentrations between the Kongsfjorden water masses and no correlation between salinity and DOC concentration based on the entire dataset.

PCA was performed using seven molecular bulk parameters (MW_w, $\#C_w$, H/C_w, DBE/O_w, DBE/C_w, O/C_w, and DBE_w) and water masses as factors to visualise sample groups. Neither in Kongsfjorden nor in Arnarfjörður the molecular characteristics of water masses formed distinct clusters in the PCA or differed significantly from each other (ANOSIM, MANOVA, $p > 0.05$). In Scoresby Sund in contrast, different water mass clusters were observed. The first two principal components (PC1 and PC2, Fig. 3) explained ~90% of the variance. The different water masses clustered along PC2, which explained 37% of the variance and was mostly related to the molecular

size (MW_w, $\#C_w$). GMW samples and most of SGW samples were found at negative PC2 values, while AW and MPW samples were mostly found at positive values. GSDW samples showed no distinct cluster, while PW showed negative values for PC1. PC1 explained 53.6% of the variance and was mostly influencedd by O/C_w, DBE/C_w, and H/C_w. Based on ANOSIM there was a weak significant difference between the different water masses ($R = 0.2$, $p < 0.01$). MANOVA showed that water masses differed significantly ($p < 0.01$) for all bulk parameters ($p < 0.01$, DBE/O_w: $p < 0.05$) except O/C_w and DBE_w ($p > 0.05$).

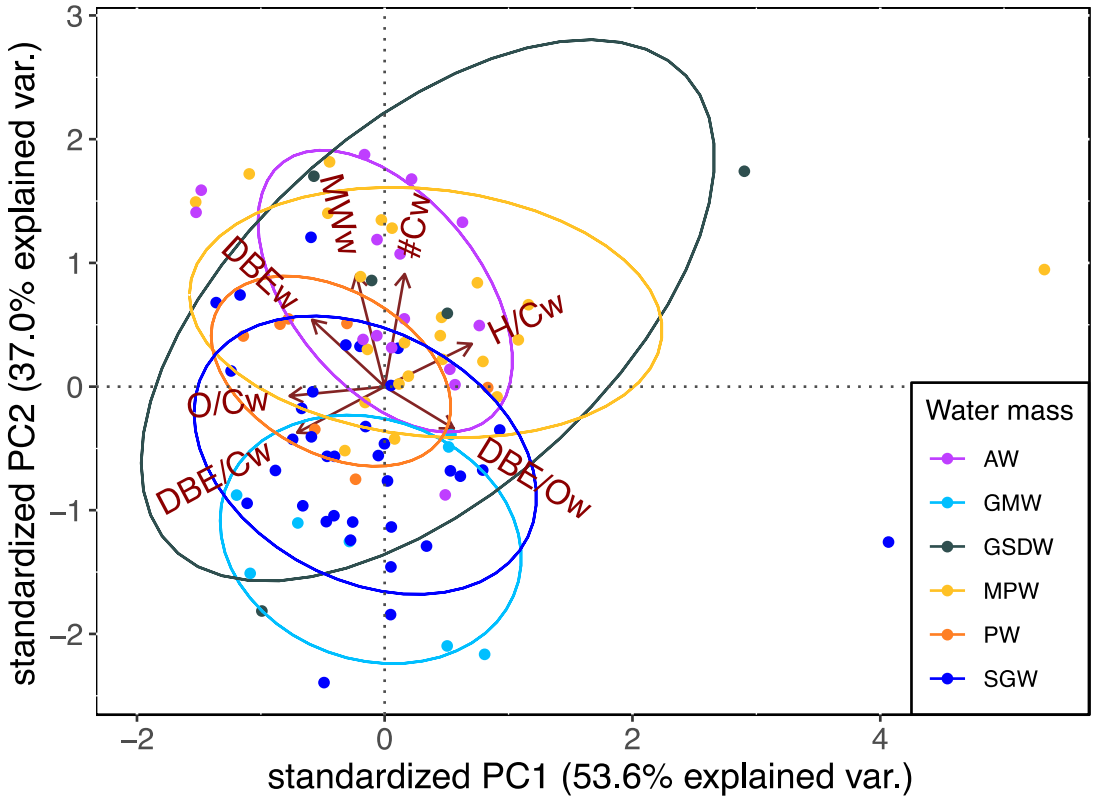

Figure 3: Principal component analysis (PCA) of molecular bulk parameters of DOM identified through high-resolution mass spectrometry for each sample from Scoresby Sund. Scores represent water masses depicted in different colours, including confidence ellipses. Magenta: Atlantic water (AW), turquoise: Glacial meltwater (GMW), grey: Greenland Sea deep water (GSDW), yellow: modified polar water (MPW), orange: Polar water (PW), blue: Surface glacial water (SGW). Loadings are depicted as red arrows.

4.4.2.3 Macronutrient distribution

All nutrient concentrations were low at the surface of Kongsfjorden. Silicate and nitrate concentrations were lowest at the surface of the fjords inside (< 1 µmol L^{-1}, < 1.5 µmol L^{-1}, respectively), highest at the bottom (up to 5 µmol L^{-1} and 10 µmol L^{-1}, respectively) and intermediate (up to 3 µmol L^{-1} and 4-6 µmol L^{-1}, respectively) in the upper inflowing AW at the mouth of the fjord. Phosphate concentrations were only low in the upper 50 m of the inner fjord and increased with depth. Bottom water phosphate

concentrations were up to 0.8 µmol L^{-1}. The incoming AW showed concentrations of up to 0.4 µmol L^{-1} in the upper 70 m. Ammonium concentrations peaked between 70 m and 100 m within the fjord (~1 µmol L^{-1}), while being low in its surface, bottom, and at the fjord's mouth. Similar to nutrient distribution in Kongsfjorden, in Arnarfjörður all nutrients were low in SW and showed highest concentrations at the bottom of the fjord (ammonium: 1.5-2 µmol L^{-1}, nitrate: 3-5 µmol L^{-1}, phosphate: 0.6-1 µmol L^{-1}, silicate: 4-8 µmol L^{-1}). Nutrient concentrations in Scoresby Sund were described in detail in Seifert et al. (2019).

Generally, nutrient concentrations were low in areas where dDA was found. dDA concentrations correlated negatively with phosphate, nitrate and silicate ($\tau = 0.30$, $\tau = 0.35$, $\tau = 0.42$, respectively, $p < 0.05$) but not with ammonium.

4.4.3 *Pseudo-nitzschia* abundance and distribution

Four different *Pseudo-nitzschia* species were identified via light microscopy (Table 2): Since the species group *P. delicatissima / pseudodelicatissima* could not be distinguished morphologically it will be referred to as *P. (pseudo-)delicatissima* in the following. *P. (pseudo-)delicatissima* was present in all three fjords and most abundant in Arnarfjörður. *P. pungens* was found at one station in Kongsfjorden and two in Arnarfjörður. The species *P. seriata* was exclusively found at one station in Arnarfjörður, while *P. granii* was only found in Kongsfjorden.

Table 2: *Pseudo-nitzschia* cell densities identified by light microscopy. Fjord, station number (St.), water mass (WM), sampling depth, and dissolved domoic acid concentration (dDA) are listed. WM abbreviations: IW (Kongsfjorden, Intermediate water), TAW (Transformed Atlantic water), SGW (Surface glacial water), GMW (Glacial meltwater), SW (Arnarfjörður, Surface water). *P. delicatissima / pseudodelicatissima* (*P. (pseudo-)delicatissima*), *P. pungens*, *P. seriata* and *P. granii* were monitored during the cruise.

Fjord	St.	WM	Depth (m)	dDA (pmol L^{-1})	*P. (pseudo-) delicatissima* (cells L^{-1})	*P. pungens* (cells L^{-1})	*P. seriata* (cells L^{-1})	*P. granii* (cells L^{-1})
Kongs-fjorden	551	IW	17.7	< LOD	127370			382111
Kongs-fjorden	556	IW	11.4	37	2149985			
Kongs-fjorden	558	IW	15	26	253236			50647
Kongs-fjorden	559	TAW	15	31	1570065	1175325		
Kongs-fjorden	560	TAW	65	< LOD	729425			1916291
		TAW	14.8	< LOQ	212635			2203735
Scoresby Sund	595	SGW	18.5	< LOQ	402013			
Scoresby Sund	599	GMW	1.5	< LOD	54510			
Arnar-fjörður	603	SW	19.2	29	13144061			
		SW	4	26	4594429			
Arnar-fjörður	605	SW	18.5	NA	13359185			
		SW	3.1	21	96483000			
Arnar-fjörður	606	SW	12.7	76	81168238	2522431		
		SW	1.7	29	41451956			
Arnar-fjörður	608	SW	6.5	82	107203333	42115595		
		SW	3	99	201006250	16422638		
Arnar-fjörður	610	SW	30	NA	152033818		33501042	
		SW	2.2	95	16080500		8040250	

Pseudo-nitzschia ASVs were found in all three fjords (Fig. 4). ASVs that were annotated as *P. cuspidata*, *P. multiseries*, or *Nitzschia* sp. were only found in Arnarfjörður. ASVs annotated as *P. delicatissima* were found in Arnarfjörður and in lower numbers also in Kongsfjorden whereas *P. seriata* ASVs were only identified in Scoresby Sund.

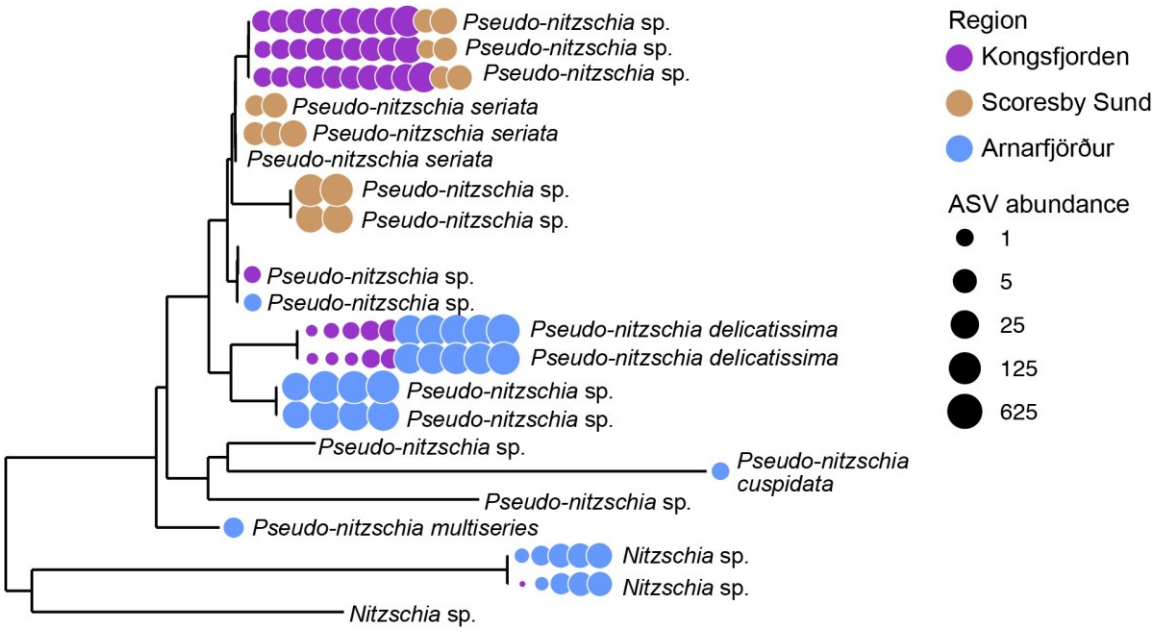

Figure 4: Distribution and abundance of ASVs annotated as *Pseudo-nitzschia* spp. and *Nitzschia* sp. Each tree tip represents an ASV sequence. Species names at tips are labelled according to ASV annotations derived from the PR^2 database. Dot colours represent the respective area from which a respective ASV has been retrieved. Dot sizes represent the library size normalized ASV abundance.

4.4.4 Distribution of domoic acid and *Pseudo-nitzschia* species

Quantifiable amounts of dDA were mostly found in the upper water column (upper 50 m in Scoresby Sund and Arnarfjörður, upper 200 m in Kongsfjorden). Throughout the cruise, dDA was quantified with lowest concentrations in Kongsfjorden (≤ 38 pmol L^{-1}, Fig. 5). DA carbon yield showed an equal distribution. *P. (pseudo-)delicatissima* and total *Pseudo-nitzschia* cell densities correlated significantly with dDA concentrations (τ = 0.60, p = 0.01, and τ = 0.49, p < 0.01, respectively).

4.4.4.1 Kongsfjorden

The highest dDA concentration and DA carbon yield in Kongsfjorden was found within the fjord (38 pmol L^{-1} and 12 ppm, respectively, Fig. 5a). Average concentrations of dDA were highest in the fjord's SW and IW and slightly lower in TAW and in AW, while CAW did not contain any dDA. dDA concentrations did not differ significantly between the different water masses (p > 0.05). Three *Pseudo-nitzschia* species were found in

the fjord's inside. *P. (pseudo-)delicatissima* were found at four stations with highest cell densities (2149985 cells L^{-1}) close to the inside of the fjord. *P. pungens* were found at only one station at which *P. (pseudo-)delicatissima* were also found and *P. granii* cells were identified at two stations. ASVs of *Pseudo-nitzschia* sp. were detected in the surface water throughout the fjord. Few ASVs of *P. delicatissima* were identified both at the mouth and the inside of the fjord, as well as of *Nitzschia* sp. in the fjord's middle.

4.4.4.2 Scoresby Sund

Inside Scoresby Sund, dDA concentrations were low. In Scoresby Sund, dDA was primarily found in the upper 100 m of the outer fjord. The highest dDA concentration in Scoresby Sund was 58 pmol L^{-1} at the mouth of the fjord (Fig. 5b) in the surface (SGW), in concentrations not significantly different from PW below ($p > 0.05$). In addition, low pDA (12 and 14 pmol L^{-1}) was quantified at both easternmost stations at the mouth of the fjord, where dDA was highest. The SGW dDA concentration was significantly higher ($p < 0.01$) than in MPW (freshened and warmed water at ~200 m depth). DA carbon yield was significantly higher in SGW compared to MPW and AW ($p < 0.05$), whereas GSDW did not contain any DA with only one exception at station 572. At two stations in the middle of the fjord, *P. (pseudo-)delicatissima* cells were counted in comparatively low densities (54510 and 402013 cells L^{-1}), but dDA was not quantifiable. Inside Nordvestfjord, *P. seriata* ASVs were identified at three stations close to the glacier. A high number of ASVs of *Pseudo-nitzschia* sp. were discovered at the mouth of the fjord, where high dDA concentrations were found.

4.4.4.3 Arnarfjörður

In Arnarfjörður, dDA was found in all samples and concentrations were highest of the entire cruise area (Fig. 5c). dDA concentrations and DA carbon yields correlated ($\tau = 0.80$, $p < 0.05$) and were highest in the SW (maximum of 124 pmol dDA L^{-1} at the mouth), which differed significantly from bottom water ($p < 0.05$). dDA in intermediate water was not statistically different from SW and BW.

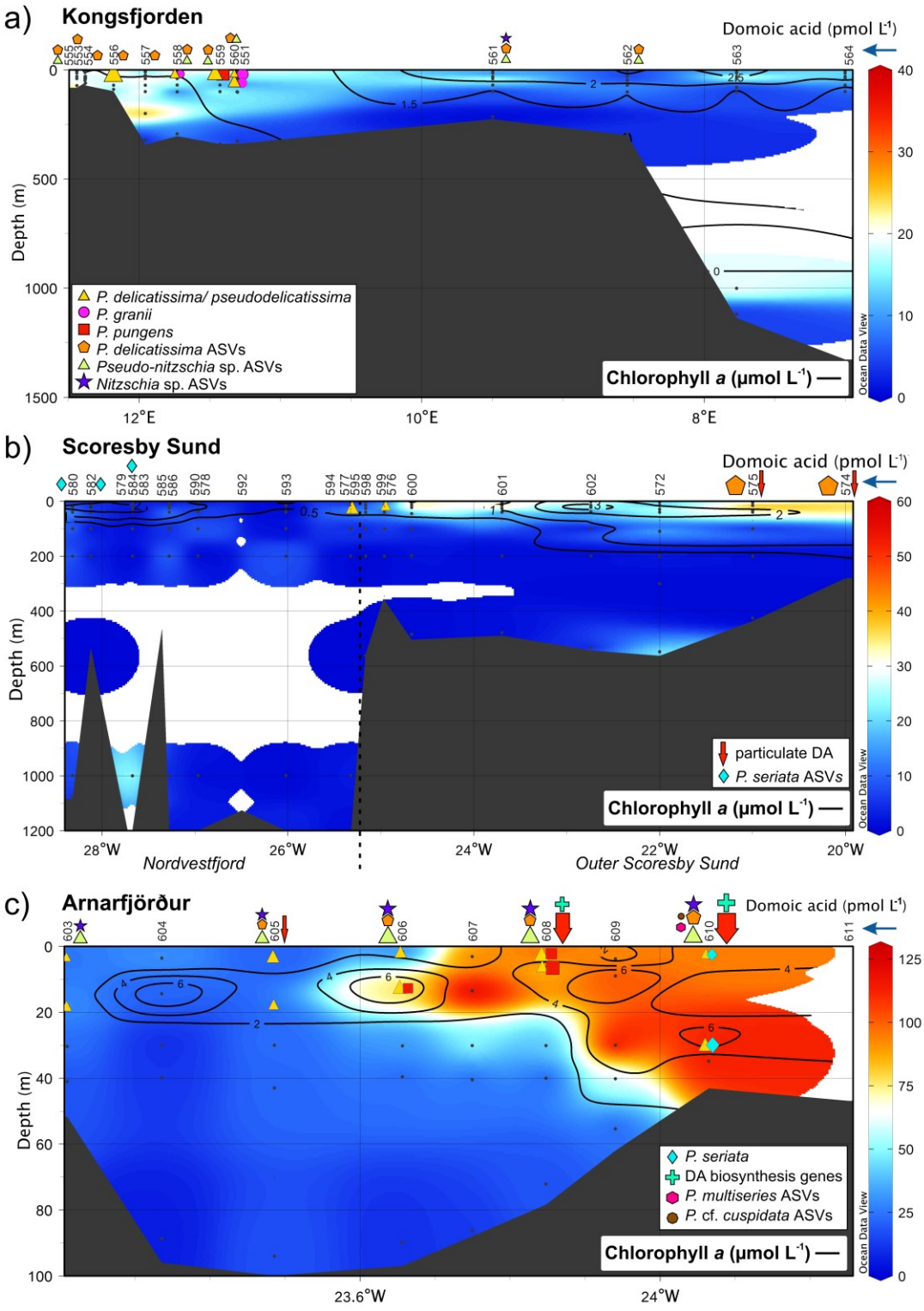

Figure 5: Vertical distribution of dissolved domoic acid (colours) and chlorophyll *a* concentration (contours) in Kongsfjorden (a), Scoresby Sund (b), and Arnarfjörður (c). Black dots under the station numbers represent samples. Symbols within the water column denote the occurrence of *Pseudo-nitzschia* cells. Symbols next to or above station numbers indicate at which stations *Pseudo-nitzschia* and *Nitzschia* amplicon sequence variants (ASVs) were found. Red arrows next to station numbers indicate the quantification of pDA with the size of the arrows accounting for pDA amounts. Turquoise plusses right to station numbers indicate the expression of domoic acid biosynthetic genes. Symbol size accounts for the number/amount found, respectively. Blue arrows at the upper right corners mark the fjord's mouth. The dotted line in Scoresby Sund divides Nordvestfjord and Outer Scoresby Sund.

Microscopic *Pseudo-nitzschia* counts were highest for all species within the entire cruise area with a predominance of *P. (pseudo-)delicatissima* in the whole fjord's surface. *P. seriata* was only found at one station at the fjord's mouth and *P. pungens* occurred in the middle of the fjord. Their cell densities were highest at stations 608 and 610. *Pseudo-nitzschia* sp., *Nitzschia* sp., and *P. delicatissima* ASVs were found throughout the fjord with highest numbers at the same stations, which also showed highest pDA (206 and 233 pmol pDA L^{-1}, respectively) and dDA (124 and 114 pmol dDA L^{-1}, respectively, Fig. 5c). Additionally, we found ASVs for mRNA encoding the DA biosynthesis gene cluster at both stations, suggesting active DA synthesis (Fig. 6). At station 610, few *P. multiseries* and *P.* cf. *cuspidata* ASVs were identified.

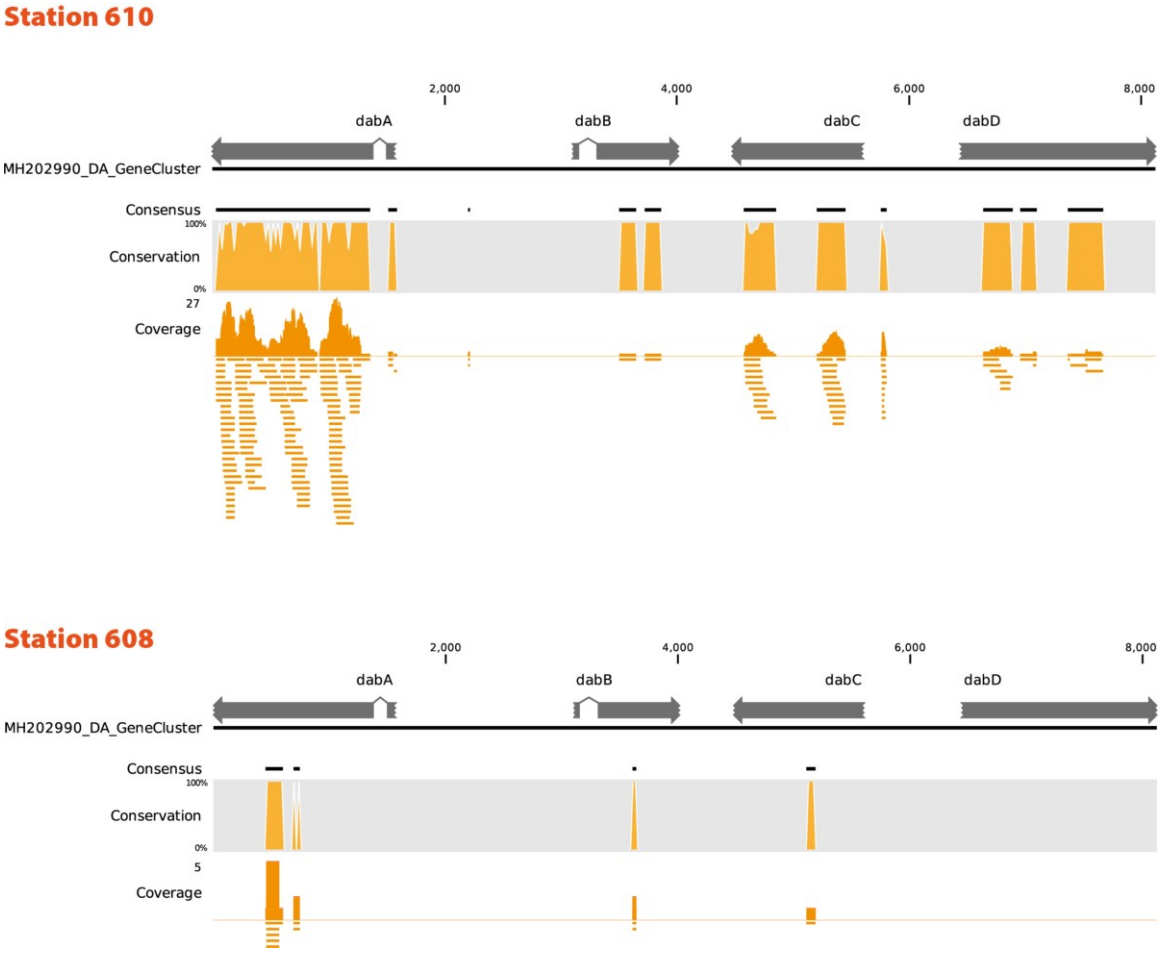

Figure 6: Alignment of metatranscriptome reads to the domoic acid biosynthesis gene cluster. Grey arrows represent coding regions of the domoic acid (DA) gene cluster. Conservation values represent percentage nucleotide base identities between aligned reads and the DA gene cluster. Coverage depicts numbers and positions of reads aligned to the DA gene cluster.

4.4.5 Domoic acid contribution to dissolved organic matter

DA carbon yield decreased with depth (Fig. 7, $\tau = -0.26$, $p < 0.05$) and correlated strongly with dDA ($\tau = 0.89$, $p < 0.05$). dDA also correlated moderately with total *Pseudo-nitzschia* counts ($\tau = 0.48$, $p < 0.05$), *P. (pseudo-)delicatissima* counts ($\tau = 0.56$, $p < 0.05$), and weakly with chlorophyll *a* concentrations ($\tau = 0.22$, $p < 0.05$).

DA carbon yield and carbon weighed summed peak intensities that represent the molecular formula of DA in the high-resolution mass spectrometry showed only a weak correlation ($\tau = 0.18$, $p < 0.05$). There was no linear relationship between the two parameters.

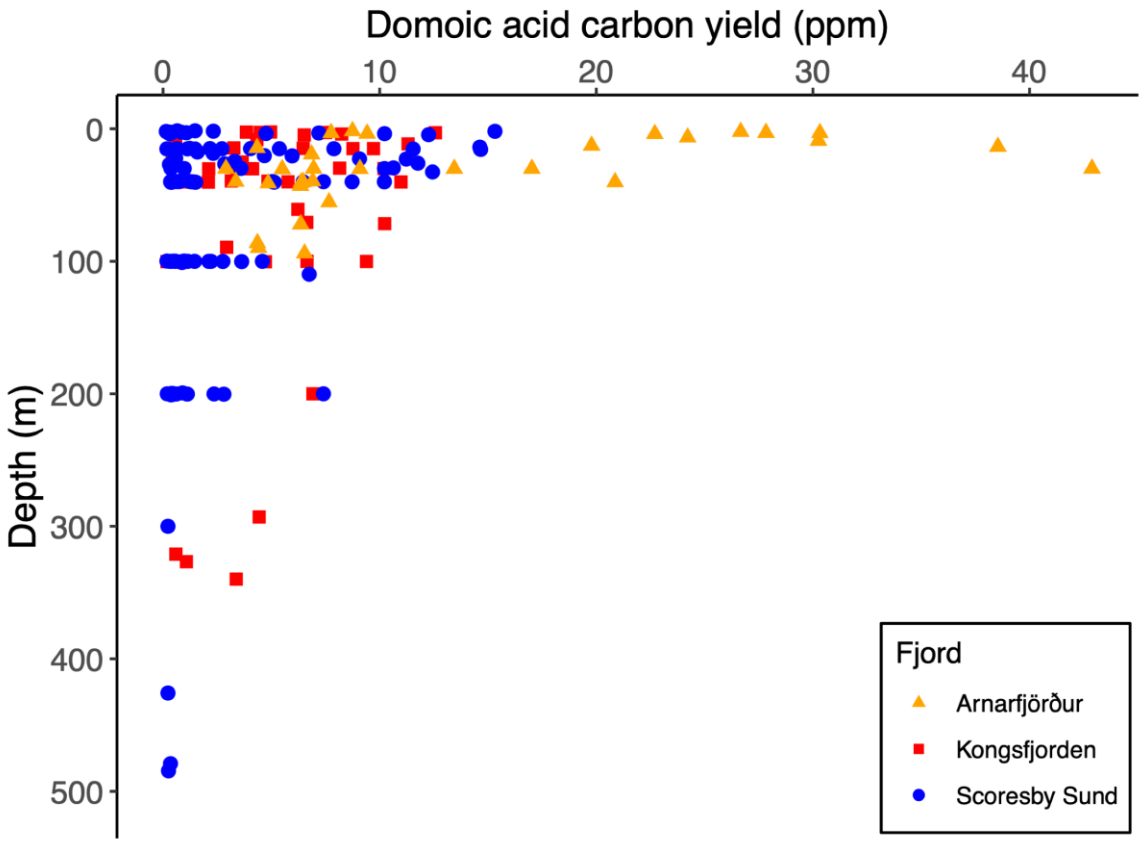

Figure 7: Depth distribution of domoic acid carbon yield (Molar fraction of carbon that is explained by the carbon contributed by DA). Red squares: Kongsfjorden, blue dots: Scoresby Sund, yellow triangles: Arnarfjörður

4.4.6 Distribution of chlorophyll *a*

Chlorophyll *a* concentrations ranged between 0.01 and 11.7 µg L^{-1} and were highest in Arnarfjörður (Fig. 5). Overall, there was a weak correlation between chlorophyll *a* and dDA concentrations ($\tau = 0.22$, $p < 0.05$). Within the inside of Kongsfjorden, concentrations were only enhanced in the SW in the upper 5 m. Chlorophyll *a* was also enhanced in the upper 50 m of the inflowing AW at the mouth of Kongsfjorden (up to

3.6 µg L^{-1}). The distribution of chlorophyll *a* in Scoresby Sund has been previously described in detail by Seifert et al. (2019). Higher chlorophyll *a* concentrations (up to 6.6 µg L^{-1}) were found at 20-30 m depth in SGW close to the glacier and within the outer Scoresby Sund in SGW and PW. In Arnarfjörður, chlorophyll *a* was comparatively high in SW and highest at the fjords mouth, with concentrations between 4 and 8 µg L^{-1} in the upper 40 m of the water column. Within the fjord, highest chlorophyll *a* concentrations (7-9 µg L^{-1}) occurred at 10-15 m depth (Fig. 5c).

4.5 Discussion

4.5.1 Sources and distribution of domoic acid

With few exceptions, pDA was quantified, where dDA concentrations were highest throughout the cruise. Especially in Arnarfjörður, where dDA concentrations and *Pseudo-nitzschia* cell densities were highest, pDA values were also highest (up to 233 pmol L^{-1}). Since the amount of dDA released can vary with environmental conditions, dDA may represent low or large parts of total DA (Delegrange et al., 2018; Trick et al., 2018; Wang et al., 2007). Consequently, dDA could also be detected, where pDA was absent, which has been observed before, presumably due to cellular regulation of dDA release (Trainer et al., 2009). Surprisingly, pDA was also discovered at the mouth of Scoresby Sund, where no *Pseudo-nitzschia* cells were counted. This finding implies that pDA was most likely associated with other particles or species e.g. grazers that fall into the size range of the plankton net (20 - 200 µm).

We also observed dDA in deep water of the study areas. dDA is a comparatively stable compound that can add to the DOM pool in deeper regions uncoupled from its production (Geuer et al., 2019). It is mainly degraded either by photooxidation at the Ocean's surface (Bouillon et al., 2006; Fisher et al., 2006) or bacterial degradation within the water column (Hagström et al., 2007). Due to its low particle reactivity, downward transport by accumulation is not very likely for DA (Lail et al., 2007). It was previously suggested that dDA residence times in the water column are comparable to pDA residence times (Umhau et al., 2018), which matches our observations.

Generally, microscopic species distinctions did not completely match the ASVs found for *Pseudo-nitzschia* species throughout the cruise. In Kongsfjorden, ASVs were found at the mouth of the fjord, where no *Pseudo-nitzschia* cells were counted. Only in Arnarfjörður, microscopic counts of *P. (pseudo-)delicatissima* matched the ASVs of *P. delicatissima* found at the same stations and depths. Using light microscopic species distinction, one of the distinguishable groups is the *P. (pseudo-)delicatissima* group

(Trainer et al., 2008). Albeit it was impossible to distinguish *P. delicatissima* and *P. pseudodelicatissima* via microscopy, the ASVs trees suggest that they are likely *P. delicatissima* (Fig. 4). Some of the counted *P. (pseudo-)delicatissima* cells, however, might also belong to the *P. pseudodelicatissima* complex. Within the *P. pseudodelicatissima* complex, it is also morphologically difficult to distinguish species, such as *P. cuspidata* (Lundholm et al., 2003; Pan et al., 2001), for which ASVs were found. The microscopically determined species *P. pungens*, *P. seriata*, and *P. granii* were not represented in the DNA data at the respective stations. We could not resolve the exact *Pseudo-nitzschia* species composition with the genomic data, as the reference database lacks resolution within the *Pseudo-nitzschia* species complex.

Overall, total *Pseudo-nitzschia* cell densities correlated with dDA concentrations. Much of the dDA quantified within our study area was thus likely excreted close to its producers. *P. (pseudo-)delicatissima* cell densities showed an even better correlation with dDA and were found at all stations at which *Pseudo-nitzschia* cells were identified. This implies, that in all three fjords at least some of the dDA could be excreted by *P. delicatissima* or *P. pseudodelicatissima*, species of which some strains have been shown to produce DA (Fuentes and Wikfors, 2013; Moschandreou et al., 2010) suggesting in turn that some of the other species did not produce DA.

In the inner Kongsfjorden, *Pseudo-nitzschia* cells were exclusively found, where dDA concentrations were highest (Fig. 5), whereas at the mouth of the fjord ASVs of *Pseudo-nitzschia* sp., *Nitzschia* sp., and *P. delicatissima* were also found where dDA concentrations were low. Overall, dDA concentrations were lower than the maximum concentrations found in the other fjords. *Pseudo-nitzschia* species counted in Kongsfjorden were *P. (pseudo-) delicatissima*, *P. granii* and at one station *P. pungens*. Of these, *P. delicatissima*, *P. granii*, and *P. pungens* have been reported in Kongsfjorden previously with *P. granii* broadly contributing to the phytoplankton composition in summer (Hegseth et al., 2019; Rytter Hasle and Riddervold Heimdal, 1998). *P. granii* only occurred in Kongsfjorden and dDA was below limit of quantification where its cell numbers were highest. Generally, *P. granii* is known to occur in the Arctic (Von Quillfeldt et al., 2003) and to produce DA, however not in an Arctic strain (Fuentes and Wikfors, 2013) and might thus not contribute to dDA.

Some strains of *P. pungens* have been observed to produce DA (Bates et al., 2018; Rhodes et al., 2013), but in comparatively low concentrations compared to other species (Lema et al., 2017) and might contribute to dDA in Kongsfjorden in addition to *P. delicatissima* or *P. pseudodelicatissima*. *Nitzschia* sp. ASVs were only found at one

station with low dDA concentrations. The genus *Nitzschia* has previously been discovered in the Arctic (Johnsen et al., 2018; Kauko et al., 2018; Leu et al., 2015) and the species *N. frigida* was previously observed close to Svalbard (Leu et al., 2010). This species is, however, not known to produce DA (Harðardóttir et al., 2019; Lundholm et al., 2018).

Low abundances of *P. (pseudo-)delicatissima* were found where the outer Scoresby Sund branches into Nordvestfjord and might be in part responsible for the low dDA concentrations quantified at the respective stations. Within Nordvestfjord close to the glacier, few numbers of *P. seriata* ASVs and low dDA concentrations were found. *P. seriata* has been shown to produce DA at the western coast of Greenland before (Hansen et al., 2011), and is thus a potential source for DA in Nordvestfjord, also for dDA found in lower areas of the water column, potentially derived from particle transport after a bloom (Umhau et al., 2018).

Microscopically, *P. seriata* was only counted in Arnarfjörður, where also high cell densities of *P. (pseudo-)delicatissima* were found. However, *P. seriata* is a known DA producing Arctic and western Icelandic species, which increases DA production in the presence of predators (Hansen et al., 2011; Lundholm et al., 2018; Tammilehto et al., 2015) and is likely to contribute to the particularly high dDA concentrations at the mouth of Arnarfjörður, as are *P. pungens* and *P. delicatissima* (Fuentes and Wikfors, 2013; Lema et al., 2017; Rhodes et al., 2013). *P. pseudodelicatissima*, which is known to occur in the west of Iceland (Lundholm et al., 2003), could also have contributed to dDA (Moschandreou et al., 2010). Around Iceland, several *Nitzschia* species have been reported (Hasle and Syvertsen, 1997; Jiang et al., 2001; Koc and Scherer, 1996), however, they are not known to produce DA. At station 610, small numbers of ASVs of *P. multiseries* and *P.* cf. *cuspidata* were found. Depending on the specific strain, *P. cuspidata* might be involved in DA production (Lundholm et al., 2003), which holds also true for *P. multiseries* (reviewed in Bates et al., 2018).

Transcripts for DAb genes were identified in the RNA metatranscriptome samples of stations 610 and 608 (Fig. 6). These genes have previously been discovered to be involved in the biosynthesis pathway of DA (Brunson et al., 2018) and have been found in two different *Pseudo-nitzschia* species (Brunson et al., 2018; Harðardóttir et al., 2019). Our study is the first record of these transcripts in ecological samples in an area, where also DA was quantified. The presence of these DAb gene transcripts reveals that at the respective stations, DA was actively produced at the time of sampling. This

finding matches well to dDA, pDA and *Pseudo-nitzschia* cell and ASV numbers, which were highest at these stations.

Chlorophyll *a* and dDA concentrations correlated well in Arnarfjörður. Generally, high dDA and species counts for *Pseudo-nitzschia* only matched the areas of high chlorophyll *a* concentration in Arnarfjörður and not in the other two fjords, which both rather showed post-bloom conditions (Hegseth et al., 2019; Seifert et al., 2019). Chlorophyll *a* was low in the inner Kongsfjorden (< 1 µg L^{-1}) and nutrients were depleted, while chlorophyll *a* peaked at the fjord's mouth, all in consistence with previous post spring bloom observations (Hegseth et al., 2019). In contrast to the other fjords in our study, chlorophyll *a* did not correlate with dDA. Chlorophyll *a* weakly correlated with dDA concentrations in Scoresby Sund and higher dDA concentrations occurred at the chlorophyll *a* maximum in the outer Scoresby Sund, which matched post-bloom conditions with high numbers of copepods and faecal pellets (Seifert et al., 2019). Relatively large amounts of dDA were found in this area and in the fjords mouth. Although no *Pseudo-nitzschia* cells were counted on the respective stations, small pDA amounts were quantified as well as a high number of *Pseudo-nitzschia* sp. ASVs. It is thus likely that DA was produced at the respective stations. The absence of *Pseudo-nitzschia* cells might be attributed to the post-bloom conditions at the time of our study (Seifert et al., 2019). The presence of dDA in some deep areas of the fjord could also be explained by these post-bloom conditions, i.e. through the leakage of sinking *Pseudo-nitzschia* cells. For the western Arctic Ocean it could be shown that under higher temperature and lower salinity, the diatom diversity shifts to a higher number of *Pseudo-nitzschia* species (Sugie et al., 2020) and that dDA release increases under low salinities (Ayache et al., 2019). With an increase of temperature and higher influence of glacial meltwater, the contribution of *Pseudo-nitzschia* to blooms and the simultaneous occurrence of dDA could thus increase in the future.

4.5.2 The impact of varying nutrient regimes on domoic acid

dDA concentrations showed a moderate inverse correlation with silicate and weak inverse correlation with phosphate and nitrate concentrations, which was also observed in a previous field study (Schnetzer et al., 2007). Laboratory experiments demonstrated that phosphate and silicate limitation can trigger and increase DA production in different species (Bates et al., 1991; Fehling et al., 2004; Pan et al., 1996a, 1996b). In case of limitation, DA does not only increase in the cells but also in the medium (Fehling et al., 2004; Pan et al., 1996a). The best inverse correlation in the field was found between dDA and silicate, which could be explained with silicate limitation in

particular causing high leakages of DA (up to 67%) into the surrounding medium (Fehling et al., 2004). Especially if silicate to nitrogen ratios are low, cellular DA is elevated (Ryan et al., 2017). Apart from toxicity, *Pseudo-nitzschia* species composition can be influenced by the ratio of silicate and nitrogen, which in turn impacts the DA amount (Thorel et al., 2017). Nitrogen is essential for the synthesis of DA (Bates et al., 1993, 1991; Pan et al., 1998). In our study nitrate concentrations also weakly inversely correlated with dDA. It has previously been suggested that ammonium, albeit toxic to its producers in high amounts (Bates et al., 1993), serves as an energetically even better nitrogen source for the synthesis of DA than nitrate (Pan et al., 1998). Ammonium did not inversely correlate with dDA in our study area and thus, although nitrate concentrations were low, nitrogen was likely not a limiting nutrient. It has been previously suggested that nutrient limitation might be responsible for a high DA content without high cell counts (Wohlrab et al., 2019). This might also be a likely scenario for our study area, where phosphate and silicate might be limiting. If it is considered that a lot of DA is released by the cells under these limitations (Fehling et al., 2004), it can be expected that dDA concentrations mirror this effect.

4.5.3 Dissolved domoic acid and its contribution to dissolved organic matter in different water masses

Our results discussed above showed that *Pseudo-nitzschia* alters parts of the chemical signals of dissolved organic matter in the water column by changing the content of dDA. Therefore, we were interested to assess the contribution of dDA to the total DOM and to explore if molecular chemical fingerprints in DOM in general mirror the biological processes in the water column. DA carbon yield, i.e. the fraction of DOC that can be explained by carbon derived from DA, strongly correlated with dDA concentrations ($\tau = 0.89$, $p < 0.05$) and thus also showed similar distributions in the fjords. This strong correlation between dDA and DA carbon yield also explains the correlation of DA carbon yield with *Pseudo-nitzschia* cell counts and chlorophyll *a*. Generally, the DA carbon yield decreased with depth (Fig. 7), as was previously observed (Geuer et al., 2019). Particularly in the upper water of Arnarfjörður, where dDA concentrations reached high values, its contribution to total DOM was high. Overall, DA carbon yield within the fjords were in the range of the values previously observed for the Atlantic Ocean (Geuer et al., 2019). We could thus show that dDA indeed contributed to DOM, especially where dDA concentrations were comparatively high.

AW was an important component in all three fjords. In consistence with previous data during our summer conditions, its inflow heavily influenced Kongsfjorden and led to

warmer and nutrient rich water at intermediate depth (Svendsen et al., 2002; Tverberg et al., 2019). Within Scoresby Sund, AW entered at 200 m depth and filled the deep regions of Nordvestfjord (Seifert et al., 2019), while Iceland coastal water influencing the summer stratified Arnarfjörður is a mixture of AW and PW (Marine and Malmberg, 1999; Stefánsson and Ólafsson, 1991).

Our oceanographic data agreed well with previous findings in Kongsfjorden during summer: The inner fjord is influenced by glacial outflow, whose effects diminish towards the outer fjord (Hop et al., 2002) (Fig 2a). The upper water masses of the inner fjord showed a layer of SW, IW, and TAW, which originate from the mixing of low saline surface water with the inflowing AW (Tverberg et al., 2019). While Scoresby Sund and Arnarfjörður were highly stratified, it was apparent that water masses in Kongsfjorden were subject to mixing. In Arnarfjörður we observed the previously described summer stratification with an approximately 40 m thick warm SW layer and BW of 3 °C with a salinity of 34.5 (Jónsdóttir, 2015) along with an intermediate water mass, which was a mixture of both (Fig. 2c). Primary production around Iceland is usually high from May to August (Zhai et al., 2012), which was also observed particularly at the fjord's mouth during our study. Biogeochemical differences divide outer Scoresby Sund and Nordvestfjord, mainly due to nutrient input into the fjord at its mouth and surface meltwater discharge at its inside (Seifert et al., 2019). The influence of glacier meltwater (Bach, 2016) and icebergs, in particular by the Daugaard-Jensen Glacier, led to low saline surface water (salinity < 30) throughout the fjord (Seifert et al., 2019), most pronouncedly in Nordvestfjord (Fig. 2b) (Dowdeswell et al., 1992). Via the fjord's mouth, EGC water that flows southwards along the east Greenland coast (Aagaard and Coachman, 1968) enters the fjord. Its different layers consist of PW at the surface, AW at 200 m depth and GSDW, which entered at approximately 500 m depth and constituted the outer Scoresby Sund's bottom water.

Most water masses we detected in our summer conditions were not original water masses in a strict oceanographic sense but were affected by mixing and reflected a post bloom situation. DOC, DOM, and DA differed significantly where physical water mass properties and stratification were large. In Arnarfjörður, where stratification is common for early summer (Jónsdóttir, 2015), dDA and DOC concentrations differed significantly between SW and BW.

In Scoresby Sund, SGW contained significantly more DOC compared to AW, GSDW, and GMW. dDA concentrations were also highest at the mouth of the fjord in SGW and differed significantly from AW, MPW, and GMW, which did not contain any dDA. Since

GMW in the surface primarily consists of meltwater discharge (Seifert et al., 2019), such low dDA and DOC concentrations were expected. The same holds true for AW and GSDW, since both are the deepest water masses and lower DOC in AW and deep water has previously been observed in the Arctic (Bussmann and Kattner, 2000).

PW dDA concentrations were on average second highest and we assume that dDA was transported into the fjord via this water mass, since both pDA and dDA were found along the Greenland shelf north of the fjord and might be transported southwards with the EGC (Aagaard and Coachman, 1968). Transcripts of *Pseudo-nitzschia* at the respective station indicate that dDA was additionally derived from autochthonous production. There was almost no dDA detected in AW and DA carbon yield was furthermore significantly higher in MPW compared to AW, which is in line with the observation that AW forms a distinct layer in deeper fjord areas (Seifert et al., 2019). Although we previously found dDA in the deep Atlantic and suggested that dDA is a relatively stable molecule (Geuer et al., 2019) that is likely transported to the deep-sea via sinking particles, such as zooplankton faecal pellets or transparent exopolymer aggregates (Umhau et al., 2018), it is reasonable that its concentrations were comparatively low, because AW entered the fjord at 200 m depth.

Obviously, the differences in DOC and dDA concentrations were insignificant for those water masses that were strongly affected by mixing, as observed in Kongsfjorden, where AW gradually mixes with the other water masses (Tverberg et al., 2019). Furthermore, our study was carried out after the spring bloom (Hegseth et al., 2019), which might imply that a transformation of DOC as observed before resulting in constant DOC concentrations along the salinity gradient (Osterholz et al., 2014) might have already taken place.

4.5.4 Biogeochemical impacts on chemical fingerprints of dissolved organic matter

FT-ICR-MS has been previously shown to yield complex chemical information on marine DOM (e.g. Hertkorn and Kettrup, 2005; Koch et al., 2005). The technique yields thousands of molecular formulas for each sample that can be evaluated as fingerprints on a semi-quantitative level. In our approach here, we tried to explore if these chemical fingerprints can represent water masses and biological-chemical processes in the three fjords. To test for differences, we reduced the complexity of the dataset by calculating few indicator parameters (O/C_w, H/C_w, DBE_w, DBE/C_w, MW_w, $\#C_w$), which we used for statistical comparison.

In Kongsfjorden, molecular fingerprints did not differ significantly with water mass. This is consistent with the findings for dDA and DOC, which were likely affected by water mass mixing (see above). These results also match previous findings for Svalbard fjords including Kongsfjorden, where the DOM pool mainly consisted of semi-refractory and refractory material introduced by AW and DOM from spring blooms was rapidly turned over (Osterholz et al., 2014). Furthermore, our statistical analyses for the indicator parameters showed no significant differences between water masses in Arnarfjörður. Usually, the water column of Arnarfjörður is mixed before it becomes stratified in summer (Jónsdóttir, 2015), which is likely one of the reasons, why there were no pronounced differences in chemical fingerprints of different water masses, even if the concentration of DOC differed between them.

In contrast, significant differences in chemical fingerprints (particularly molecular weight and carbon number) were observed between water masses in Scoresby Sund. The only exception was GSDW, which was not separated in the PCA. Since it forms the bottom layer of the outer Scoresby Sund, a release of DOM from sediment could influence this water mass at some stations (Rossel et al., 2016). Despite an overlap of the water masses in the PCA, which can be explained mainly by mixing, we still observed significant differences between samples based on most indicator parameters. The only exceptions were O/C_w and DBE_w, which did not differ significantly between groups and thus did not seem to be as important when differentiating between water masses. This has been observed before, while other molecular parameters showed differences when correlated with latitude (Roth et al., 2013). In addition, O/C was shown to not significantly change with DOM age (Flerus et al., 2012). O/C_w mainly influenced PC1 and thus had a less pronounced effect on the group formation of water masses compared to parameters influencing PC2 (Fig. 3). DBE is independent of i.a. the number of O (Koch and Dittmar, 2006), thus it is not surprising that the effects of both DBE/C_w and DBE/O_w were more pronounced.

GMW formed the most distinctive group and was negatively related to molecular size and partially related to aromaticity (represented as DBE/C_w; negative PC1 scores). A higher aromaticity might indicate a higher yield of terrestrial DOM in this water mass as observed in the discharge of Svalbard glaciers (Grzesiak et al., 2015), which seems reasonable considering that the runoff of glacial meltwater partially stems from meltwater rivers (Seifert et al., 2019).

The observed differences of water masses on a molecular level support our results for dDA and DOC concentrations. GMW and AW form two distinctive groups SGW and

GSDW show only partial overlaps, while MPW and PW show a high overlap in the biplot. The molecular differences between the water masses thus seem to be mirrored in the concentration differences. Water stratification thus allows at least a partial distinction of DOM in different water masses by their molecular fingerprint, particularly under strong glacial influence, and the formation of a distinctive group in the PCA underpins the pronounced influence by meltwater on fjord water chemistry.

4.6 Conclusions

In this study, we confirmed that *Pseudo-nitzschia* occurrence and dDA concentrations matched very well, especially in areas with high dDA concentrations. We showed that dDA was present in three different Arctic fjords. *Pseudo-nitzschia* and DA occurrence were not related to high primary production in any of the fjord systems. On the contrary, post bloom conditions with low availability of phosphate and silicate might partially be responsible for the DA production observed in our study area. Overall, dDA, pDA, *Pseudo-nitzschia* counts, and ASVs numbers matched well. Especially in areas, where dDA was high, the other parameters were high as well, although microscopic species distinctions did not completely match the ASVs found for *Pseudo-nitzschia* species in all areas of this study. Furthermore, this study underlines that dDA remains in the water column at least equally long as pDA. For the first time, we presented findings of gene transcripts involved in DA biosynthesis in field samples, where also DA was quantified and source organisms were counted.

In Scoresby Sund, an increased meltwater discharge of very low salinity and poor in nutrients is likely, which could result in a decrease in primary production. However, the share of *Pseudo-nitzschia* in local blooms might increase with the resulting lower salinity and higher temperatures. Less glacial discharge in Scoresby Sund would probably lead to higher nutrient availability, a less pronounced stratification and different bloom onset times. Potentially, *Pseudo-nitzschia* blooms would furthermore show a higher toxicity, as observed in Arnarfjörður, due to phosphate or silicate limitation.

The water stratification within the fjords allows at least a partial chemical distinction between DOM pools of the different water masses. As soon as water masses start mixing, however, these differences are obscured. The formation of a distinctive group in the PCA underpins the pronounced influence on fjord water chemistry by glacial runoff.

Acknowledgements

We thank the captain and the crew of RV Maria S. Merian for their advice and invaluable assistance. Furthermore, we want to thank the participants of the cruise MSM56 for their help during sampling. Thank you to Fabian Moye, Laura Käse, and Jan Tebben for statistical discussions and Thomas Max for help during pDA analysis.

This study was financially supported in the framework of the project “Inorganics in organics: Chemical and biological controls on micronutrient and carbon fluxes in the polar ocean” (Koch; IP76010001) by the strategy fund of the Alfred Wegener Institute, Helmholtz Centre for Polar and Marine Research.

References

Aagaard, K., Coachman, L., 1968. The East Greenland Current north of Denmark Strait: part I. *Arctic* 21, 181–200.

Ayache, N., Hervé, F., Martin-Jézéquel, V., Amzil, Z., Caruana, A.M.N., 2019. Influence of sudden salinity variation on the physiology and domoic acid production by two strains of *Pseudo-nitzschia australis*. *J. Phycol.* 55, 186–195. doi:10.1111/jpy.12801

Bach, L.T., 2016. Documentation of glaciers and mountain chains in the Nordvestfjord of Scorsby Sound (East Greenland, July 2016) by landscape photography during Maria S. Merian cruise MSM56. doi:10.1594/PANGAEA.863608

Bargu, S., Lefebvre, K.A., Silver, M.W., 2006. Effect of dissolved domoic acid on the grazing rate of krill *Euphausia pacifica*. *Mar. Ecol. Prog. Ser.* 312, 169–175. doi:10.3354/meps312169

Bates, S.S., Bird, C.J., de Freitas, A.S.W., Foxall, R., Gilgan, M., Hanic, L.A., Johnson, G.R., McCulloch, A.W., Odense, P., Pocklington, R., Quilliam, M.A., Sim, P.G., Smith, J.C., Subba Rao, D. V., Todd, E.C.D., Walter, J.A., Wright, J.L.C., 1989. Pennate Diatom *Nitzschia pungens* as the Primary Source of Domoic Acid, a Toxin in Shellfish from Eastern Prince Edward Island, Canada. *Can. J. Fish. Aquat. Sci.* 46, 1203–1215. doi:10.1139/f89-156

Bates, S.S., Freitas, A.S.W. de, Milley, J.E., Pocklington, R., Quilliam, M.A., Smith, J.C., Worms, J., 1991. Controls on Domoic Acid Production by the Diatom *Nitzschia pungens* f. *multiseries* in Culture: Nutrients and Irradiance. *Can. J. Fish. Aquat. Sci.* 48, 1136–1144. doi:10.1139/f91-137

Bates, S.S., Hubbard, K.A., Lundholm, N., Montresor, M., Leaw, C.P., 2018. *Pseudo-nitzschia*, *Nitzschia*, and domoic acid: New research since 2011. *Harmful Algae* 79, 3–43. doi:10.1016/j.hal.2018.06.001

Bates, S.S., Worms, J., Smith, J.C., 1993. Effects of Ammonium and Nitrate on Growth and Domoic Acid Production by *Nitzschia pungens* in Batch Culture. *Can. J. Fish. Aquat. Sci.* 50, 1248–1254. doi:10.1139/f93-141

Bouillon, R.-C., Knierim, T.L., Kieber, R.J., Skrabal, S.A., Wright, J.L.C., 2006. Photodegradation of the algal toxin domoic acid in natural water matrices. *Limnol. Oceanogr.* 51, 321–330. doi:10.4319/lo.2006.51.1.0321

Brunson, J.K., McKinnie, S.M.K., Chekan, J.R., McCrow, J.P., Miles, Z.D., Bertrand, E.M., Bielinski, V.A., Luhavaya, H., Oborník, M., Smith, G.J., Hutchins, D.A., Allen, A.E., Moore, B.S., 2018. Biosynthesis of the neurotoxin domoic acid in a bloom-forming diatom. *Science* 361, 1356–1358. doi:10.1126/science.aau0382

Bussmann, I., Kattner, G., 2000. Distribution of dissolved organic carbon in the central Arctic Ocean: The influence of physical and biological properties. *J. Mar. Syst.* 27, 209–219. doi:10.1016/S0924-7963(00)00068-3

Callahan, B.J., McMurdie, P.J., Rosen, M.J., Han, A.W., Johnson, A.J.A., Holmes, S.P., 2016. DADA2: High-resolution sample inference from Illumina amplicon data. *Nat. Methods* 13, 581–583. doi:10.1038/nmeth.3869

Chen, L., Reeve, J., Zhang, L., Huang, S., Wang, X., Chen, J., 2018. GMPR: A robust normalization method for zero-inflated count data with application to microbiome sequencing data. *PeerJ* 6, e4600. doi:10.7717/peerj.4600

Cottier, F.R., Nilsen, F., Skogseth, R., Tverberg, V., Skardhamar, J., Svendsen, H., 2010. Arctic fjords: A review of the oceanographic environment and dominant physical processes. *Geol. Soc. Spec. Publ.* 344, 35–50. doi:10.1144/SP344.4

del Campo, J., Kolisko, M., Boscaro, V., Santoferrara, L.F., Nenarokov, S., Massana, R., Guillou, L., Simpson, A., Berney, C., de Vargas, C., Brown, M.W., Keeling, P.J., Wegener Parfrey, L., 2018. EukRef: Phylogenetic curation of ribosomal RNA to enhance understanding of eukaryotic diversity and distribution. *PLoS Biol.* 16, 1–14. doi:10.1371/journal.pbio.2005849

Delegrange, A., Lefebvre, A., Gohin, F., Courcot, L., Vincent, D., 2018. *Pseudo-nitzschia* sp. diversity and seasonality in the southern North Sea, domoic acid levels and associated phytoplankton communities. *Estuar. Coast. Shelf Sci.* 214, 194–206. doi:10.1016/j.ecss.2018.09.030

Dittmar, T., Koch, B.P., Hertkorn, N., Kattner, G., 2008. A simple and efficient method for the solid-phase extraction of dissolved organic matter (SPE-DOM) from seawater. *Limnol. Oceanogr. Methods* 6, 230–235. doi:10.4319/lom.2008.6.230

Dowdeswell, J.A., Whittington, R.J., Hodgkins, R., 1992. The sizes, frequencies, and freeboards of East Greenland icebergs observed using ship radar and sextant. *J. Geophys. Res.* 97, 3515–3528. doi:10.1029/91JC02821

Fehling, J., Davidson, K., Bolch, C.J., Bates, S.S., 2004. Growth and domoic acid production by *Pseudo-nitzschia seriata* (Bacillariophyceae) under phosphate and silicate limitation. *J. Phycol.* 40, 674–683. doi:10.1111/j.1529-8817.2004.03213.x

Fisher, J.M., Reese, J.G., Pellechia, P.J., Moeller, P.L., Ferry, J.L., 2006. Role of Fe(III), phosphate, dissolved organic matter, and nitrate during the photodegradation of domoic acid in the marine environment. *Environ. Sci. Technol.* 40, 2200–2205. doi:10.1021/es051443b

Flerus, R., Koch, B.P., Schmitt-Kopplin, P., Witt, M., Kattner, G., 2011. Molecular level investigation of reactions between dissolved organic matter and extraction solvents using FT-ICR MS. *Mar. Chem.* 124, 100–107. doi:10.1016/j.marchem.2010.12.006

Flerus, R., Lechtenfeld, O.J., Koch, B.P., McCallister, S.L., Schmitt-Kopplin, P., Benner, R., Kaiser, K., Kattner, G., 2012. A molecular perspective on the ageing of marine dissolved organic matter. *Biogeosciences* 9, 1935–1955. doi:10.5194/bg-9-1935-2012

Fofonoff, N., Millard, R., 1983. Algorithms for computation of fundamental properties of seawater, *UNESCO Technical Papers in Marine Sciences*. Paris.

Fuentes, M.S., Wikfors, G.H., 2013. Control of domoic acid toxin expression in *Pseudo-nitzschia multiseries* by copper and silica: Relevance to mussel aquaculture in New England (USA). *Mar. Environ. Res.* 83, 23–28. doi:10.1016/j.marenvres.2012.10.005

Geuer, J.K., Krock, B., Leefmann, T., Koch, B.P., 2019. Quantification, extractability and stability of dissolved domoic acid within marine dissolved organic matter. *Mar. Chem.* 215, 103669. doi:10.1016/j.marchem.2019.103669

Grzesiak, J., Górniak, D., Świątecki, A., Aleksandrzak-Piekarczyk, T., Szatraj, K., Zdanowski, M.K., 2015. Microbial community development on the surface of Hans and Werenskiold Glaciers (Svalbard, Arctic): a comparison. *Extremophiles* 19, 885–897. doi:10.1007/s00792-015-0764-z

Hagström, J.A., Granéli, E., Maneiro, I., Barreiro, A., Petermann, A., Svensen, C., 2007. Release and degradation of amnesic shellfish poison from decaying *Pseudo-nitzschia multiseries* in presence of bacteria and organic matter. *Harmful Algae* 6, 175–188. doi:10.1016/j.hal.2006.08.002

Hansen, L.R., Soylu, S. í, Kotaki, Y., Moestrup, Ø., Lundholm, N., 2011. Toxin production and temperature-induced morphological variation of the diatom *Pseudo-nitzschia seriata* from the Arctic. *Harmful Algae* 10, 689–696. doi:10.1016/j.hal.2011.05.004

Harðardottir, S., Pančic, M., Tammilehto, A., Krock, B., Møller, E.F., Nielsen, T.G., Lundholm, N., 2015. Dangerous Relations in the Arctic Marine Food Web: Interactions between Toxin Producing *Pseudo-nitzschia* Diatoms and *Calanus* Copepodites. *Mar. Drugs* 13, 3809–3835. doi:10.3390/md13063809

Harðardóttir, S., Wohlrab, S., Hjort, D.M., Krock, B., Nielsen, T.G., John, U., Lundholm, N., 2019. Transcriptomic responses to grazing reveal the metabolic pathway leading to the biosynthesis of domoic acid and highlight different defense strategies in diatoms. *BMC Mol. Biol.* 20, 1–14. doi:10.1186/s12867-019-0124-0

Hasle, G.R., Syvertsen, E.E., 1997. Marine diatoms, in: Thomas, C.R. (Ed.), Identifying Marine Phytoplankton. Academic Press, San Diego, pp. 5–385.

Haugan, P.M., 1999. Structure and heat content of the West Spitsbergen Current. *Polar Res. 1*8, 183–188. doi:10.3402/polar.v18i2.6572

Hegseth, E.N., Assmy, P., Wiktor, J.M., Wiktor, J.J., Kristiansen, S., Leu, E., Tverberg, V., Gabrielsen, T.M., Skogseth, R., Cottier, F., 2019. Phytoplankton Seasonal Dynamics in Kongsfjorden, Svalbard and the Adjacent Shelf, in: Hop, H., Wiencke, C. (Eds.), The Ecosystem of Kongsfjorden, Svalbard. Advances in Polar Ecology, Vol. 2. Springer, Cham, pp. 173–227. doi:10.1007/978-3-319-46425-1_6

Hegseth, E.N., Tverberg, V., 2013. Effect of Atlantic water inflow on timing of the phytoplankton spring bloom in a high Arctic fjord (Kongsfjorden, Svalbard). *J. Mar. Syst.* 113–114, 94–105. doi:10.1016/j.jmarsys.2013.01.003

Hertkorn, N., Kettrup, A., 2005. Molecular level structural analysis of natural organic matter and of humic substances by multinuclear and higher dimensional NMR spectroscopy, in: Use of Humic Substances to Remediate Polluted Environments: From Theory to Practice. Springer, pp. 391–435.

Hodal, H., Falk-Petersen, S., Hop, H., Kristiansen, S., Reigstad, M., 2012. Spring bloom dynamics in Kongsfjorden, Svalbard: Nutrients, phytoplankton, protozoans and primary production. *Polar Biol.* 35, 191–203. doi:10.1007/s00300-011-1053-7

Hop, H., Person, T., Hegseth, E.N., Kovacs, K.M., Wiencke, C., Kwasniewski, S., Eiane, K., Mehlum, F., Gulliksen, B., Wlodarska-Kowalczuk, M., Lydersen, C., Weslawski, J.M., Cochrane, S., Gabrielsen, G.W., Leakey, R.J.G., Lønne, O.J., Zajaczkowski, M., Falk-Petersen, S., Kendall, M., Wängberg, S.-Å., Bischof, K., Voronkov, A.Y., Kovaltchouk, N.A., Wiktor, J., Poltermann, M., di Prisco, G., Papucci, C., Gerland, S., 2002. The marine ecosystem of Kongsfjorden, Svalbard. *Polar Res.* 21, 167–208. doi:10.1016/j.polar.2016.11.001

Jiang, H., Seidenkrantz, M.-S., Knudsen, K.L., Eiríksson, J., 2001. Diatom surface sediment assemblages around Iceland and their relationships to oceanic environmental variables. *Mar. Micropaleontol.* 41, 73–96. doi:10.1016/S0377-8398(00)00053-0

Johnsen, G., Norli, M., Moline, M., Robbins, I., von Quillfeldt, C., Sørensen, K., Cottier, F., Berge, J., 2018. The advective origin of an under-ice spring bloom in the Arctic Ocean using multiple observational platforms. *Polar Biol.* 41, 1197–1216. doi:10.1007/s00300-018-2278-5

Jónsdóttir, I.R., 2015. A 2000 year record of marine climate variability from Arnarfjörður, NW Iceland. 58 p. University of Iceland.

Karbowski, C., Finstad, B., Karbowski, N., Hedger, R., 2019. Sea lice in Iceland: assessing the status and current implications for aquaculture and wild salmonids. *Aquac. Environ. Interact.* 11, 149–160. doi:10.3354/aei00302

Kattner, G., Becker, H., 1991. Nutrients and organic nitrogenous compounds in the marginal ice zone of the Fram Strait. *J. Mar. Syst.* 2, 385–394. doi:10.1016/0924-7963(91)90043-T

Kauko, H.M., Olsen, L.M., Duarte, P., Peeken, I., Granskog, M.A., Johnsen, G., Fernández-Méndez, M., Pavlov, A.K., Mundy, C.J., Assmy, P., 2018. Algal colonization of young arctic sea ice in spring. *Front. Mar. Sci.* 5. doi:10.3389/fmars.2018.00199

Koc, N., Scherer, R.P., 1996. Neogene Diatom Biostratigraphy of the Iceland Sea Site 907, in: Thiede, J., Myhre, A.M., Firth, J. V., Johnson, G.L., Ruddiman, W.F. (Eds.), Proceedings of the Ocean Drilling Program, Scientific Results. Bergen. doi:10.2973/odp.proc.sr.151.108.1996

Koch, B.P., Dittmar, T., 2006. From mass to structure: An aromaticity index for high-resolution mass data of natural organic matter. *Rapid Commun. Mass Spectrom.* 20, 926–932. doi:10.1002/rcm.2386

Koch, B.P., John, U., Amann, R., Assmy, P., Bach, L., Burau, C., Edvardsen, B., Fernández-Méndez, M., Friedrichs, A., Geuer, J.K., Hoppema, M., Huhn, O., Iversen, M., Konrad, C., Kühne, N., Lechtenfeld, O.J., Mackensen, A., McCallister, S.L., Nystedt, E., Schmitt-Kopplin, P., Schwalfenberg, K., Seifert, M., Zielinski, O., Editorial, 2017. Molecular ecological chemistry in Arctic fjords at different stages of deglaciation, Cruise No. MSM56, July 2 - July 25, 2016, Longyearbyen (Svalbard, Norway) - Reykjavík (Iceland), MARIA S. MERIAN-Berichte. doi:10.2312/cr_msm56

Koch, B.P., Ludwichowski, K.U., Kattner, G., Dittmar, T., Witt, M., 2008. Advanced characterization of marine dissolved organic matter by combining reversed-phase liquid chromatography and FT-ICR-MS. *Mar. Chem.* 111, 233–241. doi:10.1016/j.marchem.2008.05.008

Koch, B.P., Witt, M., Engbrodt, R., Dittmar, T., Kattner, G., 2005. Molecular formulae of marine and terrigenous dissolved organic matter detected by electrospray ionization Fourier transform ion cyclotron resonance mass spectrometry. *Geochim. Cosmochim. Acta* 69, 3299–3308. doi:10.1016/j.gca.2005.02.027

Lail, E.M., Skrabal, S.A., Kieber, R.J., Bouillon, R.C., Wright, J.L.C., 2007. The role of particles on the biogeochemical cycling of domoic acid and its isomers in natural water matrices. *Harmful Algae* 6, 651–657. doi:10.1016/j.hal.2007.01.005

Lechtenfeld, O.J., Koch, B.P., Gašparović, B., Frka, S., Witt, M., Kattner, G., 2013. The influence of salinity on the molecular and optical properties of surface microlayers in a karstic estuary. *Mar. Chem.* 150, 25–38. doi:10.1016/j.marchem.2013.01.006

Leefmann, T., Frickenhaus, S., Koch, B.P., 2019. UltraMassExplorer: a browser-based application for the evaluation of high-resolution mass spectrometric data. Rapid Commun. *Mass Spectrom.* 33, 193–202. doi:10.1002/rcm.8315

Lema, K.A., Latimier, M., Nézan, É., Fauchot, J., Le Gac, M., 2017. Inter and intra-specific growth and domoic acid production in relation to nutrient ratios and concentrations in *Pseudo-nitzschia*: phosphate an important factor. *Harmful Algae* 64, 11–19. doi:10.1016/j.hal.2017.03.001

Leu, E., Mundy, C.J., Assmy, P., Campbell, K., Gabrielsen, T.M., Gosselin, M., Juul-Pedersen, T., Gradinger, R., 2015. Arctic spring awakening - Steering principles behind the phenology of vernal ice algal blooms. *Prog. Oceanogr.* 139, 151–170. doi:10.1016/j.pocean.2015.07.012

Leu, E., Wiktor, J., Søreide, J.E., Berge, J., Falk-Petersen, S., 2010. Increased irradiance reduces food quality of sea ice algae. *Mar. Ecol. Prog. Ser.* 411, 49–60. doi:10.3354/meps08647

Li, P., Tao, J., Lin, J., He, C., Shi, Q., Li, X., Zhang, C., 2019. Stratification of dissolved organic matter in the upper 2000 m water column at the Mariana Trench. *Sci. Total Environ.* 668, 1222–1231. doi:10.1016/j.scitotenv.2019.03.094

Lundholm, N., Krock, B., John, U., Skov, J., Cheng, J., Pančić, M., Wohlrab, S., Rigby, K., Nielsen, T.G., Selander, E., Harðardóttir, S., 2018. Induction of domoic acid production in diatoms—Types of grazers and diatoms are important. *Harmful Algae* 79, 64–73. doi:10.1016/j.hal.2018.06.005

Lundholm, N., Moestrup, Ø., Hasle, G.R., Hoef-Emden, K., 2003. A study of the *Pseudo-nitzschia pseudodelicatissima/cuspidata* complex (Bacillariophyceae): What is *P. pseudodelicatissima*? *J. Phycol.* 39, 797–813. doi:10.1046/j.1529-8817.2003.02031.x

Maldonado, M.T., Hughes, M.P., Rue, E.L., Wells, M.L., 2002. The effect of Fe and Cu on growth and domoic acid production by *Pseudo-nitzschia multiseries* and *Pseudo-nitzschia australis*. *Limnol. Oceanogr.* 47, 515–526. doi:10.4319/lo.2002.47.2.0515

Marine, V., Malmberg, S.-A., 1999. Near-surface circulation in Icelandic waters derived from satellite tracked drifters. *Rit Fiskid.* 16, 23–39.

Martin, M., 2011. Cutadapt removes adapter sequences from high-throughput sequencing reads. *EMBnet.journal* 17.1, 10–12.

McMurdie, P.J., Holmes, S., 2013. phyloseq: An R Package for Reproducible Interactive Analysis and Graphics of Microbiome Census Data. *PLoS One* 8, e61217. doi:10.1371/journal.pone.0061217

Melnikov, I.A., 2018. Characterization of the Biodiversity of Modern Sea Ice in the North Pole Region. *Dokl. Earth Sci.* 480, 792–795. doi:10.1134/S1028334X18060132

Melnikov, I.A., Kolosova, E.G., Welch, H.E., Zhitina, L.S., 2002. Sea ice biological communities and nutrient dynamics in the Canada Basin of the Arctic Ocean. *Deep. Res. Part I Oceanogr. Res. Pap.* 49, 1623–1649. doi:10.1016/S0967-0637(02)00042-0

Moschandreou, K.K., Papaefthimiou, D., Katikou, P., Kalopesa, E., Panou, A., Nikolaidis, G., 2010. Morphology, phylogeny and toxin analysis of *Pseudo-nitzschia pseudodelicatissima* (Bacillariophyceae) isolated from the Thermaikos Gulf, Greece. *Phycologia* 49, 260–273. doi:10.2216/PH09-42.1

Osterholz, H., Dittmar, T., Niggemann, J., 2014. Molecular evidence for rapid dissolved organic matter turnover in Arctic fjords. *Mar. Chem.* 160, 1–10. doi:10.1016/j.marchem.2014.01.002

Pan, Y., Bates, S.S., Cembella, A.D., 1998. Environmental stress and domoic acid production by *Pseudo-nitzschia*: A physiological perspective. *Nat. Toxins* 6, 127–135. doi:10.1002/(sici)1522-7189(199805/08)6:3/4<127::aid-nt9>3.3.co;2-u

Pan, Y., Parsons, M., Busman, M., Moeller, P., Dortch, Q., Powell, C., Doucette, G., 2001. *Pseudo-nitzschia* sp. cf. *pseudodelicatissima* - a confirmed producer of domoic acid from the northern Gulf of Mexico. *Mar. Ecol. Prog. Ser.* 220, 83–92. doi:10.3354/meps220083

Pan, Y., Subba Rao, D. V., Mann, K.H., 1996a. Changes in domoic acid production and cellular chemical composition of the toxigenic diatom *Pseudo-nitschia multiseries* under phosphate limitation. *J. Phycol.* 32, 371–381. doi:10.1111/j.0022-3646.1996.00371.x

Pan, Y., Subba Rao, D. V, Mann, K.H., Brown, R.G., Pocklington, R., 1996b. Effects of silicate limitation on production of domoic acid, a neurotoxin, by the diatom *Pseudo-nitzschia multiseries*. I. Batch culture studies. *Mar. Ecol. Prog. Ser.* 131, 225/233. doi:10.3354/meps131225

Prince, E., Irmer, F., Pohnert, G., 2013. Domoic Acid Improves the Competitive Ability of *Pseudo-nitzschia delicatissima* against the Diatom *Skeletonema marinoi*. *Mar. Drugs* 11, 2398–2412. doi:10.3390/md11072398

Reeh, N., Olesen, O.B., 1986. Velocity Measurements On Daugaard-Jensen Gletscher, Scoresby Sund, East Greenland. *Ann. Glaciol.* 8, 146–150. doi:10.3189/s0260305500001336

Rhodes, L., Jiang, W., Knight, B., Adamson, J., Smith, K., Langi, V., Edgar, M., 2013. The genus *Pseudo-nitzschia* (Bacillariophyceae) in New Zealand: Analysis of the last decade's monitoring data. New Zeal. *J. Mar. Freshw. Res.* 47, 490–503. doi:10.1080/00288330.2013.803489

Richlen, M.L., Zielinski, O., Holinde, L., Tillmann, U., Cembella, A., Lyu, Y., Anderson, D.M., 2016. Distribution of *Alexandrium fundyense* (Dinophyceae) cysts in Greenland and Iceland, with an emphasis on viability and growth in the Arctic. *Mar. Ecol. Prog. Ser.* 547, 33–46. doi:10.3354/meps11660

Rignot, E., Kanagaratnam, P., 2006. Changes in the velocity structure of the Greenland Ice Sheet. *Science* 311, 986–990. doi:10.1126/science.1121381

Rossel, P.E., Bienhold, C., Boetius, A., Dittmar, T., 2016. Dissolved organic matter in pore water of Arctic Ocean sediments: Environmental influence on molecular composition. *Org. Geochem.* 97, 41–52. doi:10.1016/j.orggeochem.2016.04.003

Roth, V.N., Dittmar, T., Gaupp, R., Gleixner, G., 2013. Latitude and pH driven trends in the molecular composition of DOM across a north south transect along the Yenisei River. *Geochim. Cosmochim. Acta* 123, 93–105. doi:10.1016/j.gca.2013.09.002

Ryan, J.P., Kudela, R.M., Birch, J.M., Blum, M., Bowers, H.A., Chavez, F.P., Doucette, G.J., Hayashi, K., Marin, R., Mikulski, C.M., Pennington, J.T., Scholin, C.A., Smith, G.J., Woods, A., Zhang, Y., 2017. Causality of an extreme harmful algal bloom in Monterey Bay, California, during the 2014–2016 northeast Pacific warm anomaly. *Geophys. Res. Lett.* 44, 5571–5579. doi:10.1002/2017GL072637

Rytter Hasle, G., Riddervold Heimdal, B., 1998. The net phytoplankton in Kongsfjorden, Svalbard, July 1988, with general remarks on species composition of Arctic phytoplankton. *Polar Res.* 17, 31–52. doi:10.3402/polar.v17i1.6605

Schnetzer, A., Miller, P.E., Schaffner, R.A., Stauffer, B.A., Jones, B.H., Weisberg, S.B., DiGiacomo, P.M., Berelson, W.M., Caron, D.A., 2007. Blooms of *Pseudo-nitzschia* and domoic acid in the San Pedro Channel and Los Angeles harbor areas of the Southern California Bight, 2003-2004. *Harmful Algae* 6, 372–387. doi:10.1016/j.hal.2006.11.004

Seifert, M., Hoppema, M., Burau, C., Friedrichs, A., Geuer, J.K., John, U., Koch, B.P., Konrad, C., van der Jagt, H., Iversen, M.H., 2019. Influence of glacial meltwater on summer biogeochemical cycles in Scoresby Sund, East Greenland. *Front. Mar. Sci.* 6. doi:10.3389/fmars.2019.00412

Silvert, W., Subba Rao, D. V, 1992. Dynamic Model of the Flux of Domoic Acid, a Neurotoxin, through a *Mytilus edulis* Population. *Can. J. Fish. Aquat. Sci.* 49, 400-405.

Sleighter, R.L., Hatcher, P.G., 2008. Molecular characterization of dissolved organic matter (DOM) along a river to ocean transect of the lower Chesapeake Bay by ultrahigh resolution electrospray ionization Fourier transform ion cyclotron resonance mass spectrometry. *Mar. Chem.* 110, 140–152. doi:10.1016/j.marchem.2008.04.008

Sleighter, R.L., Liu, Z., Xue, J., Hatcher, P.G., 2010. Multivariate statistical approaches for the characterization of dissolved organic matter analyzed by ultrahigh resolution mass spectrometry. *Environ. Sci. Technol.* 44, 7576–7582. doi:10.1021/es1002204

Stefánsson, U., Ólafsson, J., 1991. Nutrients and fertility of Icelandic waters, Rit Fiskideildar. Marine Research Institute, Reykjavík, 56 p.

Sugie, K., Fujiwara, A., Nishino, S., Kameyama, S., Harada, N., 2020. Impacts of Temperature, CO_2, and Salinity on Phytoplankton Community Composition in the Western Arctic Ocean. *Front. Mar. Sci.* 6. doi:10.3389/fmars.2019.00821

Svendsen, H., Beszczynska-Møller, A., Hagen, J.O., Lefauconnier, B., Tverberg, V., Gerland, S., Ørbæk, J.B., Bischof, K., Papucci, C., Zajaczkowski, M., Azzolini, R., Bruland, O., Wiencke, C., Winther, J.-G., Dallmann, W., 2002. The physical environment of Kongsfjorden-Krossfjorden, an Arctic fjord system in Svalbard. *Polar Res.* 21, 133–166.

Tammilehto, A., Nielsen, T.G., Krock, B., Møller, E.F., Lundholm, N., 2015. Induction of domoic acid production in the toxic diatom *Pseudo-nitzschia seriata* by calanoid copepods. *Aquat. Toxicol.* 159, 52–61. doi:10.1016/j.aquatox.2014.11.026

Thorel, M., Claquin, P., Schapira, M., Le Gendre, R., Riou, P., Goux, D., Le Roy, B., Raimbault, V., Deton-Cabanillas, A.F., Bazin, P., Kientz-Bouchart, V., Fauchot, J., 2017. Nutrient ratios influence variability in *Pseudo-nitzschia* species diversity and particulate domoic acid production in the Bay of Seine (France). *Harmful Algae* 68, 192–205. doi:10.1016/j.hal.2017.07.005

Trainer, V.L., Hickey, B.M., Bates, S.S., 2008. Toxic diatoms, in: Walsh, P.J., Smith, S.L., Fleming, L.E., Solo-Gabriele, H., Gerwick, W.H. (Eds.), Oceans and Human Health: Risks and Remedies from the Sea. Elsevier Science Publishers, New York, pp. 219–237.

Trainer, V.L., Wells, M.L., Cochlan, W.P., Trick, C.G., Bill, B.D., Batgh, K.A., Beall, B.F., Herndon, J., Lundholm, N., 2009. An ecological study of a massive bloom of toxigenic *Pseudo-nitzschia cuspidata* off the Washington State coast. *Limnol. Oceanogr.* 54, 1461–1474. doi:10.4319/lo.2009.54.5.1461

Trick, C.G., Trainer, V.L., Cochlan, W.P., Wells, M.L., Beall, B.F., 2018. The successional formation and release of domoic acid in a *Pseudo-nitzschia* bloom in the Juan de Fuca Eddy: A drifter study. *Harmful Algae* 79, 105–114. doi:10.1016/j.hal.2018.08.007

Tverberg, V., Skogseth, R., Cottier, F., Sundfjord, A., Walczowski, W., Inall, M.E., Falck, E., Pavlova, O., Nilsen, F., 2019. The Kongsfjorden Transect: Seasonal and Inter-annual Variability in Hydrography, in: Hop, H., Wiencke, C. (Eds.), The Ecosystem of Kongsfjorden, Svalbard. Springer Nature Switzerland AG, pp. 49–104. doi:10.1007/978-3-319-46425-1_3

Umhau, B.P., Benitez-Nelson, C.R., Anderson, C.R., McCabe, K., Burrell, C., 2018. A Time Series of Water Column Distributions and Sinking Particle Flux of *Pseudo-Nitzschia* and Domoic Acid in the Santa Barbara Basin, California. *Toxins* (Basel). 10, 480. doi:10.3390/toxins10110480

Van Meerssche, E., Pinckney, J.L., 2017. The influence of salinity in the domoic acid effect on estuarine phytoplankton communities. *Harmful Algae* 69, 65–74. doi:10.1016/j.hal.2017.10.003

Von Quillfeldt, C.H., Ambrose, W.G., Clough, L.M., 2003. High number of diatom species in first-year ice from the Chukchi Sea. *Polar Biol.* 26, 806–818. doi:10.1007/s00300-003-0549-1

Wang, Z., King, K.L., Ramsdell, J.S., Doucette, G.J., 2007. Determination of domoic acid in seawater and phytoplankton by liquid chromatography-tandem mass spectrometry. *J. Chromatogr. A* 1163, 169–176. doi:10.1016/j.chroma.2007.06.054

Wohlrab, S., John, U., Klemm, K., Eberlein, T., Forsberg Grivogiannis, A.M., Krock, B., Frickenhaus, S., Bach, L.T., Rost, B., Riebesell, U., Van de Waal, D.B., 2019. Ocean acidification increases domoic acid contents during a spring to summer succession of coastal phytoplankton. *Harmful Algae* 101697. doi:10.1016/j.hal.2019.101697

Wünsch, U.J., Acar, E., Koch, B.P., Murphy, K.R., Schmitt-Kopplin, P., Stedmon, C.A., 2018. The Molecular Fingerprint of Fluorescent Natural Organic Matter Offers Insight into Biogeochemical Sources and Diagenetic State. *Anal. Chem.* 90, 14188–14197. doi:10.1021/acs.analchem.8b02863

Xiao, C., Wu, X., Liu, T., Xu, G., Chi, R., 2017. Microbial Community Structure of Activated Sludge for Biosolubilization of Two Different Rock Phosphates. *Appl. Biochem. Biotechnol.* 182, 742–754. doi:10.1007/s12010-016-2358-3

Zhai, L., Gudmundsson, K., Miller, P., Peng, W., Guðfinnsson, H., Debes, H., Hátún, H., White, G.N., Hernández Walls, R., Sathyendranath, S., Platt, T., 2012. Phytoplankton phenology and production around Iceland and Faroes. *Cont. Shelf Res.* 37, 15–25. doi:10.1016/j.csr.2012.01.013

5 Manuscript III

Does dissolved domoic acid improve growth rates and iron content in low iron *Pseudo-nitzschia subcurvata*?

Jana K. Geuer[1*], Scarlett Trimborn[1,2], Florian Koch[1,3], Tina Brenneis[1], Bernd Krock[1], Boris P. Koch[1,3]

[1]Alfred Wegener Institute Helmholtz Centre for Polar and Marine Research, Bremerhaven, Germany

[2]Marine Botany, University of Bremen, Bremen, Germany

[3]Department of Technology, University of Applied Sciences Bremerhaven, Bremerhaven, Germany

* Correspondence: Corresponding Author: jana.geuer@awi.de

Keywords:

- Antarctica
- copper
- incubation experiment
- Diatoms (Bacillariophyceae)
- Phytoplankton
- toxin
- high nutrient low chlorophyll (HNLC) regions

5.1 Abstract

Many regions of Antarctica are classified as high nutrient low chlorophyll (HNLC) areas. In these, iron availability is limiting primary productivity and subsequent carbon export. Domoic acid (DA) has previously been detected in the Southern Ocean and suggested to act as a ligand that facilitates iron assimilation for *Pseudo-nitzschia* spp., species that contribute to Antarctic diatom blooms. An incubation experiment using the Antarctic species *Pseudo-nitzschia subcurvata* was performed in Antarctic seawater at low and high iron concentrations. Dissolved DA was added to one set of each of the two treatments. This was done to verify whether DA positively affects the growth of the non-toxic species *Pseudo-nitzschia subcurvata* and increases their cellular iron content, particularly under low iron conditions. We hypothesize that (i) DA is taken up under low iron conditions (ii) that more iron is taken up if DA is available and (iii) that the growth rate increases in the presence of DA. However, our results indicated that almost no DA was taken up by the cells and that low iron treatments did not profit from DA addition, nor did they result in elevated cellular iron content. No increase of the growth rate was observed in treatments where DA was added. However, the cellular copper content increased under low iron conditions when DA was added. This study highlights that dissolved DA in naturally occurring concentrations does not increase bioavailability of iron for *P. subcurvata* and that only species producing DA might profit from it.

5.2 Introduction

Marine and terrestrial primary production similarly contribute to global net primary production (Field et al., 1998). Phytoplankton fix marine carbon (Falkowski, 1994), a process which also requires nitrogen and phosphorous (Redfield, 1958), as well as trace elements such as iron, manganese, zinc, copper, cadmium, cobalt, and molybdenum (Quigg et al., 2003). Iron is a particularly important trace element as it is involved in many metabolic pathways including respiration and photosynthesis (Geider and La Roche, 1994). Many areas of the Southern Ocean (SO) are rich in macronutrients, but harbor low primary productivity making them so-called high nutrient low chlorophyll (HNLC) areas (Allanson et al., 1981). One of the most important limiting factors for phytoplankton growth in the SO is iron availability (Martin et al., 1990; De Baar et al., 1995). Important sources of iron to the SO are upwelling of iron rich deep water (Blain et al., 2007), iron rich sediments (Martin et al., 1990), atmospheric dust deposition (Martin, 1990), hydrothermal vents (Tagliabue et al., 2014), and icebergs (Smith et al., 2007). However, iron bioavailability critically depends on its

chemical speciation and resulting solubility (Boye et al., 2001). The speciation of iron can control phytoplankton community composition (Trimborn et al., 2017) with some phytoplankton species possessing more efficient mechanisms to adapt to low iron concentrations than others (Meyerink et al., 2017; Bender et al., 2018).

Domoic acid (DA) is primarily produced by different species of the diatom *Pseudo-nitzschia* (Bates et al., 1989) and is well known for its neurotoxicity, causing amnesic shellfish poisoning (Quilliam et al., 1989). While *Pseudo-nitzschia* species have a cosmopolitan distribution (Hasle, 2002; Trainer et al., 2012), not all species are capable of DA production (Silver et al., 2010; Lelong et al., 2012) and the amounts of DA produced can differ greatly. Depending on the species, blooms and different environmental conditions, the particulate DA (pDA) content can vary by eight orders of magnitude, between 2.5×10^{-9} pmol cell^{-1} (7.8×10^{-7} pg cell^{-1}) to 0.25 pmol cell^{-1} (78 pg cell^{-1}; Cerino et al., 2005; Trainer et al., 2000). pDA with $2.7\ 10^{-3}$ pmol cell^{-1} (0.85 pg cell^{-1}) quantified in the SO was two orders of magnitude lower. During the same study, dissolved DA (dDA) in the range of 6-707 pmol L^{-1} was measured (Silver et al., 2010). In a recent study, dDA up to 20 pmol L^{-1} was found in the SO (Geuer et al., 2019). The amount of DA released by cells can differ greatly (between 11% up to 83% of total DA) (Wang et al., 2007; Delegrange et al., 2018).

Although the primary ecological function of DA is still not well understood, various effects of the substance on its environment have been described. The diatom species *Pseudo-nitzschia seriata* increased DA production when exposed to exudates of predatory copepods (Tammilehto et al., 2015). Copepod escape response level decreased after ingestion of toxic *Pseudo-nitzschia* cells suggesting a role of DA as defense mechanism (Harðardóttir et al., 2018). Phosphate limitation also stimulated DA production (Lema et al., 2017). Furthermore, DA has been suggested to act as a ligand, binding both iron and copper (Rue and Bruland, 2001). Increased DA production under iron limitation and an even higher production under copper stress coupled to observations of increased DA release into the surrounding medium support such a role (Maldonado et al., 2002). DA was also suggested to act as a copper ligand as part of an efficient iron uptake system (Wells et al., 2005). Iron in connection with DA production is likely to improve competitiveness of *Pseudo-nitzschia* spp. over other diatoms (Prince et al., 2013). Generally, *Pseudo-nitzschia* spp. are known to adapt to low iron environments by modifying their cellular iron content (Marchetti et al., 2006) as well as their cell morphology by increased surface to volume (A:V) ratios (Marchetti and Harrison, 2007). Thus, *Pseudo-nitzschia* spp. show high species richness in open ocean HNLC regions (Marchetti et al., 2008, 2015). Furthermore, many *Pseudo-*

nitzschia spp. are among the best adapted species to low iron concentrations within the SO (Smetacek et al., 2004; Marchetti et al., 2006; Hoppe et al., 2013; Russo et al., 2015). In the species *P. granii*, which is associated with open ocean HNLC areas, genes were discovered, which encode iron storage and iron concentration proteins, showing that HNLC *Pseudo-nitzschia* spp. possess mechanisms for an efficient iron uptake (Marchetti et al., 2017).

At least seven different *Pseudo-nitzschia* spp. (*P. heimii, P. lineola, P. turgidula, P. prolongatoides, P. turgiduloides*, *P. subcurvata*, and *P. antarctica*) occur in the Weddell Sea and contribute to the diatom diversity (Kang and Fryxell, 1993; Almandoz et al., 2008; Lelong et al., 2012). *P. lineola* and *P. turgidula* are cosmopolitan species, while *P. prolongatoides, P. turgiduloides*, and *P. subcurvata* are endemic to the SO (Hasle and Syvertsen, 1997; Bates et al., 2018). Of the species found within Antarctica, DA production has been verified for *P. turgidula* and *P. lineola* (Rhodes et al., 1996; Silver et al., 2010). DA production in endemic *Pseudo-nitzschia* spp. of Antarctica, however, has barely been described (Kegel et al., 2013; Bates et al., 2018). *P. subcurvata* are reported to not produce DA (Fryxell et al., 1991), while the species *P. prolongatoides* and *P. antarctica* have not yet been tested for DA production (Lelong et al., 2012; Bates et al., 2018). Generally, the connection between DA, iron and Antarctic *Pseudo-nitzschia* species has been rarely studied (Bates et al., 2018), even though *Pseudo-nitzschia* are important contributors to local blooms under low iron concentrations.

In this study, we used the Antarctic species *Pseudo-nitzschia subcurvata*, which does not produce DA, to test whether this species benefits from the addition of dDA. We hypothesize that (i) the growth rates of *P. subcurvata* in low iron conditions potentially increase, if DA is available and (ii) that DA is taken up by the cells, (iii) thereby also enhancing its intracellular iron content.

5.3 Materials and Methods

5.3.1 Experimental conditions

The experiment was conducted under trace metal clean conditions according to GEOTRACES guidelines (Cutter et al., 2017). All equipment was soaked for one week in a 1% aqueous detergent solution (Citranox®, Alconox, Sigma-Aldrich, Germany), rinsed thoroughly with ultrapure water (UPW, Milli-Q®, Millipore A 10 system, Merck KGaA, Germany), and then placed in a hydrochloric acid (HCl) bath (1 mol L^{-1}, HPLC grade, Merck KGaA) for another week. Then, the items were rinsed with UPW again,

dried in a clean bench (Class 100, Opta, Germany), and stored in two polyethylene (PE) bags until use.

Monocultures of the diatom *Pseudo-nitzschia subcurvata* (isolated at 49° S, 02° E during ANT-XXI/4 in April 2004) were kept for more than two years in stock cultures in iron-deplete and -replete natural Antarctic seawater medium. Before the start of the main experiment, *P. subcurvata* was pre-acclimated for two weeks in dilute batch cultures in four different treatments (Table 1). To the Control treatment, no additions were made. To the treatments +DA and +FeDA dDA was added and to the treatments +Fe and +FeDA iron was added.

Table 1: Experimental setup. The treatments differed by concentrations of total dissolved iron (Fe) and dissolved domoic acid (DA). Addition of DA and iron was denoted by +. Initial dissolved copper concentrations are also shown.

Treatment	Domoic acid (nmol L^{-1})	Iron (nmol L^{-1})	Copper (nmol L^{-1})
+FeDA	3.5	1.72 ± 0.01	1.75 ± 0.04
+Fe	0	1.59 ± 0.13	1.63 ± 0.05
+DA	3.5	0.66 ± 0.08	1.28 ± 0.35
Control	0	0.75 ± 0.08	1.41 ± 0.09

Triplicate polycarbonate (PC) bottles were filled with 4.2 L of sterile filtered (0.2 µm, acid-cleaned Sartobran capsule, Sartorius, Germany) naturally low iron Antarctic seawater (0.7 nmol L^{-1} iron, collected at 59° 61' S, 148° 64' W in January 2017), spiked with macronutrients (100 µmol L^{-1} NO_3^-, 6.25 µmol L^{-1} PO_4^3 and 100 µmol L^{-1} Si^-), and vitamins (30 nmol L^{-1} B_1, 23 nmol L^{-1} B_7, and 0.228 nmol L^{-1} B_{12}) ($F/2^R$ medium; Guillard and Ryther, 1962).

In order to remove trace metals, all macronutrients and vitamins were passed through a chelex column (Chelex® 100, Merck KGaA). +Fe and +FeDA treatments were additionally spiked with iron (Fe(III), ICP-MS standard, TraceCERT®, Fluka, Germany) to obtain a final iron concentration of 1.7 nmol L^{-1}. To all treatments, zinc (0.16 nmol L^{-1}), copper (0.08 nmol L^{-1}), cobalt (0.09 nmol L^{-1}), molybdenum (0.05 nmol L^{-1}), and manganese (1.9 nmol L^{-1}) were added maintaining the ratio of the original f/2 recipe and representing trace metal concentrations typical for Antarctic open ocean waters. No ethylenediaminetetraacetic acid (EDTA) was added to avoid changing natural trace metal interactions of seawater (Gerringa et al., 2000). Treatments with DA addition were adjusted to a final concentration of 3500 pmol L^{-1} (Table 1) assuming an 11% release of dDA (Wang et al., 2007) from the particulate phase of a high pDA *Pseudo-nitzschia* bloom event (Smith et al., 2018). For all four treatments, abiotic treatments were prepared in duplicate being exposed for the same

time to the same four different experimental conditions except they were not inoculated with cells. All treatments were tested for bacterial DNA presence using polymerase chain reaction. The treatments were not axenic.

During the preacclimation phase as well as during the main experiment, cultures were maintained at 2 °C under a light : dark cycle of 16 : 8 h in front of light emitting diodes (LEDs, SolarStinger SunStrip Daylight, Econlux, Germany) at 100 µmol photons m^{-2} s^{-1} at color temperature of 8100 K. All treatments were harvested during exponential growth of the cells at a density of 0.6-1.2 x 10^5 cells mL^{-1} after six up to seven days, with no pH shifts occurring (Table 2).

5.3.2 Seawater iron chemistry and macronutrient concentrations

To prevent pH drifts in the cultures, the pH was monitored regularly at the growth temperature using a pH-Meter (827, Metrohm AG, Germany), which was calibrated (3-point calibration) with buffers certified from the National Institute of Standards and Technology before use. Upon harvest of the experiments, samples for dissolved inorganic carbon (DIC) were filtered through cartridges (0.2 µm, Thermo Scientific, Germany) into 5 mL air-tight borosilicate bottles with no headspace and stored at 4 °C until analysis. Quantification was performed via colorimetric analysis on an autoanalyzer (QuAAtro, SEAL Analytical GmbH, Germany). At the time of harvest, salinity was determined for every sample as well.

For the determination of total dissolved metal concentrations (Mn, Fe, Co, Cu, Zn), 100 mL of seawater was filtered under a laminar flow bench (Class 100, Opta). All used labware was cleaned as described in Dick et al., (2008). Prior to analysis, all seawater samples were acidified to pH 1.7 with sub-boiled HNO3 (distilled 65% HNO3, pro analysis, Merck KGaA) and irradiated for 1.5 h using a UV power supply system (7830) and photochemical lamp (7825) from ArcGlass to provide total dissolved concentrations of Cu and Co (Biller and Bruland, 2012). Mn, Fe, Co, Cu, and Zn concentrations in seawater samples were analyzed via external calibration using a SeaFAST system (Elemental Scientific, Germany) coupled to an Element2 mass spectrometer (Thermo Scientific). Standards for external calibration were prepared from Antarctic seawater and spiked with commercially available inductively coupled plasma mass spectrometry (ICP-MS) single element standards (SCP Science; 1000 mg L^{-1}). The SeaFAST system eliminates matrix components, such as Na, Mg, and Cl from the seawater and preconcentrates the samples by a factor 40. This procedure reduces possible interferences by the matrix and enables analyzing expected low concentrations of elements of interest. The Nass-7 reference material

(Natural Research Council Canada) was used to validate the quality of the analysis of trace elements in seawater at the beginning and end of a batch run. Since the element concentrations of the reference material are much higher than the concentrations expected in our seawater samples, the reference material was analyzed in a 1:10 dilution. The analysis of the Nass-7 reference material (n=10) showed good results for Mn, Fe, Co, and Cu, for which average and standard deviation were in range of the certified material. Recovery rates were Mn (99.9%), Fe (99.7%), Co (101%), Cu (93.2%), and Zn (170.2%).

5.3.3 Dissolved and particulate domoic acid

For dDA quantification, 1000 mL of sample were filtered via a combusted filter (glass microfiber filters, GF/F, ~0.7 µm, Whatman GmbH, Germany) at the end of the experiment. The aqueous phase was acidified to pH 2 and stored at 4 °C for a maximum of two days. The samples were then processed via solid-phase extraction. Cartridges (PPL, 200 mg, Agilent Technologies GmbH, Germany) were conditioned with 6 mL of methanol (100%, LiChrosolv®, HPLC grade, Merck KGaA) and 6 mL of acidified UPW (pH2, acidified with HCl, Suprapur®, Merck KGaA). Subsequently, the samples were loaded onto the cartridge. After loading, the cartridges were washed by filling them three times with acidified UPW before drying them with clean N_2. Two additions of 500 µL methanol were used to elute into weighed combusted screw top vials (Agilent Technologies GmbH). To determine the exact volume of the extract, the filled vials were weighed again and the actual volume of methanol extract as well as the enrichment factor of each sample was calculated. The samples were then stored at -20 °C until further analysis.

Corresponding filters for pDA analysis were stored in centrifuge tubes (Falcon™, Fisher Scientific, Germany) at -20 °C until further processing. For pDA extraction, the filters were thawed and transferred into microcentrifuge tubes (Eppendorf, Germany) filled with 0.9 g of ceramic beads. 1 mL of methanol was added to each sample, which was shaken at 6500 rpm for 45 seconds (MagNA Lyser, Roche, Switzerland). Subsequently, the samples were centrifuged for 15 min at 18111 x g (Centrifuge 5424 R, Eppendorf). In two steps, the supernatant was transferred onto a filter unit insert (0.45 µm, Durapore®, Merck KGaA) on a micro tube (Sarstedt, Germany), centrifuged for 30 seconds at 18111 x g, transferred into combusted screw top vials (Agilent Technologies GmbH) and stored at -20 °C until analysis. A process blank underwent the same procedure starting with filtration of 1000 mL of UPW.

Both dDA and pDA were analyzed via reversed phase ultrahigh performance liquid chromatography coupled to a triple quadrupole mass spectrometer (RP-UPLC-MS/MS, ACQUITY UPLC with Xevo TQ-XS, Waters) with electrospray ionization in positive mode. Total run time was 4.5 min at a flow rate of 0.6 mL min^{-1} with an aqueous formate buffer as mobile phase A, (pH 5.8, 20 mM ammonium formate, Riedel-de Haën, formic acid, Merck KGaA) and acetonitrile (LiChrosolv®, Merck KGaA) as mobile phase B. From 0-3.8 min, a gradient from 1-99% B was run, followed by isocratic conditions for 0.2 min. In a 0.3 min linear gradient the initial conditions were restored and the column equilibrated for another 0.2 min. Separation was performed on a C18 column with pre-column (2.1 x 50 mm, 1.7 µm, ACQUITY, Waters GmbH with BEH C18, 1.7 µm, VanGuard™, Waters GmbH, Germany) at 35 °C. DA was detected with mass transitions *m/z* 312 > 266 and 312 > 193. For dDA quantification the calibration curve was prepared in the extract of one of the abiotic treatments without DA addition to account for potential matrix effects. The calibration curve for pDA quantification was prepared in UPW. To determine limit of detection (LOD) and limit of quantification (LOQ), a calibration curve with DA concentrations of 0.25, 0.5, 1, 5, 10, 50 µg L^{-1} was measured 5 times. The calibration curves were prepared in an abiotic extract of the respective matrix and the limits calculated as described previously (Geuer et al., 2019). For dDA quantification, LOD was 2.8 µg L^{-1} (9 pmol L^{-1}) and LOQ was 8.7 µg L^{-1} (28 pmol L^{-1}) in water, accounting for an enrichment factor of 1000. LOD for pDA was 0.65 µg L^{-1} (2095 pmol L^{-1}) and LOQ was 1.97 µg L^{-1} (6349 pmol L^{-1}) in cell extract.

5.3.4 Growth rate and cell volume

Right after sampling, determination of cell density was performed at least every second day using a Multisizer™ 3 Particle Counter® (Beckman Coulter, Germany). Additionally, another set of subsamples was taken and fixed with 10% acid Lugol's solution and stored in the dark at 2 °C. To determine start and end point cell densities, cells were counted in Utermöhl chambers (Hydrobios, Germany) under an inverted microscope (Axio Observer D1, Zeiss, Germany) according to the method described by Utermöhl (1958). To this end, samples were allowed to settle for 24 hours before counting at least 400 cells in stripes. Growth rates were calculated from cell densities derived by light microscopy using the following formula:

$$\mu = \ln(N_{t_{end}} : N_{t_0})/t \quad (1)$$

where µ (d^{-1}) is the growth rate, N_{t0} and N_{tend} are the initial and final cell densities, respectively and t is the time between the sampled time points of the experiment.

To determine cell sizes, Lugol fixed samples from the end point of each sample were used. The length and width of 25 cells per sample were measured using the program AxioVision (Release 4.8.2, Carl Zeiss Microscopy GmbH, Germany) from pictures that were previously taken using a camera connected to the inverted microscope (Axio Observer, Carl Zeiss Microscopy GmbH) at a magnification of 640 x. The cell height was assumed to be half the cell width. From these dimensions, cellular biovolume and cell surface and subsequently cellular surface to volume ratios (A:V) were calculated using the formula for prism on parallelogram-base according to Hillebrand et al. (1999).

5.3.5 Organic matter

Dissolved and particulate organic matter was sampled at the end of the experiment. For the analyses of particulate organic carbon (POC) and particulate organic nitrogen (PON), 300 mL of sample were filtered through a precombusted (15 h, 500 °C) filter (GF/F, 0.7 µm, Whatman GmbH). The filters were stored in combusted (15 h, 500 °C) glass petri dishes at -20 °C. All POC samples were taken in duplicate. Between the two filtrations, a blank filter was put onto the filtration unit and pressure was applied for a few seconds. Prior to POC analysis, the samples were dried for 12 h at 60 °C. After drying, the filters were acidified with 200 µL of 0.2 N HCl (reagent grade, Sigma-Aldrich). The filters were again dried for 12 h at 60 °C. The dry filters were folded under clean air, packed into tin cups and stored at room temperature and a humidity of 32% until quantification. Analysis was performed on an Elemental Analyzer (Euro EA – CHNSO, HEKAtech GmbH, Germany). Combusted filter blanks were subtracted from the obtained yields. For cellular quotas, POC and PON were normalized to filtered volume and cell volume. For POC production, the cell-volume-normalized POC content was multiplied by the growth rate.

5.3.5.1 Pigment analysis

For pigment content, 200 mL of sample were filtered (GF/F, ~0.7 µm, Whatman GmbH). The filters were flash frozen in liquid nitrogen and subsequently stored at -80 °C. Before analysis, a 24 h dark extraction at 4 °C in 90% acetone was performed. After centrifugation (5 min, 4 °C, 18111 x g) and filtration (0.45 µm, Nalgene, Thermo Scientific) pigment concentrations were determined by RP high performance liquid chromatography (HPLC). The LaChrom Elite® HPLC system was equipped with a chilled autosampler (L-2200) connected to a DAD detector (L-2450, both VWR Hitachi International GmbH, Germany). For data analysis, the software EZChrom Elite (Ver. 3.1.3.; Agilent Technologies) was used. Separation was performed on a Spherisorb ODS-2 column (5 µm particle size, 25 cm x 4.6 mm, Waters) guarded by a

guard cartridge (LiChrospher 100-RP-18, Merck KGaA). A gradient was run as described in Wright (1991). Peaks of the pigments chlorophyll *a* and c_2, fucoxanthin, diadinoxanthin, diatoxanthin and β-carotene were identified and quantified against known standard concentrations (DHI Lab Products, Denmark).

5.3.6 Intracellular trace metal content

The cellular metal content was determined by filtering 500 mL over trace metal clean filters (0.2 µm, PC, Whatman GmbH). The filters were stored in clean reaction tubes (Eppendorf). For intracellular iron content, 500 mL were filtered over trace metal clean filters again. After filtration, the filters were rinsed with oxalic acid to remove cell surface bound metals (Hassler and Schoemann, 2009). After rinsing, the filters were stored in clean reaction tubes. Before analysis, the filters were digested in 5 mL HNO_3 (distilled 65%, p.a. Merck, USA) for 16 h at 180 °C with 0.5 mL HF (40%, Suprapur®, Merck KGaA) (Twining and Baines, 2013). Subsequently, 0.5 mL UPW was added. By evaporation under a glass hood at 140 °C, the cell extract was reduced to 0.5 mL. After the addition of 0.2 mL HNO_3 (distilled 65%, Merck, USA) and moving the solution to a clean vial, 10 µL Rh (1 mg L^{-1}) was added as internal standard. The sample was filled up to 10 mL with UPW and analyzed on an ICP-MS (Attom, Nu Instruments, UK). As reference samples to ensure low background trace metals and the quality of digestion, acid (5 mL 65% distilled HNO_3, 0.5 mL HF), two filter blanks and BCR-414 (Plankton reference material, Sigma-Aldrich) were processed and analyzed. BCR-414 recovery rates were Mn (87.1%), Fe (93.1%), Co (81.2%), Cu (81.5%), and Zn (85.1%). Intracellular iron quotas were normalized per cell volume.

5.3.7 Statistical analyses

To test normality of the data the Shapiro-Wilk test was applied. Normally distributed data was tested for statistical differences in means using analysis of variance (ANOVA). For non-normally distributed data Wilcoxon signed-rank test and Wilcoxon rank-sum test were used. Correlations between variables were tested using a correlation matrix based on Person correlation. The significance level for all tests was chosen as $\alpha = 0.05$ and significance was assumed when $p \leq 0.05$. Statistical tests were performed using R in the software application RStudio®.

5.4 Results

5.4.1 Iron chemistry and domoic acid concentrations

The salinity of all treatments during the experiment was 33.8 ± 0.2 (n = 12). DIC and pH did not show any significant differences between the treatments (Table 2).

Table 2: *P. subcurvata* grown under absence / addition of dissolved iron (Fe) and domoic acid (DA), respectively. Measured pH, and dissolved inorganic carbon (DIC) concentrations are shown. No DA was detected in the treatments without DA addition. Dissolved domoic acid (dDA) concentration and its relative recovery compared to the initial concentration are depicted as average ± standard deviation (n = 3). dDA was below the limit of detection (b.d.) in samples without DA addition. Particulate domoic acid (pDA) was above the limit of detection (LOD = 2095 pmol L^{-1} in cell extract) but below the limit of quantitation (LOQ = 6349 pmol L^{-1}). A theoretical calculated quantification of pDA for the treatments above LOD was performed (pDA amount). The results are shown as mean (n = 3).

		Control	+DA	+Fe	+FeDA
pH (Seawater scale)		8.16 ± 0.04	8.09 ± 0.01	8.14 ± 0.02	8.15 ± 0.00
DIC (µmol kg^{-1})		2089 ± 4	2093 ± 2	2104 ± 17	2084 ± 3
dDA	Conc. (pmol L^{-1})	b.d.	3258 ± 71	b.d.	3147 ± 124
	Recovery (%)	-	92 ± 2	-	89 ± 4
pDA	Amount (amol $cell^{-3}$)	-	0.035 (n=2)	-	0.034 (n=1)
	Contribution dDA (%)	-	~0.09	-	~0.12

dDA was below detection in non-amended controls but could be almost fully recovered in the different incubations of *P. subcurvata*, to which DA was added (Table 2), with a recovery rate for dDA of 92 ± 2% for treatment +DA and 89 ± 4% for treatment +FeDA. Recovery rates did not differ significantly between these treatments.

pDA was only quantified in the treatments with dDA addition. pDA levels were very low and only above detection in two bottles of +DA and in one bottle of the +FeDA treatment (Table 2). The approximate amount of pDA in these samples was 0.034 amol $cell^{-1}$. This pDA amount accounted on average for 0.10 ± 0.02% of the initially added DA.

5.4.2 Growth, cell volume, metal content and POC production

Growth rates differed significantly between low iron and +Fe treatments. Treatments Control and +DA showed significantly lower growth rates (for both: 0.44 ± 0.01 d^{-1}) compared to the +FeDA and +Fe treatments (0.53 ± 0.02 and 0.53 ± 0.01 d^{-1}; respectively, Fig. 1a). A:V ratios differed significantly between all treatments (Fig. 1b). The +DA treatment showed the highest A:V ratio (2.36 ± 0.01 $µm^{-1}$), while the +Fe treatment had the lowest ratio (1.99 ± 0.03). A:V ratio was significantly higher for low compared to high iron treatments.

POC production in the +DA treatment was lowest (6.8 ± 0.5 fmol μm^{-3} d^{-1}, Fig. 1c) while highest POC production was found in the +FeDA treatment (12.0 ± 1.2 fmol μm^{-3} d^{-1}). All treatment means differed significantly from each other. The POC content was highest in the +FeDA (23.2 ± 2.1 fmol μm^{-3}), followed by the +Fe treatment (18.9 ± 0.7 fmol μm^{-3}). In the Control and +DA treatment a significantly lower POC was observed (17.5 ± 0.6, 15.6 ± 1.4 fmol μm^{-3}, respectively, Table 3). Compared to all other treatments, +DA showed the highest C:N ratio (6.5 ± 0.2 mol mol^{-1}). There was no statistical difference between the other treatments. The PON content in +DA was significantly lower than in the other treatments (2.4 ± 0.2 fmol μm^{-3}), while it was highest in +FeDA (3.9 ± 0.2 fmol μm^{-3}, Table 3).

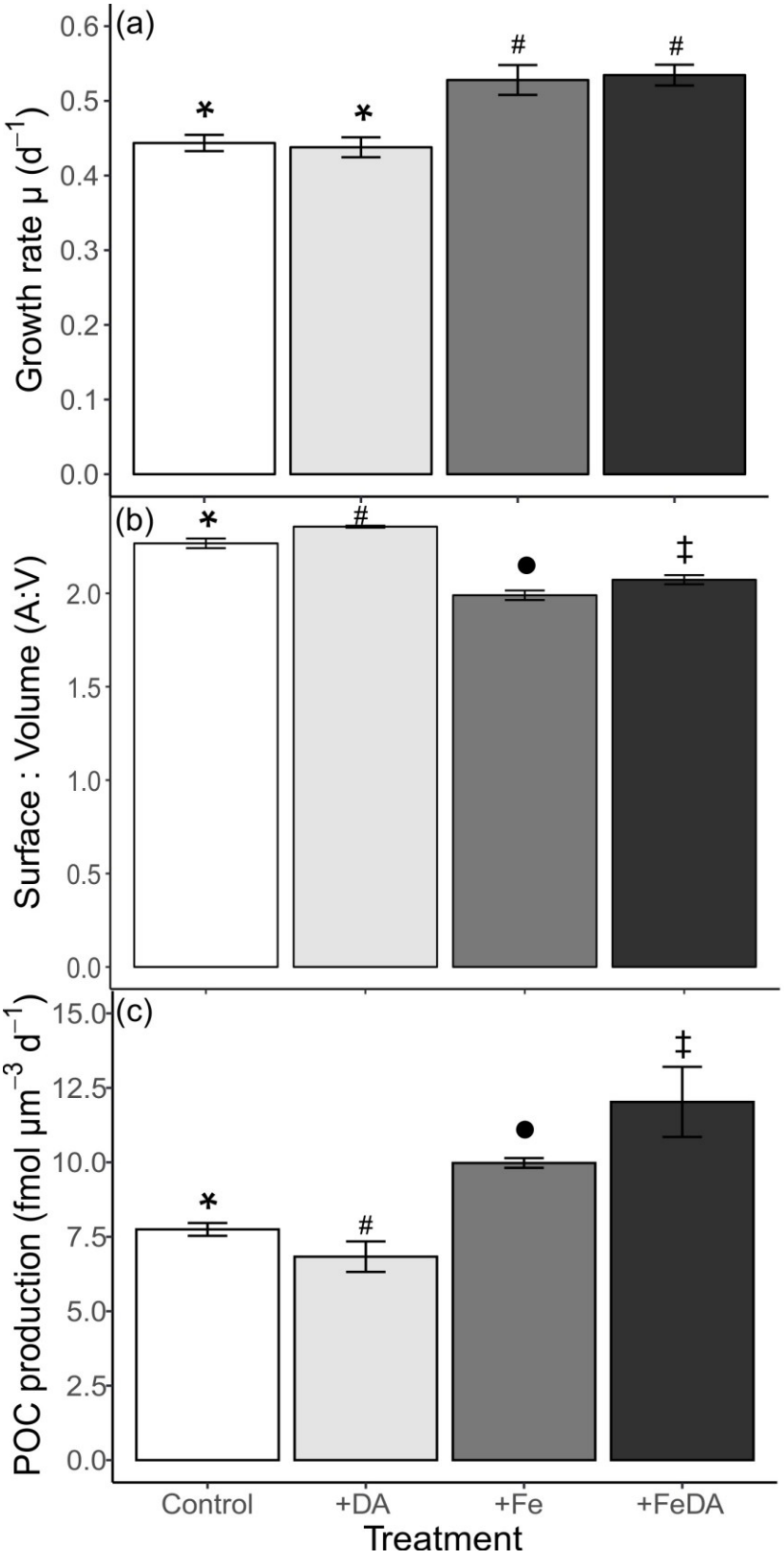

Figure 5 (a) Growth rates, (b) surface to volume ratio (A:V) and (c) particulate organic carbon (POC) production rates of the four different treatments. Low iron treatments (Control and +DA) are depicted in white and light grey, high iron treatments (+Fe and +FeDA) in grey and dark grey. Error bars represent the standard deviation between biological triplicates. Different symbols on top of the bars denote significant differences between the treatments ($p < 0.05$).

Cellular iron contents did not differ significantly between the treatments. The +Fe treatment showed the highest average iron content of 1.09 ± 0.61 amol μm^{-3}. In contrast, the cellular copper content was highest in +DA and differed significantly from the other treatments. Standard deviations for iron to carbon (Fe:C) ratios were high, particularly for treatment +Fe, which did not differ significantly from any other treatment (57.0 ± 30.4). Lowest Fe:C ratios were found in the Control and +FeDA treatment (23.1 ± 5.1 and 19.2 ± 4.7, respectively), a significantly higher Fe:C ratio was found in treatment +DA (50.2 ± 12.7, Table 3).

Table 3: Elemental composition of the cells: cell-volume-normalized particulate organic carbon and nitrogen (POC, PON) contents, molar carbon to nitrogen ratios (C:N), cell-volume-normalized iron and copper contents and molar iron to carbon (Fe:C) ratios for the four different treatments. All values are depicted as average ± standard deviation (n = 3). Significant differences between the treatments are denoted by different superscript symbols ($p < 0.05$).

	Control	**+DA**	**+Fe**	**+FeDA**
POC content (fmol μm^{-3})	17.5 ± 0.8*	15.6 ± 1.4*	18.9 ± 0.7$^{\#}$	23.2 ± 2.1•
PON content (fmol μm^{-3})	2.9 ± 0.2*	2.4 ± 0.2$^{\#}$	3.2 ± 0.1*	3.9 ± 0.2•
C:N (mol mol^{-1})	5.9 ± 0.3*	6.5 ± 0.2$^{\#}$	5.9 ± 0.0*	5.7 ± 0.3*
Iron content (amol μm^{-3})	0.41 ± 0.10*	0.77 ± 0.15*	1.09 ± 0.61*	0.44 ± 0.12*
Copper content (amol μm^{-3})	0.04 ± 0.03*	0.21 ± 0.11$^{\#}$	0.03 ± 0.04*	0.02 ± 0.02*
Fe:C (µmol mol^{-1})	23.1 ± 5.1*	50.2 ± 12.7$^{\#}$	57.0 ± 30.4*,$^{\#}$	19.2 ± 4.7*

5.4.2.1 Pigment concentrations

The concentration of the pigments diatoxanthin and β – carotene did not differ significantly between the treatments (Table 4). Diatoxanthin could not be quantified in Control and +DA treatments and was low in +Fe treatments. For pigments chlorophyll *a* and c_2, fucoxanthin and diadionoxanthin, both low iron treatments showed significantly lower concentrations than the +Fe treatments. Both chlorophyll c_2 and fucoxanthin were highest in the +FeDA treatment.

Table 4: Cellular pigment content in *P. subcurvata* grown in the four different treatments, normalized to cell volume. Chlorophyll c_2 and *a*, fucoxanthin, diadinoxanthin, diatoxanthin and β – carotene are listed. No diatoxanthin was detected (n.d.) in treatments Control and +DA. All values are mean of the triplicates ± standard deviation. Different symbols in superscript denote statistical differences between the treatments ($p < 0.05$).

	Control	**+DA**	**+Fe**	**+FeDA**
Chlorophyll c_2 (amol μm^{-3})	0.66 ± 0.09*	0.56 ± 0.03*	0.79 ± 0.05$^{\#}$	1.04 ± 0.14•
Chlorophyll *a* (amol μm^{-3})	3.04 ± 0.42*	3.00 ± 0.25*	4.71 ± 0.44$^{\#}$	5.57 ± 0.95$^{\#}$
Fucoxanthin (amol μm^{-3})	3.02 ± 0.38*	2.96 ± 0.08*	4.23 ± 0.31$^{\#}$	6.16 ± 1.22•
Diadinoxanthin (amol μm^{-3})	0.85 ± 0.11*	0.77 ± 0.03*	1.36 ± 0.14$^{\#}$	1.42 ± 0.27$^{\#}$
Diatoxanthin (amol μm^{-3})	n.d.	n.d.	0.06 ± 0.02*	0.08 ± 0.04*
β - carotene (amol μm^{-3})	0.10 ± 0.02*	0.09 ± 0.04*	0.16 ± 0.02*	0.16 ± 0.04*

5.5 Discussion

To determine whether dDA facilitates iron uptake for *Pseudo-nitzschia* spp. investigations on the potential production of dDA and pDA in iron-limiting conditions using species from HNLC regions are required to further elucidate the role of DA (Marchetti et al., 2008). This study furthers our understanding of whether DA plays a role in iron acquisition by *P. subcurvata*. This species is a prominent bloom-forming species of the largest HNLC region, the SO. We show that *P. subcurvata* did not take up any added DA, even under low iron conditions. Additionally and contrary to our hypothesis, the cells were not positively influenced by the addition of dDA in terms of growth rate, physiology and carbon content. Furthermore, there was no statistically significant difference in iron content between the different treatments.

5.5.1 Experimental conditions, recovery of dissolved domoic acid and low iron conditions

dDA was exclusively quantified in both +DA treatments and not found in treatments without dDA addition (Table 2). This outcome was expected as DA production by *P. subcurvata* has not been reported (Fryxell et al., 1991). In both +DA treatments, even though the recovery rate of dDA was 91 ± 3%, the amount of DA measured in the cells accounted for approximately 0.1%. Thus, the 10% loss of dDA cannot be explained by cellular uptake. The here observed loss of dDA could potentially be explained by adsorption and photodegradation. DA adsorbs to natural clays in a comparatively low amount compared with other common non-polar organic substances. Furthermore, the adsorption is enhanced if metal ions are present (Burns and Ferry, 2007). In an experiment investigating the production of DA and chemical cues, a PC membrane was used (Tammilehto et al., 2015). The authors suspected the PC membrane to hold back only lipophilic components. Bottles used for incubation in this experiment were also made from PC. The hydrophilic DA should thus not adsorb onto the surface of the treatment bottles in large amounts. DA is photochemically degraded in natural seawater if subjected to radiation (Bouillon et al., 2006; Fisher et al., 2006). The photodegradation rate usually decreases with decreasing radiation energy and is strongest at wavelengths in the UV range (280 – 400 nm) with a maximum at 330 nm (Bouillon et., 2006). Photodegradation still occurs at higher wavelengths and is promoted if Fe(III) ions and DOM are present (Fisher et al., 2006). In fact, all our treatments were illuminated 16 h per day with 100 µmol photons m^{-2} s^{-1} at 8100 K in this experiment, covering the range of wavelengths representative for daylight, but being out of the UV range in which photodegradation is most efficient.

Thus, it is likely that only a slight loss of dDA by photodegradation occurred in this experiment.

Iron concentrations in the medium without iron addition were 0.66 ± 0.08 nmol L^{-1} and 0.75 ± 0.08 nmol L^{-1}, respectively (Table 1). For both treatments without iron addition, the growth rate and POC production was significantly lower than for iron enriched treatments, while the A:V ratio was higher, indicating that the cells were physiologically iron limited (Maldonado et al., 2002; Marchetti and Harrison, 2007; Zhu et al., 2016). This is supported by light harvesting pigments (fucoxanthin, chlorophyll *a* and c_2, Table 4) being significantly lower in the low iron treatments (Koch et al., 2019; Koch and Trimborn 2019, Pagnone et al., unpublished data).

5.5.2 Effects of the experimental conditions on growth, size and elemental and pigment composition

Low iron treatments (Control and +DA) showed a significantly lower growth rate than high iron treatments (+Fe and +FeDA, Fig. 1a). Under iron deficiency and copper stress, growth rates of temperate *Pseudo-nitzschia* species have been shown to decrease by as much as 50% (Maldonado et al., 2002). In this experiment, the growth rates for both low iron treatments were 20% lower than for the +Fe treatments (Fig. 1a). In a previous temperature experiment with *P. subcurvata* the growth rate at 2°C was 0.6 d^{-1} under ample supply of iron (Zhu et al., 2017) and thus similar to our +Fe treatments. In agreement with our results, another experiment by Zhu et al., (2016), reported a 20% difference in growth rate of *P. subcurvata* at 0°C between low and high iron conditions. Cell numbers of *Pseudo-nitzschia* have been reported to increase when dDA was added to the medium (Trick et al., 2010) and an increased growth rate was previously observed upon the addition of dDA (Wells et al., 2005). Similarly, Prince et al. (2013) showed increased growth of *P. delicatissima* under iron replete conditions when dDA was added to the culture (Prince et al., 2013). In this study, however, we did not observe an increase in growth rate when dDA was added even at low iron conditions, findings contrary to our initial hypothesis. This is consistent with observations for DA producing *Pseudo-nitzschia* species. Even though an increased release of dDA in iron limited treatments was observed, exponential phase growth rates remained lower for these treatments than for iron sufficient treatments (Maldonado et al., 2002; Sobrinho et al., 2017).

A:V ratios were higher for the low iron treatments compared to the +Fe treatments. Enhanced A:V ratios are beneficial for cells since they help increase nutrient uptake, release of waste products and heat as well as uptake and loss of other compounds

(Lewis, 1976). Increasing A:V ratios under low iron environments is a common adaptation strategy of phytoplankton since it facilitates the uptake of trace metals (Raven and Kübler, 2002; Koch and Trimborn, 2019). The increase in A:V ratio was previously reported for *Pseudo-nitzschia* spp. grown under low iron conditions and hypothesized to facilitate iron uptake (Marchetti and Harrison, 2007). In this study, the average difference in A:V ratio between low and high iron treatments was 13%, which is in the range of what was previously observed for other species (9 – 40%, Marchetti and Harrison, 2007) and indicative of an acclimation to low iron condition. Surprisingly, the A:V ratio was highest in the +DA treatment, suggesting enhanced iron limitation stress for this treatment.

In our experiment, POC production was lowest in the low iron treatments (Fig. 1c). This is in line with previous studies, which showed generally a reduction of POC under iron deficiency in various phytoplankton species (e.g. Hoppe et al., 2013; Hutchins et al., 1999; Koch et al., 2019; Trimborn et al., 2019), the same as in temperate *Pseudo-nitzschia* species (Marchetti and Harrison, 2007), but also for the Antarctic *P. subcurvata* (Zhu et al., 2016).

Except for the +DA treatment, no changes in C:N ratios were observed (Table 3), with values being consistent with other temperate oceanic *Pseudo-nitzschia* spp. (Marchetti and Harrison, 2007). Similarly, the C:N ratio of *P. subcurvata* remained constant in response to different iron availabilities (Zhu et al., 2016) as well as temperature and pCO_2 (Zhu et al., 2017). Only for *P. pseudodelicatissima,* an increase of the C:N ratio with decreasing iron availability was reported (Sugie and Yoshimura, 2013). The authors suggested a rapid decrease in N relative to C assimilation under iron limitation. For our experiment, this was only observed in the +DA treatment, in which PON was lowest while POC remained similar in all treatments. Nitrogen assimilation can be limited by iron availability, since iron is essential for enzymes that reduce nitrate and nitrite (Morel et al., 1991; Milligan and Harrison, 2000). Milligan and Harrison (2000) suggested that during low iron availability the ability to process photons becomes limited within the photosynthetic electron transport chain, impacting also nitrite reduction as limiting step in nitrogen assimilation, which is a common phenomenon in iron limited phytoplankton (Hutchins et al., 1999). Nitrate reductase reduction was previously observed for low iron conditions, resulting also in a reduced nitrate assimilation capacity, which can be compensated by recycling proteins (Koch et al., 2019). Thus, an increase of C:N ratios may be triggered by iron limitation but often no changes are observed (Milligan and Harrison, 2000; Price, 2005; Koch et al., 2019). Hence, based on our data it appears that the combination of low iron availability and

DA addition caused higher iron stress and affected nitrogen metabolism relative to the low iron treatment alone.

Photosynthetic pigment contents in phytoplankton usually are reduced when iron is limiting, a process called chlorosis (Greene et al., 1991, 1992; Geider and La Roche, 1994). Chlorophyll *a* content was reduced in both low iron treatments (Table 4). The synthesis of chlorophyll *a* is negatively impacted by iron deficiency, which decreases its cellular content. An associated decrease in growth rate and carbon fixation was also observed in this and other experiments (Davey and Geider, 2001). *P. subcurvata* decreased their light harvesting pigments fucoxanthin, chlorophyll *a* and c_2 under iron limitation, which was previously observed in the Antarctic diatom *Phaeocystis antarctica* (Van Leeuwe and Stefels, 2007; Koch et al., 2019). Pigments of the xanthophyll cycle (diadinoxanthin und diatoxanthin) have been shown to decrease under iron limitation in the Antarctic diatom *Chaetoceros brevis*, while β – carotene content was not affected by iron limitation (Van Oijen et al., 2004). In our experiment, only the diadinoxanthin content was significantly lower in the low iron treatments. Diatoxanthin was not detected in these treatments, implying no increase in de-epoxidation of diadinoxanthin and thus no higher investment in photoprotective mechanisms (Olaizola et al., 1994; Van Oijen et al., 2004).

5.5.3 Uptake and potential effects of domoic acid on cellular metal contents under low iron conditions

The amount of DA in the cellular fraction of the treatments containing DA was below LOQ. Only in three out of six treatments with DA addition, pDA was detected at all (Table 2). Thus, there was no considerable uptake of dDA, which was not surprising, since DA not necessarily increases iron uptake by out-competing other ligands but by increasing bioavailability due to increased iron exchange among ligands and cell surface (Albrecht-Gary and Crumbliss, 1998; Maldonado et al., 2002). Rue and Bruland (2001) discovered that the strength, with which DA binds to iron and copper in combination with its concentration relative to other naturally occurring ligands does have the potential to affect their chemical speciation and thus their bioavailability and detoxification. In our experiment, DA was added at ecologically relevant concentrations previously reported for *Pseudo-nitzschia* blooms (Wang et al., 2007; Smith et al., 2018). The amount of DA present in the medium was thus high enough to act as a ligand, also for non-producing species (Maldonado et al., 2002). Furthermore, iron was added as Fe(III), which was shown to bind well to DA (Bates et al., 2001; Rue and Bruland, 2001) and was also used in previous experiments investigating DA and iron

uptake (Maldonado et al., 2002; Wells et al., 2005). Still, the cellular iron content did not differ significantly between the treatments (Table 3). However, the Fe:C ratio was significantly higher in +DA compared to the Control treatment. Treatments with iron addition did not show higher Fe:C ratios. The Fe:C in +FeDA was similar to the Control treatment, while in +Fe, the standard deviation within the triplicate was high. In contrast, other experiments using *Pseudo-nitzschia* describe Fe:C ratios usually higher by one to two orders of magnitude in high iron compared to low iron treatments (Maldonado et al., 2002; Marchetti et al., 2006). For *P. subcurvata*, iron limited Fe:C ratios of 25 µmol mol^{-1} (0°C) to 50 µmol mol^{-1} (4°C) were reported, while iron replete Fe:C ratios were higher (~70 and 210 µmol mol^{-1}, respectively) (Zhu et al., 2016). Fe:C ratios in our experiment were comparable to their iron limited Fe:C ratios. Surprisingly, in our experiment, iron addition did not result in elevated Fe:C ratios. Since *Pseudo-nitzschia* spp. generally adapt well to low iron concentrations (Marchetti et al., 2006; Sobrinho et al., 2017), the limiting effect of iron might be relatively low in this experiment, resulting in changes less prominent. With regard to DA addition, elevated Fe:C was observable in the +DA treatment but not in the +FeDA treatment, which showed equally low values as in the Control treatment. In another experiment under iron limitation, an increased iron uptake rate was observed when DA was added to present concentrations of FeEDTA (Maldonado et al., 2002). The authors, however, observed the same for iron replete treatments, even though the effect was lower. Thus, from our results it remains unclear whether dDA addition improves cellular iron acquisition.

The cellular copper content was significantly higher in the +DA treatment (Table 3). Rue and Bruland (2001) proved that relative to natural copper-binding organic ligands rather low concentrations of dDA are required to compete with other ligands for free copper ions. Since more copper than iron ions usually are available for complexation in natural seawater, complex formation between DA and copper is likely, even if DA has a higher theoretical complexation capacity for iron (Ladizinsky, 2003). In a study where *P. multiseries* was grown in low and high copper containing media (19.6 and 396 nmol L^{-1}, respectively) both dDA and pDA were lower in the low copper treatment (Fuentes and Wikfors, 2013). In contrast Ladizinsky, (2003) and Wells et al. (2005) observed a DA production increase and high dDA release when copper was deficient. In our experiment, the average copper concentration was 1.5 ± 0.2 nmol L^{-1} and thus not limiting (Lelong et al., 2013). An elevated copper uptake has been previously observed in iron limited oceanic diatoms (Peers et al., 2005; Koch and Trimborn, 2019). Copper is required for iron acquisition by diatoms (Peers et al., 2005). It was

also previously shown, that copper is essential for several *Pseudo-nitzschia* species to adapt to iron limiting environments (Wells et al., 2005; Lelong et al., 2013). Wells et al. (2005) suggested a high affinity iron uptake system in some *Pseudo-nitzschia* species involving copper uptake with the help of dDA. Iron complexed by siderophores would thus be assessed. Further tests of this hypothesis confirmed copper requirements in iron limited *P. delicatissima*, but in their experiment no production of DA was observed (Lelong et al., 2013). The authors interpreted that either their strain did not possess such an iron uptake system or not enough siderophores bound to iron were present in their experiment. The *P. subcurvata* used in this experiment also did not produce DA, but our results indicate that copper might be useful for iron limited cells in that they better access it when dDA was added to the medium. However, it remains uncertain if the elevated copper content was involved in obtaining the higher Fe:C ratio in the +DA treatment in comparison with the Control treatment.

Furthermore, no advantages for cells in treatment +DA were observed compared to the Control treatment in terms of growth, morphology and element ratios. Instead, treatment +DA showed increased A:V ratios, decreased POC production and higher cellular iron and copper values, indicating that cells of this treatment were in an even higher need for iron. *Pseudo-nitzschia* spp. are known to adapt better to low iron concentrations compared to other oceanic diatoms (Marchetti et al., 2006; Hoppe et al., 2013; Russo et al., 2015; Sobrinho et al., 2017). It was suggested, that *Pseudo-nitzschia* may cope with low iron conditions by using an efficient iron uptake system (Wells et al., 2005) and storing excess iron (Marchetti et al., 2006). Consistent with this hypothesis, in the species *P. granii,* genes for an iron independent photosynthetic and a putative iron transport system were expressed under low iron concentrations (Cohen et al., 2018). The results of our experiment indicate a relatively good adaptation of cells to the low iron concentration in the low iron treatments.

It is important to keep in mind that the biological function of DA as ligand for *Pseudo-nitzschia* is still not fully understood (Sobrinho et al., 2017). An increased uptake of iron was previously observed in a non-producing strain that took up more iron when DA was added (Maldonado et al., 2002). The authors suggested that dDA might increase the rate of exchange of iron among ligands in solution and the cell surface and might help with iron uptake even if the respective species might not possess the proposed uptake mechanisms (Albrecht-Gary and Crumbliss, 1998; Maldonado et al., 2002). In our experiments, no strong ligands were added to the treatments, but natural seawater was used that might have contained other ligands and dDA. However, the amount of dDA added in the experiment of Maldonado et al. (2002) was approximately

three orders of magnitude higher. Lelong et al. (2013) postulated that if DA is used as an iron uptake system, it might not occur in every *Pseudo-nitzschia* species, which might also apply to *P. subcurvata* used in this experiment. To further elucidate the role of DA as ligand, the mechanism of DA production in combination with iron uptake mechanisms should further be assessed. For the non-DA-producing species *P. subcurvata*, however, DA does not appear to play an important role as ligand increasing iron bioavailability in naturally occurring concentrations.

5.6 Conclusions

P. subcurvata was well adapted to deal with low iron conditions and the cells did not draw down the DA added, as only very small amounts were found in the cells and >90% remained as dDA in the media. The availability of dDA did not result in any physiological advantages for *P. subcurvata* under low iron conditions, showing that using DA does not seem to be a strategy to directly acquire more iron when it is scarce. In addition, while the cellular iron content did not increase the cellular copper content increased in the +DA treatment, possibly due to the added DA. Further investigations would, however, be required to investigate whether copper might be involved in subsequently increasing iron uptake. This study highlights that if dDA is produced and released as a ligand, it might only be advantageous to *Pseudo-nitzschia* and *Nitzschia* species, which are also capable of producing and taking up DA or that dDA would be required in higher concentrations than naturally occurring in the SO. Thus, it would be of interest to compare these results to other HNLC species capable of producing DA. This study confirmed that there still is considerable need for research in terms of the ecological and physiological role of DA, especially when iron is scarce.

Conflict of Interest

The authors declare that the research was conducted in the absence of any commercial or financial relationships that could be construed as a potential conflict of interest.

Author Contributions

ST, BPK, JKG, BK, FK, and TB designed this study. JKG and TB conducted the experiment. TB, JKG and FK acquired the data. JKG, ST, FK, BK, and BPK analyzed and interpreted the data. JKG wrote the manuscript with contributions and critical feedback from all co-authors.

Funding

JKG, BK, and BPK were funded by the strategy fund of the Alfred Wegener Institute Helmholtz Centre for Polar and Marine Research in the framework of the project “Inorganics in organics: Chemical and biological controls on micronutrient and carbon fluxes in the polar ocean” (Koch; IP76010001). ST, TB, and FK were funded by the Helmholtz Association (HGF Young Investigators Group EcoTrace, VH-NG-901). FK was furthermore supported by the Deutsche Forschungsgemeinschaft (SPP1158, KO5563/1-1‘ViTMeD’).

Acknowledgments

We would like to express our sincere thanks to C. Völkner for quantification of metals and advice for sample preparation and thank D. Wilhelms-Dick for performing pretests for the experiment. Furthermore, we would like to thank J. Tebben and W. Geibert for advice and lively discussions during planning this study. We sincerely thank B. Meyer-Schlosser for the pigment analysis and K.-U. Ludwichowski for nutrient analysis. M. Camoying and F. Pausch are thanked for their valuable help in the laboratory and M. Camoying for fruitful discussions about the results.

References

Albrecht-Gary, A.-M., and Crumbliss, A. L. (1998). „Coordination Chemistry of Siderophores: Thermodynamics and Kinetics of Iron Chelation and Release“, in *Metal Ions in Biological Systems*, eds. A. Sigel and H. Sigel (Marcel Dekker, Inc.), 239–327. doi:10.1002/cber.19971301203.

Allanson, B. R., Hart, R. C., and Lutjeharms, J. R. E. (1981). Observations on the nutrients, chlorophyll and primary production of the Southern Ocean south of Africa. *South African J. Antarct. Res.* 10/11, 3–14.

Almandoz, G. O., Ferreyra, G. A., Schloss, I. R., Dogliotti, A. I., Rupolo, V., Paparazzo, F. E., et al. (2008). Distribution and ecology of *Pseudo-nitzschia species* (Bacillariophyceae) in surface waters of the Weddell Sea (Antarctica). *Polar Biol.* 31, 429–442. doi:10.1007/s00300-007-0369-9.

Bates, S. S., Bird, C. J., de Freitas, A. S. W., Foxall, R., Gilgan, M., Hanic, L. A., et al. (1989). Pennate Diatom *Nitzschia pungens* as the Primary Source of Domoic Acid, a Toxin in Shellfish from Eastern Prince Edward Island, Canada. *Can. J. Fish. Aquat. Sci.* 46, 1203–1215. doi:10.1139/f89-156.

Bates, S. S., Hubbard, K. A., Lundholm, N., Montresor, M., and Leaw, C. P. (2018). *Pseudo-nitzschia*, *Nitzschia*, and domoic acid: New research since 2011. *Harmful Algae* 79, 3–43. doi:10.1016/j.hal.2018.06.001.

Bates, S. S., Léger, C., Satchwell, M., and Boyer, G. L. (2001). The effects of iron on domoic acid production by *Pseudo-nitzschia multiseries*. in *Harmful Algal Blooms (2000)*, eds. G. A. Hallegraeff, S. I. Blackburn, C. J. Bolch, and R. J. Lewis (Paris), 320–323.

Bender, S. J., Moran, D. M., Mcilvin, M. R., Zheng, H., Mccrow, J. P., Badger, J., et al. (2018). Iron triggers colony formation in *Phaeocystis antarctica*: connecting molecular mechanisms with iron biogeochemistry. *Biogeosciences Discuss.* doi:10.5194/bg-2017-558.

Biller, D. V., and Bruland, K. W. (2012). Analysis of Mn, Fe, Co, Ni, Cu, Zn, Cd, and Pb in seawater using the Nobias-chelate PA1 resin and magnetic sector inductively coupled plasma mass spectrometry (ICP-MS). *Mar. Chem.* 130–131, 12–20. doi:10.1016/j.marchem.2011.12.001.

Blain, S., Quéguiner, B., Armand, L., Belviso, S., Bombled, B., Bopp, L., et al. (2007). Effect of natural iron fertilization on carbon sequestration in the Southern Ocean. *Nature* 446, 1070–1074. doi:10.1038/nature05700.

Bouillon, R.-C., Knierim, T. L., Kieber, R. J., Skrabal, S. A., and Wright, J. L. C. (2006). Photodegradation of the algal toxin domoic acid in natural water matrices. *Limnol. Oceanogr.* 51, 321–330. doi:10.4319/lo.2006.51.1.0321.

Boye, M., Van Den Berg, C. M. G., De Jong, J. T. M., Leach, H., Croot, P., and De Baar, H. J. W. (2001). Organic complexation of iron in the Southern Ocean. *Deep. Res. Part I Oceanogr. Res. Pap.* 48, 1477–1497. doi:10.1016/S0967-0637(00)00099-6.

Burns, J. M., and Ferry, J. L. (2007). Adsorption of domoic acid to marine sediments and clays. *J. Environ. Monit.* 9, 1373–1377. doi:10.1039/b713101a.

Cerino, F., Orsini, L., Sarno, D., Dell' Aversano, C., Tartaglione, L., and Zingone, A. (2005). The alternation of different morphotypes in the seasonal cycle of the toxic diatom *Pseudo-nitzschia galaxiae*. *Harmful Algae* 4, 33–48. doi:10.1016/j.hal.2003.10.005.

Cohen, N. R., Gong, W., Moran, D. M., McIlvin, M. R., Saito, M. A., and Marchetti, A. (2018). Transcriptomic and proteomic responses of the oceanic diatom *Pseudo-nitzschia granii* to iron limitation. *Environ. Microbiol.* 20, 3109–3126. doi:10.1111/1462-2920.14386.

Cutter, G., Casciotti, K., Croot, P., Geibert, W., Heimbürger, L.-E., Lohan, M., et al. (2017). Sampling and Sample-handling Protocols for GEOTRACES Cruises. 3. doi:http://dx.doi.org/10.25607/OBP-2.

Davey, M., and Geider, R. J. (2001). Impact of iron limitation on the photosynthetic apparatus of the diatom *Chaetoceros muelleri* (Bacillariophyceae). *J. Phycol.* 37, 987–1000. doi:10.1046/j.1529-8817.2001.99169.x.

De Baar, H. J. W., de Jong, J. T. M., Bakker, D. C. E., Löscher, B. M., Veth, C., Bathmann, U., et al. (1995). Importance of iron for plankton blooms and carbon dioxide drawdown in the Southern Ocean. *Nature* 373, 412–415. doi:10.1038/373412a0.

Delegrange, A., Lefebvre, A., Gohin, F., Courcot, L., and Vincent, D. (2018). *Pseudo-nitzschia* sp. diversity and seasonality in the southern North Sea, domoic acid levels and associated phytoplankton communities. *Estuar. Coast. Shelf Sci.* 214, 194–206. doi:10.1016/j.ecss.2018.09.030.

Dick, D., Wegner, A., Gabrielli, P., Ruth, U., Barbante, C., and Kriews, M. (2008). Rare earth elements determined in Antarctic ice by inductively coupled plasma-time of flight, quadrupole and sector field-mass spectrometry: An inter-comparison study. *Anal. Chim. Acta* 621, 140–147. doi:10.1016/j.aca.2008.05.026.

Falkowski, P. G. (1994). The role of phytoplankton photosynthesis in global biogeochemical cycles. *Photosynth. Res.* 39, 235–258. doi:10.1007/BF00014586.

Field, C. B., Behrenfeld, M. J., Randerson, J. T., and Falkowski, P. (1998). Primary Production of the Biosphere: Integrating Terrestrial and Oceanic Components. *Science* 281, 237–240. doi:10.1126/science.281.5374.237.

Fisher, J. M., Reese, J. G., Pellechia, P. J., Moeller, P. L., and Ferry, J. L. (2006). Role of Fe(III), phosphate, dissolved organic matter, and nitrate during the photodegradation of domoic acid in the marine environment. *Environ. Sci. Technol.* 40, 2200–2205. doi:10.1021/es051443b.

Fryxell, G. A., Garza, S. A., and Roelke, D. L. (1991). Auxospore formation in an Antarctic clone of *Nitzschia subcurvata* hasle. *Diatom Res.* 6, 235–245. doi:10.1080/0269249X.1991.9705169.

Fuentes, M. S., and Wikfors, G. H. (2013). Control of domoic acid toxin expression in *Pseudo-nitzschia multiseries* by copper and silica: Relevance to mussel aquaculture in New England (USA). *Mar. Environ. Res.* 83, 23–28. doi:10.1016/j.marenvres.2012.10.005.

Geider, R. J., and La Roche, J. (1994). The role of iron in phytoplankton photosynthesis, and the potential for iron-limitation of primary productivity in the sea. *Photosynth. Res.* 39, 274–301. doi:10.1007/BF00014588.

Gerringa, L. J. A., de Baar, H. J. W., and Timmermans, K. R. (2000). A comparison of iron limitation of phytoplankton in natural oceanic waters and laboratory media conditioned with EDTA. *Mar. Chem.* 68, 335–346. doi:10.1016/S0304-4203(99)00092-4.

Geuer, J. K., Krock, B., Leefmann, T., and Koch, B. P. (2019). Quantification, extractability and stability of dissolved domoic acid within marine dissolved organic matter. *Mar. Chem.* 215, 103669. doi:10.1016/j.marchem.2019.103669.

Greene, R. M., Geider, R. J., and Falkowski, P. G. (1991). Effect of iron limitation on photosynthesis in a marine diatom. *Limnol. Oceanogr.* 36, 1772–1782. doi:10.4319/lo.1991.36.8.1772.

Greene, R. M., Geider, R. J., Kolber, Z., and Falkowski, P. G. (1992). Iron-induced changes in light harvesting and photochemical energy conversion processes in eukaryotic marine algae. *Plant Physiol.* 100, 565–575. doi:10.1104/pp.100.2.565.

Guillard, R., and Ryther, J. (1962). Studies of marine planctonic diatoms I. *Cyclotella nana* Hustedt and *Detonula confervacea* (Cleve) Gran. *Can. J. Microbiol.* 8, 229–239.

Harðardóttir, S., Krock, B., Wohlrab, S., John, U., Gissel, T., and Lundholm, N. (2018). Can domoic acid affect escape response in copepods? *Harmful Algae* 79, 50–52. doi:10.1016/j.hal.2018.08.009.

Hasle, G. R. (2002). Are most of the domoic acid-producing species of the diatom genus *Pseudo-nitzschia* cosmopolites? *Harmful Algae* 1, 137–146. doi:10.1016/S1568-9883(02)00014-8.

Hasle, G. R., and Syvertsen, E. E. (1997). “Marine diatoms,” in *Identifying marine phytoplankton*, ed. C. R. Thomas (San Diego: Academic Press), 5–385.

Hassler, C. S., and Schoemann, V. (2009). Discriminating between intra- and extracellular metals using chemical extractions: an update on the case of iron. *Limnol. Oceanogr. Methods* 7, 479–489. doi:10.4319/lom.2009.7.479.

Hillebrand, H., Dürselen, C. D., Kirschtel, D., Pollingher, U., and Zohary, T. (1999). Biovolume calculation for pelagic and benthic microalgae. *J. Phycol.* 35, 403–424. doi:10.1046/j.1529-8817.1999.3520403.x.

Hoppe, C. J. M., Hassler, C. S., Payne, C. D., Tortell, P. D., Rost, B. R., and Trimborn, S. (2013). Iron limitation modulates ocean acidification effects on Southern Ocean phytoplankton communities. *PLoS One* 8. doi:10.1371/journal.pone.0079890.

Hutchins, D. A., Franck, V. M., Brzezinski, M. A., and Bruland, K. W. (1999). Inducing phytoplankton iron limitation in iron-replete coastal waters with a strong chelating ligand. *Limnol. Oceanogr.* 44, 1009–1018. doi:10.4319/lo.1999.44.4.1009.

Kang, S.-H., and Fryxell, G. A. (1993). Phytoplankton in the Weddell Sea, Antarctica: composition, abundance and distribution in water-column assemblages of the marginal ice-edge zone during austral autumn. *Mar. Biol.* 348, 335–348.

Kegel, J. U., Del Amo, Y., and Medlin, L. K. (2013). Introduction to project MIDTAL: Its methods and samples from Arcachon Bay, France. *Environ. Sci. Pollut. Res.* 20, 6690–6704. doi:10.1007/s11356-012-1299-9.

Koch, F., Beszteri, S., Harms, L., and Trimborn, S. (2019). The impacts of iron limitation and ocean acidification on the cellular stoichiometry, photophysiology, and transcriptome of *Phaeocystis antarctica*. *Limnol. Oceanogr.* 64, 357–375. doi:10.1002/lno.11045.

Koch, F., and Trimborn, S. (2019). Limitation by Fe, Zn, Co, and B_{12} results in similar physiological responses in two antarctic phytoplankton species. *Front. Mar. Sci.* 6. doi:10.3389/fmars.2019.00514.

Ladizinsky, N. (2003). The influences of dissolved copper on the production of domoic acid by *Pseudo-nitzschia* species in Monterey Bay, California: laboratory experiments and field observations. 68 p.

Lelong, A., Bucciarelli, E., Hégaret, H., and Soudant, P. (2013). Iron and copper limitations differently affect growth rates and photosynthetic and physiological parameters of the marine diatom *Pseudo-nitzschia delicatissima*. *Limnol. Oceanogr.* 58, 613–623. doi:10.4319/lo.2013.58.2.0613.

Lelong, A., Hégaret, H., Soudant, P., and Bates, S. S. (2012). *Pseudo-nitzschia* (Bacillariophyceae) species, domoic acid and amnesic shellfish poisoning: revisiting previous paradigms. *Phycologia* 51, 168–216. doi:10.2216/11-37.

Lema, K. A., Latimier, M., Nézan, É., Fauchot, J., and Le Gac, M. (2017). Inter and intra-specific growth and domoic acid production in relation to nutrient ratios and concentrations in *Pseudo-nitzschia*: phosphate an important factor. *Harmful Algae* 64, 11–19. doi:10.1016/j.hal.2017.03.001.

Lewis, W. (1976). Surface/Volume Ratio: Implications for Phytoplankton Morphology. *Science* 192, 885–887. doi:10.1126/science.192.4242.885.

Maldonado, M. T., Hughes, M. P., Rue, E. L., and Wells, M. L. (2002). The effect of Fe and Cu on growth and domoic acid production by *Pseudo-nitzschia multiseries* and *Pseudo-nitzschia australis*. *Limnol. Oceanogr.* 47, 515–526. doi:10.4319/lo.2002.47.2.0515.

Marchetti, A., Catlett, D., Hopkinson, B. M., Ellis, K., and Cassar, N. (2015). Marine diatom proteorhodopsins and their potential role in coping with low iron availability. *ISME J.* 9, 2745–2748. doi:10.1038/ismej.2015.74.

Marchetti, A., and Harrison, P. J. (2007). Coupled changes in the cell morphology and the elemental C, N, and Si composition of the pennate diatom *Pseudo-nitzschia* due to iron deficiency. *Limnol. Oceanogr.* 52, 2270–2284.

Marchetti, A., Lundholm, N., Kotaki, Y., Hubbard, K., Harrison, P. J., and Virginia Armbrust, E. (2008). Identification and assessment of domoic acid production in oceanic *Pseudo-nitzschia* (Bacillariophyceae) from iron-limited waters in the northeast subarctic Pacific. *J. Phycol.* 44, 650–661. doi:10.1111/j.1529-8817.2008.00526.x.

Marchetti, A., Maldonado, M. T., Lane, E. S., and Harrison, P. J. (2006). Iron requirements of the pennate diatom *Pseudo-nitzschia*: Comparison of oceanic (high-nitrate, low-chlorophyll waters) and coastal species. *Limnol. Oceanogr.* 51, 2092–2101.

Marchetti, A., Moreno, C. M., Cohen, N. R., Oleinikov, I., deLong, K., Twining, B. S., et al. (2017). Development of a molecular-based index for assessing iron status in bloom-forming pennate diatoms. *J. Phycol.* 53, 820–832. doi:10.1111/jpy.12539.

Martin, J. H. (1990). Glacial-interglacial CO_2 change: The Iron Hypothesis. *Paleoceanography* 5, 1–13. doi:10.1029/PA005i001p00001.

Martin, J. H., Gordon, R. M., and Fitzwater, S. E. (1990). Iron in Antarctic waters. *Nature* 345, 156–158. doi:10.1038/345156a0.

Meyerink, S. W., Ellwood, M. J., Maher, W. A., Dean Price, G., and Strzepek, R. F. (2017). Effects of iron limitation on silicon uptake kinetics and elemental stoichiometry in two Southern Ocean diatoms, *Eucampia antarctica* and *Proboscia inermis*, and the temperate diatom *Thalassiosira pseudonana*. *Limnol. Oceanogr.* 62, 2445–2462. doi:10.1002/lno.10578.

Milligan, A. J., and Harrison, P. J. (2000). Effects of non-steady-state iron limitation on nitrogen assimilatory enzymes in the marine diatom *Thalassiosira weissflogii* (Bacillariophyceae). *J. Phycol.* 36, 78–86. doi:10.1046/j.1529-8817.2000.99013.x.

Morel, F. M. M. M., Hudson, R. J. M., and Price, N. M. (1991). Limitation of productivity by trace metals in the sea. *Limnol. Oceanogr.* 36, 1742–1755. doi:10.4319/lo.1991.36.8.1742.

Olaizola, M., La Roche, J., Kolber, Z., and Falkowski, P. G. (1994). Non-photochemical fluorescence quenching and the diadinoxanthin cycle in a marine diatom. *Photosynth. Res.* 41, 357–370. doi:10.1007/BF00019413.

Peers, G., Quesnel, S. A., and Price, N. M. (2005). Copper requirements for iron acquisition and growth of coastal and oceanic diatoms. *Limnol. Oceanogr.* 50, 1149–1158. doi:10.4319/lo.2005.50.4.1149.

Price, N. M. (2005). The elemental stoichiometry and composition of an iron-limited diatom. *Limnol. Oceanogr.* 50, 1159–1171. doi:10.4319/lo.2005.50.4.1159.

Prince, E. K., Irmer, F., and Pohnert, G. (2013). Domoic acid improves the competitive ability of *Pseudo-nitzschia delicatissima* against the diatom *Skeletonema marinoi*. *Mar. Drugs* 11, 2398–2412. doi:10.3390/md11072398.

Quigg, A., Finkel, Z. V, Irwin, A. J., Rosenthal, Y., Ho, T.-Y., Reinfelder, J. R., et al. (2003). The evolutionary inheritance of elemental stoichiometry in marine phytoplankton. *Nature* 425, 291–4. doi:10.1038/nature01953.

Quilliam, M. A., Sim, P. G., McCulloch, A. W., and McCinnes, A. G. (1989). High-performance liquid chromatography of domoic acid, a marine neurotoxin, with application to shellfish and plankton. *Int. J. Environ. Anal. Chem.* 36, 139–154. doi:10.1080/03067318908026867.

Raven, J. A., and Kübler, J. E. (2002). New light on the scaling of metabolic rate with the size of algae. *J. Phycol.* 38, 11–16. doi:10.1046/j.1529-8817.2002.01125.x.

Redfield, A. C. (1958). The biological control of chemical factors in the environment. *Am. Sci.* 46, 205–221.

Rhodes, L. L., White, D., Shyre, M., and Atkinson, M. (1996). "*Pseudo-nitzschia* species isolated from New Zealand coastal waters: domoic acid production in vitro and links with shellfish toxicity," in *Harmful and toxic algal blooms*, eds. T. Yasumoto, Y. Oshima, and M. Fukuyo (Paris: Intergovernmental Oceanographic Commission of UNESCO), 155–158.

Rue, E., and Bruland, K. (2001). Domoic acid binds iron and copper: a possible role for the toxin produced by the marine diatom *Pseudo-nitzschia*. *Mar. Chem.* 76, 127–134. doi:10.1016/S0304-4203(01)00053-6.

Russo, A. D. A. P. G., de Souza, M. S., Mendes, C. R. B., Jesus, B., Tavano, V. M., and Garcia, C. A. E. (2015). Photophysiological effects of Fe concentration gradients on diatom-dominated phytoplankton assemblages in the Antarctic Peninsula region. *J. Exp. Mar. Bio. Ecol.* 466, 49–58. doi:10.1016/j.jembe.2015.02.002.

Silver, M. W., Bargu, S., Coale, S. L., Benitez-Nelson, C. R., Garcia, A. C., Roberts, K. J., et al. (2010). Toxic diatoms and domoic acid in natural and iron enriched waters of the oceanic Pacific. *Proc. Natl. Acad. Sci.* 107, 20762–20767. doi:10.1073/pnas.1006968107.

Smetacek, V., Assmy, P., and Henjes, J. (2004). The role of grazing in structuring Southern Ocean pelagic ecosystems and biogeochemical cycles. *Antarct. Sci.* 16, 541–558. doi:10.1017/S0954102004002317.

Smith, J., Gellene, A. G., Hubbard, K. A., Bowers, H. A., Kudela, R. M., Hayashi, K., et al. (2018). *Pseudo-nitzschia* species composition varies concurrently with domoic acid concentrations during two different bloom events in the Southern California Bight. *J. Plankton Res.* 40, 1–17. doi:10.1093/plankt/fbx069.

Smith, K. L., Robison, B. H., Helly, J. J., Kaufmann, R. S., Ruhl, H. A., Shaw, T. J., et al. (2007). Free-drifting icebergs: Hot spots of chemical and biological enrichment in the Weddell Sea. *Science* 317, 478–482. doi:10.1126/science.1142834.

Sobrinho, B. F., De Camargo, L. M., Sandrini-Neto, L., Kleemann, C. R., Da Costa Machado, E., and Mafra, L. L. (2017). Growth, toxin production and allelopathic effects of *Pseudo-Nitzschia multiseries* under Iron-enriched conditions. *Mar. Drugs* 15. doi:10.3390/md15100331.

Sugie, K., and Yoshimura, T. (2013). Effects of pCO_2 and iron on the elemental composition and cell geometry of the marine diatom *Pseudo-nitzschia pseudodelicatissima* (Bacillariophyceae). *J. Phycol.* 49, 475–488. doi:10.1111/jpy.12054.

Tagliabue, A., Aumont, O., and Bopp, L. (2014). The impact of different external sources of iron on the global carbon cycle. *Geophys. Res. Lett.* 41, 920–926. doi:10.1002/2013GL059059.

Tammilehto, A., Nielsen, T. G., Krock, B., Møller, E. F., and Lundholm, N. (2015). Induction of domoic acid production in the toxic diatom *Pseudo-nitzschia seriata* by calanoid copepods. *Aquat. Toxicol.* 159, 52–61. doi:10.1016/j.aquatox.2014.11.026.

Trainer, V. L., Adams, N. G., Bill, B. D., Stehr, C. M., Wekell, J. C., Moeller, P., et al. (2000). Domoic acid production near California coastal upwelling zones, June (1998). *Limnol Ocean.* 45, 1818–1833. doi:https://doi.org/10.4319/lo.2000.45.8.1818.

Trainer, V. L., Bates, S. S., Lundholm, N., Thessen, A. E., Cochlan, W. P., Adams, N. G., et al. (2012). *Pseudo-nitzschia* physiological ecology, phylogeny, toxicity, monitoring and impacts on ecosystem health. *Harmful Algae* 14, 271–300. doi:10.1016/j.hal.2011.10.025.

Trick, C. G., Bill, B. D., Cochlan, W. P., Wells, M. L., Trainer, V. L., and Pickell, L. D. (2010). Iron enrichment stimulates toxic diatom production in high-nitrate, low-chlorophyll areas. *Proc. Natl. Acad. Sci. U. S. A.* 107, 5887–5892. doi:10.1073/pnas.0910579107.

Trimborn, S., Brenneis, T., Hoppe, C. J. M., Laglera, L. M., Norman, L., Santos-Echeandía, J., et al. (2017). Iron sources alter the response of Southern Ocean phytoplankton to ocean acidification. *Mar. Ecol. Prog. Ser.* 578, 35–50. doi:10.3354/meps12250.

Trimborn, S., Thoms, S., Bischof, K., and Beszteri, S. (2019). Susceptibility of two southern ocean phytoplankton key species to iron limitation and high light. *Front. Mar. Sci.* 6. doi:10.3389/fmars.2019.00167.

Twining, B. S., and Baines, S. B. (2013). The Trace Metal Composition of Marine Phytoplankton. *Ann. Rev. Mar. Sci.* 5, 191–215. doi:10.1146/annurev-marine-121211-172322.

Utermöhl, H. (1958). Zur Vervollkommnung der quantitativen Phytoplankton-Methodik. *Int. Vereinigung für Theor. und Angew. Limnol. Mitteilungen* 9, 1–38. doi:10.1080/05384680.1958.11904091.

Van Leeuwe, M. A., and Stefels, J. (2007). Photosynthetic responses in *Phaeocystis antarctica* towards varying light and iron conditions. *Biogeochemistry* 83, 61–70. doi:10.1007/978-1-4020-6214-8_6.

Van Oijen, T., Van Leeuwe, M. A., Gieskes, W. W. C., and De Baar, H. J. W. (2004). Effects of iron limitation on photosynthesis and carbohydrate metabolism in the Antarctic diatom *Chaetoceros brevis* (Bacillariophyceae). *Eur. J. Phycol.* 39, 161–171. doi:10.1080/0967026042000202127.

Wang, Z., King, K. L., Ramsdell, J. S., and Doucette, G. J. (2007). Determination of domoic acid in seawater and phytoplankton by liquid chromatography-tandem mass spectrometry. *J. Chromatogr. A* 1163, 169–176. doi:10.1016/j.chroma.2007.06.054.

Wells, M. L., Trick, C. G., Cochlan, W. P., Hughes, M. P., and Trainer, V. L. (2005). Domoic acid: The synergy of iron, copper, and the toxicity of diatoms. *Limnol. Oceanogr.* 50, 1908–1917. doi:10.4319/lo.2005.50.6.1908.

Wright, S. W. (1991). Improved HPLC method for the analysis of chlorophylls and carotenoids from marine phytoplankton. *Mar. Ecol. Prog. Ser.* 77, 183–196. doi:10.3354/meps077183.

Zhu, Z., Qu, P., Gale, J., Fu, F., and Hutchins, D. A. (2017). Individual and interactive effects of warming and CO2 on *Pseudo-nitzschia subcurvata* and *Phaeocystis antarctica*, two dominant phytoplankton from the Ross Sea, Antarctica. *Biogeosciences* 14, 5281–5295. doi:10.5194/bg-14-5281-2017.

Zhu, Z., Xu, K., Fu, F., Spackeen, J. L., Bronk, D. A., and Hutchins, D. A. (2016). A comparative study of iron and temperature interactive effects on diatoms and *Phaeocystis antarctica* from the Ross Sea, Antarctica. *Mar. Ecol. Prog. Ser.* 550, 39–51. doi:10.3354/meps11732.

6 Conclusions and Perspectives

This study provides new insights into the overall distribution of dDA in the East Atlantic Ocean and highlights the connection of dDA to environmental parameters and potential ligand function, using a highly sensitive quantification method.

6.1 Quantification of dissolved DA and its isomers and tracing other substances within DOM

Within the scope of this thesis, a highly sensitive method with near quantitative dDA recovery rates was developed. The method allowed quantifying the contribution of dDA to the entire pool of DOM. The method is fast and facilitates the quantification of very low dDA concentrations, which is valuable to enable the monitoring of dDA.

There are extremely few studies that managed to quantify single compounds within the highly complex matrix of marine DOM. Having identified dDA as part of DOM will allow the identification of similar molecules that contribute to marine DOM. However, an important prerequisite for such targeted approaches would be the quantitative assessment of extractability of the targets. By that, such future studies would contribute to a better understanding of the molecular composition of marine DOM.

Some of these targets, which are similar to DA, are isodomoic acids that are produced by different *Pseudo-nitzschia* and *Nitzschia* species and for which comparatively limited studies are available (Bates et al., 2018). It can be expected that domoic acid isomers should be well extractable with the method used within this thesis. With small modifications of the highly sensitive UPLC-MS/MS method presented, DA analogues could be analysed in seawater and cellular extracts. This would allow the assessment of isomer production and its release by other species, particularly by species, which have not been reported to produce DA, such as *P. subcurvata*.

Moreover, the quantification of dDA in its isomers in seawater could help in further elucidating, how and how fast dDA is degraded in the ocean. The ability to quantify DA isomers could also help in assessing, whether these substances show any ecological functions.

6.2 Distribution, stability, residence times and monitoring of dissolved domoic acid

The biogeochemical role of dDA and its distribution was studied in the entire Eastern Atlantic, including both polar sectors, where it occurred ubiquitously. The study presented in chapter 4 found high dDA concentrations, where pDA and producing organisms were abundant, suggesting that high dDA concentrations may serve as good indicator for toxic blooms. In chapter 3 and 4, dDA was quantified in the entire water column and results suggest that the residence time and persistence of dDA in the water column is at least as high as of pDA. Consequently, dDA can be found in the water column even after the blooms have ceased and its concentration varies with types of water masses. Moreover, we detected specific DA biosynthesis gene clusters in surface water cell samples where dDA concentration was high. For future approaches, assessing the presence of these gene clusters in combination with dDA concentrations could yield information on whether DA is still produced or if a remainder of a preceding bloom was detected. My results imply that dDA is persistent enough to be transported within a water mass meaning that the advection is faster than the degradation or dilution below detection. Its persistence is particularly surprising because DA contains nitrogen, which is usually assimilated fast in the ocean. In this context, it would be beneficial to better specify residence times of dDA in the water column. It is known that dDA is degraded via photooxidation in the uppermost water column and that below, bacterial degradation is an important sink (Bates et al., 2003; Hagström et al., 2007). Future experiments combining photooxidation and bacterial degradation could be performed to determine the importance of both. In addition, comparing the assimilation by *Pseudo-nitzschia* associated bacteria and other bacterial communities could help in assessing where bacterial degradation is highest. Furthermore, repeated in-situ quantifications of dDA after a toxic *Pseudo-nitzschia* bloom and their comparison with experimental results could help further resolve residence times of dDA. Knowing how long dDA will remain after a toxic bloom could help in tracing if such a bloom took place. Combined with knowledge on degradation products and their ratios it might even be possible to gain an idea about the time passed after a bloom. This could be an important contribution to monitor the occurrence of toxic *Pseudo-nitzschia* blooms in the future.

Quantifying dDA throughout the water column and in particular close to the bottom could help to estimate where and whether DA might influence benthic food webs, especially if it is considered that dDA occurred in the Ocean ubiquitously.

6.3 Assessing the ecological relevance and potential ligand function of dissolved domoic acid

In order to study the ecological role of dDA, I quantified dDA in different Arctic fjords and related its occurrence to pDA levels, *Pseudo-nitzschia* counts and a variety of other environmental parameters, such as water masses and macronutrient concentrations. A critical driver in this comparison is the question why DA is released. I found that dDA concentrations inversely correlated with silicate and phosphate in the field. A limitation of these macronutrients could be responsible for both DA production and dDA release. Measuring dDA levels in the ocean could thus help to understand the producers' reaction to their environment and support future understanding of toxic bloom dynamics. Particularly in the rapidly warming Arctic Ocean, an increase in sea ice melt will lead to changing conditions. Higher temperature and lower salinities would favour the presence of *Pseudo-nitzschia*, as it was shown for the Western Arctic Ocean (Sugie et al., 2020). In combination with low nutrient availability, an increase of DA production but also its release could likely happen. Monitoring dDA with other ecological parameters such as macronutrient concentrations, trace metal concentrations, numbers of grazers, associated bacteria and competitive phytoplankton communities could help in tracking these changes and help predicting areas that might be subject to future toxic blooms. Complementary experiments such as testing whether dDA has an effect on other local phytoplankton communities or bacterial abundance, could help to verify field observations. Furthermore, they might help in assessing dDA's effects on other organisms, particularly considering concentrations, which might actually occur in the environment.

After showing that dDA occurs in the Antarctic Ocean, a laboratory experiment with Southern Ocean endemic *Pseudo-nitzschia subcurvata* described in chapter 5 showed that the hypothesis about increasing growth rates due to dDA availability at low iron conditions could not be confirmed. Moreover, the cellular iron content did not increase if dDA was available. Thus, *P. subcurvata*, which did not produce DA, did not use it as adaptation mechanism to low iron concentrations. A likely reason is that only species producing DA might be positively affected by its presence concerning low iron concentrations. To further address the ligand function, the experiment should be repeated with species, which are known to be able to produce DA. Furthermore, the results indicated that the cells in the low iron treatment that had access to dDA contained more copper. From the results of the experiment, it could not be distinguished, whether dDA was connected to these higher copper levels. Further

experiments using copper isotopes could help in addressing, whether copper uptake is increased when dDA is added to a *Pseudo-nitzschia* culture. Overall, the interactions of dDA with its environment, particularly with trace metals, are quite complex.

Being ubiquitously distributed, dDA could be used well for molecular characterisation of DOM and it might be possible to identify other targets with similar methods. Whether dDA plays a role for primary production in HNLC regions due to its suggested ligand function could still not be deduced and should be ascertained in the future. Gaining a better understanding of the ecological relevance of dDA will help to better understand the occurrence and dynamics of toxic blooms, which seem to be greatly affected by global warming. Moreover, it will help to understand the chemical interaction of species, particularly in the rapidly changing Polar Regions.

7 References

Allanson, B. R., Hart, R. C., and Lutjeharms, J. R. E. (1981). Observations on the nutrients, chlorophyll and primary production of the Southern Ocean south of Africa. *South African J. Antarct. Res.* 10/11, 3–14.

Amato, A., Lüdeking, A., and Kooistra, W. H. C. F. (2010). Intracellular domoic acid production in *Pseudo-nitzschia multistriata* isolated from the Gulf of Naples (Tyrrhenian Sea, Italy). *Toxicon* 55, 157–161. doi:10.1016/j.toxicon.2009.07.005.

Auro, M. E., and Cochlan, W. P. (2013). Nitrogen Utilization and Toxin Production by Two Diatoms of the *Pseudo-nitzschia pseudodelicatissima* Complex: *P. cuspidata* and *P. fryxelliana*. *J. Phycol.* 49, 156–169. doi:10.1111/jpy.12033.

Ayache, N., Hervé, F., Martin-Jézéquel, V., Amzil, Z., and Caruana, A. M. N. (2019). Influence of sudden salinity variation on the physiology and domoic acid production by two strains of *Pseudo-nitzschia australis*. *J. Phycol.* 55, 186–195. doi:10.1111/jpy.12801.

Azam, F., Jiao, N., Sanders, S., Stone, R., Ogawa, H., Amagai, Y., et al. (2011). *Microbial Carbon Pump In The Ocean*., eds. N. Jiao, F. Azam, and S. Sanders The American Associeation for the Advancement of Science.

Barbaro, E., Zangrando, R., Rossi, S., Cairns, W. R. L., Piazza, R., Corami, F., et al. (2013). Domoic acid at trace levels in lagoon waters: Assessment of a method using internal standard quantification. *Anal. Bioanal. Chem.* 405, 9113–9123. doi:10.1007/s00216-013-7348-5.

Bargu, S., Lefebvre, K. A., and Silver, M. W. (2006). Effect of dissolved domoic acid on the grazing rate of krill *Euphausia pacifica*. *Mar. Ecol. Prog. Ser.* 312, 169–175. doi:10.3354/meps312169.

Bates, S. S., Bird, C. J., de Freitas, A. S. W., Foxall, R., Gilgan, M., Hanic, L. A., et al. (1989). Pennate Diatom *Nitzschia pungens* as the Primary Source of Domoic Acid, a Toxin in Shellfish from Eastern Prince Edward Island, Canada. *Can. J. Fish. Aquat. Sci.* 46, 1203–1215. doi:10.1139/f89-156.

Bates, S. S., Douglas, D. J., Doucette, G. J., and Léger, C. (1995). Enhancement of domoic acid production by reintroducing bacteria to axenic cultures of the diatom *Pseudo-nitzschia multiseries*. *Nat. Toxins* 3, 428–435. doi:10.1002/nt.2620030605.

Bates, S. S., Freitas, A. S. W. de, Milley, J. E., Pocklington, R., Quilliam, M. A., Smith, J. C., et al. (1991). Controls on Domoic Acid Production by the Diatom *Nitzschia pungens* f. *multiseries* in Culture: Nutrients and Irradiance. *Can. J. Fish. Aquat. Sci.* 48, 1136–1144. doi:10.1139/f91-137.

Bates, S. S., Gaudet, J., Kaczmarska, I., and Ehrman, J. M. (2004). Interaction between bacteria and the domoic-acid-producing diatom *Pseudo-nitzschia multiseries* (Hasle) Hasle; Can bacteria produce domoic acid autonomously? *Harmful Algae* 3, 11–20. doi:10.1016/j.hal.2003.08.001.

Bates, S. S., Hiltz, M. F., and Léger, C. (1999). Domoic acid toxicity of large new cells of *Pseudo-nitzschia multiseries* resulting from sexual reproduction. *Sixth Can. Work. Harmful Mar. Algae*, 21–26.

Bates, S. S., Hubbard, K. A., Lundholm, N., Montresor, M., and Leaw, C. P. (2018). *Pseudo-nitzschia*, *Nitzschia*, and domoic acid: New research since 2011. *Harmful Algae* 79, 3–43. doi:10.1016/j.hal.2018.06.001.

Bates, S. S., Léger, C., Satchwell, M., and Boyer, G. L. (2001). The effects of iron on domoic acid production by *Pseudo-nitzschia multiseries*. in *Harmful Algal Blooms (2000)*, eds. G. A. Hallegraeff, S. I. Blackburn, C. J. Bolch, and R. J. Lewis (Paris), 320–323.

Bates, S. S., Léger, C., Wells, M. L., and Hardy, K. (2003). Photodegradation of Domoic Acid. *Proc. Eight Can. Work. Harmful Mar. Algae*, 30–35.

Bates, S. S., Lundholm, N., Hubbard, K. A., Montresor, M., and Leaw, C. P. (2019). “Toxic and Harmful Marine Diatoms,” in *Diatoms: Fundamentals and Applications*, eds. J. Seckbach and R. Gordon (Scrivener Publishing LLC), 389–434.

Bates, S. S., Worms, J., and Smith, J. C. (1993). Effects of Ammonium and Nitrate on Growth and Domoic Acid Production by *Nitzschia pungens* in Batch Culture. *Can. J. Fish. Aquat. Sci.* 50, 1248–1254. doi:10.1139/f93-141.

Baugh, K. A., Bush, J. M., Bill, B. D., Lefebvre, K. A., and Trainer, V. L. (2006). Estimates of specific toxicity in several *Pseudo-nitzschia* species from the Washington coast, based on culture and field studies. *African J. Mar. Sci.* 28, 403–407. doi:10.2989/18142320609504187.

Bouillon, R.-C., Kieber, R. J., Skrabal, S. A., and Wright, J. L. C. (2008). Photochemistry and identification of photodegradation products of the marine toxin domoic acid. *Mar. Chem.* 110, 18–27. doi:10.1016/j.marchem.2008.02.002.

Bouillon, R.-C., Knierim, T. L., Kieber, R. J., Skrabal, S. A., and Wright, J. L. C. (2006). Photodegradation of the algal toxin domoic acid in natural water matrices. *Limnol. Oceanogr.* 51, 321–330. doi:10.4319/lo.2006.51.1.0321.

Brunson, J. K., McKinnie, S. M. K., Chekan, J. R., McCrow, J. P., Miles, Z. D., Bertrand, E. M., et al. (2018). Biosynthesis of the neurotoxin domoic acid in a bloom-forming diatom. *Science* 361, 1356–1358. doi:10.1126/science.aau0382.

Burns, J. M., and Ferry, J. L. (2007). Adsorption of domoic acid to marine sediments and clays. *J. Environ. Monit.* 9, 1373–1377. doi:10.1039/b713101a.

Busse, L. B., Venrick, E. L., Antrobus, R., Miller, P. E., Vigilant, V., Silver, M. W., et al. (2006). Domoic acid in phytoplankton and fish in San Diego, CA, USA. *Harmful Algae* 5, 91–101. doi:10.1016/j.hal.2005.06.005.

Carlson, C. a., and Ducklow, H. W. (1995). Dissolved organic carbon in the upper ocean of the central equatorial Pacific Ocean, 1992: Daily and finescale vertical variations. *Deep Sea Res. Part II Top. Stud. Oceanogr.* 42, 639–656. doi:10.1016/0967-0645(95)00023-J.

Carlson, C. A., Ducklow, H. W., and Michaels, A. F. (1994). Annual flux of dissolved organic carbon from the euphotic zone in the northwestern Sargasso Sea. *Nature* 371, 405–408.

Cendes, F., Andermann, F., Carpenter, S., Zatorre, R. J., and Cashman, N. R. (1995). Temporal lobe epilepsy caused by domoic acid intoxication: Evidence for glutamate receptor–mediated excitotoxicity in humans. *Ann. Neurol.* 37, 123–126. doi:10.1002/ana.410370125.

Cerino, F., Orsini, L., Sarno, D., Dell'Aversano, C., Tartaglione, L., and Zingone, A. (2005). The alternation of different morphotypes in the seasonal cycle of the toxic diatom *Pseudo-nitzschia galaxiae*. *Harmful Algae* 4, 33–48. doi:10.1016/j.hal.2003.10.005.

Clayden, J., Read, B., and Hebditch, K. R. (2005). Chemistry of domoic acid, isodomoic acids, and their analogues. *Tetrahedron* 61, 5713–5724. doi:10.1016/j.tet.2005.04.003.

Cusack, C. K., Bates, S. S., Quilliam, M. a, Patching, J. W., and Raine, R. (2002). Confirmation of domoic acid production by *Pseudo-nitzschia australis* (Bacillariophyceae) isolated from Irish waters. *J. Phycol.* 1112, 1106–1112. doi:10.1046/j.1529-8817.2002.01054.x.

Daigo, K. (1959). Studies on the Constituents of *Chondria armata*. II. Isolation of an Anthelmintical Constituent. *J. Japanese Pharm. Assoc.* 79, 353–356.

Delegrange, A., Lefebvre, A., Gohin, F., Courcot, L., and Vincent, D. (2018). *Pseudo-nitzschia* sp. diversity and seasonality in the southern North Sea, domoic acid levels and associated phytoplankton communities. *Estuar. Coast. Shelf Sci.* 214, 194–206. doi:10.1016/j.ecss.2018.09.030.

Dittmar, T., Koch, B. P., Hertkorn, N., and Kattner, G. (2008). A simple and efficient method for the solid-phase extraction of dissolved organic matter (SPE-DOM) from seawater. *Limnol. Oceanogr. Methods* 6, 230–235. doi:10.4319/lom.2008.6.230.

Doucette, G. J., King, K. L., Thessen, A. E., and Dortch, Q. (2008). The effect of salinity on domoic acid production by the diatom *Pseudo-Nitzschia multiseries*. *Nov. Hedwigia Beih* 133, 31–46.

Douglas, D. J., and Bates, S. S. (1992). Production of Domoic Acid, a Neurotoxic Amino Acid, by an Axenic Culture of the Marine Diatom *Nitzschia pungens* f. *multiseries* Hasle. *Can. J. Fish. Aquat. Sci.* 49, 85–90. doi:10.1139/f92-010.

Douglas, D. J., Bates, S. S., Bourque, L. A., and Selvin, R. C. (1993). “Domoic acid production by axenic and non-axenic cultures of the pennate diatom *Nitzschia pungens* f. *multiseries*,” in *Toxic Phytoplankton Blooms in the Sea*, eds. T. J. Smayada and Y. Shimizu (Elsevier Science Publishers B.V. (Biomedical Division)), 595–600.

Falk, M., Seto, P. F., and Walter, J. A. (1991). Solubility of domoic acid in water and in non-aqueous solvents. *Can. J. Chem.* 69, 1740–1744. doi:10.1139/v91-255.

Fehling, J., Davidson, K., Bolch, C. J., and Bates, S. S. (2004). Growth and domoic acid production by *Pseudo-nitzschia seriata* (Bacillariophyceae) under phosphate and silicate limitation. *J. Phycol.* 40, 674–683. doi:10.1111/j.1529-8817.2004.03213.x.

Fisher, J. M., Reese, J. G., Pellechia, P. J., Moeller, P. L., and Ferry, J. L. (2006). Role of Fe(III), phosphate, dissolved organic matter, and nitrate during the photodegradation of domoic acid in the marine environment. *Environ. Sci. Technol.* 40, 2200–2205. doi:10.1021/es051443b.

Furey, A., Lehane, M., Gillman, M., Fernandez-Puente, P., and James, K. J. (2001). Determination of domoic acid in shellfish by liquid chromatography with electrospray ionization and multiple tandem mass spectrometry. *J. Chromatogr. A* 938, 167–174. doi:10.1016/S0021-9673(01)01385-1.

Garthwaite, L., Ross, K. M., Miles, C. O., Hansen, R. P., Foster, D., Wilkins, A. L., et al. (1998). Polyclonal antibodies to domoic acid, and their use in immunoassays for domoic acid in sea water and shellfish. *Nat. Toxins* 6, 93–104. doi:10.1002/(sici)1522-7189(199805/08)6:3/4<93::aid-nt15>3.3.co;2-0.

Hagström, J. A., Granéli, E., Maneiro, I., Barreiro, A., Petermann, A., and Svensen, C. (2007). Release and degradation of amnesic shellfish poison from decaying *Pseudo-nitzschia multiseries* in presence of bacteria and organic matter. *Harmful Algae* 6, 175–188. doi:10.1016/j.hal.2006.08.002.

Hansell, D., Carlson, C. A., Repeta, D. J., and Schlitzer, R. (2009). Dissolved Organic Matter in the Ocean: A controversy stimulates new insights. *Oceanography* 22, 202–11. doi:10.5670/oceanog.2009.109.

Hansen, L. R., Soylu, S. í, Kotaki, Y., Moestrup, Ø., and Lundholm, N. (2011). Toxin production and temperature-induced morphological variation of the diatom *Pseudo-nitzschia seriata* from the Arctic. *Harmful Algae* 10, 689–696. doi:10.1016/j.hal.2011.05.004.

Harðardóttir, S., Krock, B., Wohlrab, S., John, U., Gissel, T., and Lundholm, N. (2018). Can domoic acid affect escape response in copepods? *Harmful Algae* 79, 50–52. doi:10.1016/j.hal.2018.08.009.

Harðardottir, S., Pančic, M., Tammilehto, A., Krock, B., Møller, E. F., Nielsen, T. G., et al. (2015). Dangerous Relations in the Arctic Marine Food Web: Interactions between Toxin Producing *Pseudo-nitzschia* Diatoms and *Calanus* Copepodites. *Mar. Drugs* 13, 3809–3835. doi:10.3390/md13063809.

Harðardóttir, S., Wohlrab, S., Hjort, D. M., Krock, B., Nielsen, T. G., John, U., et al. (2019). Transcriptomic responses to grazing reveal the metabolic pathway leading to the biosynthesis of domoic acid and highlight different defense strategies in diatoms. *BMC Mol. Biol.* 20, 1–14. doi:10.1186/s12867-019-0124-0.

Hasle, G. R. (2002). Are most of the domoic acid-producing species of the diatom genus *Pseudo-nitzschia* cosmopolites? *Harmful Algae* 1, 137–146. doi:10.1016/S1568-9883(02)00014-8.

Hong, Z., Zhang, Y., Zou, Z., Zhu, R., and Gao, Y. (2015). Influences of Domoic Acid Exposure on Cardiac Development and the Expression of Cardiovascular Relative Genes in Zebrafish (*Daniorerio*) Embryos. *J. Biochem. Mol. Toxicol.* 29, 246–260. doi:10.1002/jbt.

Hopkinson, C. S., Vallino, J. J., and Nolin, A. (2002). Decomposition of dissolved organic matter from the continental margin. *Deep. Res. II* 49, 4461–4478. doi:10.1016/S0967-0645(02)00125-X.

Hoppe, C. J. M., Hassler, C. S., Payne, C. D., Tortell, P. D., Rost, B. R., and Trimborn, S. (2013). Iron limitation modulates ocean acidification effects on Southern Ocean phytoplankton communities. *PLoS One* 8. doi:10.1371/journal.pone.0079890.

Huang, C. X., Dong, H. C., Lundholm, N., Teng, S. T., Zheng, G. C., Tan, Z. J., et al. (2019). Species composition and toxicity of the genus *Pseudo-nitzschia* in Taiwan Strait, including *P. chiniana* sp. nov. and *P. qiana* sp. nov. *Harmful Algae* 84, 195–209. doi:10.1016/j.hal.2019.04.003.

Kaczmarska, I., Ehrman, J. M., Bates, S. S., Green, D. H., Léger, C., and Harris, J. (2005). Diversity and distribution of epibiotic bacteria on *Pseudo-nitzschia multiseries* (Bacillariophyceae) in culture, and comparison with those on diatoms in native seawater. *Harmful Algae* 4, 725–741. doi:10.1016/j.hal.2004.10.001.

Kirchman, D. L., Suzuki, Y., Garside, C., and Ducklow, H. W. (1991). High turnover rates of dissolved organic carbon during a spring phytoplankton bloom. *Lett. to Nat.* 352, 612–614.

Kotaki, Y. (2008). “Ecobiology of Amnesic Shellfish Toxin Producing Diatoms,” in *Seafood and Freshwater Toxins: Pharmacology, Physiology and Detection*, ed. L. M. Botana (Boca Raton: CRC Press), 383–396.

Kudela, R. M., Anderson, C., Birch, J. M., Bowers, H., Caron, D. A., Chao, Y., et al. (2015). Harmful algal bloom hotspots really are hot: A case study from Monterey Bay, California. in *AGU Fall Meeting Abstracts*.

Ladizinsky, N. (2003). The influences of dissolved copper on the production of domoic acid by *Pseudo-nitzschia* species in Monterey Bay, California: laboratory experiments and field observations. California State University. 68p.

Lail, E. M., Skrabal, S. A., Kieber, R. J., Bouillon, R. C., and Wright, J. L. C. (2007). The role of particles on the biogeochemical cycling of domoic acid and its isomers in natural water matrices. *Harmful Algae* 6, 651–657. doi:10.1016/j.hal.2007.01.005.

Lelong, A., Bucciarelli, E., Hégaret, H., and Soudant, P. (2013). Iron and copper limitations differently affect growth rates and photosynthetic and physiological parameters of the marine diatom *Pseudo-nitzschia delicatissima*. *Limnol. Oceanogr.* 58, 613–623. doi:10.4319/lo.2013.58.2.0613.

Lelong, A., Hégaret, H., Soudant, P., and Bates, S. S. (2012). *Pseudo-nitzschia* (Bacillariophyceae) species, domoic acid and amnesic shellfish poisoning: revisiting previous paradigms. *Phycologia* 51, 168–216. doi:10.2216/11-37.

Lema, K. A., Latimier, M., Nézan, É., Fauchot, J., and Le Gac, M. (2017). Inter and intra-specific growth and domoic acid production in relation to nutrient ratios and concentrations in *Pseudo-nitzschia*: phosphate an important factor. *Harmful Algae* 64, 11–19. doi:10.1016/j.hal.2017.03.001.

Li, Y., Harir, M., Uhl, J., Kanawati, B., Lucio, M., Smirnov, K. S., et al. (2017). How representative are dissolved organic matter (DOM) extracts? A comprehensive study of sorbent selectivity for DOM isolation. *Water Res.* 116, 316–323. doi:10.1016/j.watres.2017.03.038.

Liefer, J. D., Robertson, A., MacIntyre, H. L., Smith, W. L., and Dorsey, C. P. (2013). Characterization of a toxic *Pseudo-nitzschia* spp. bloom in the Northern Gulf of Mexico associated with domoic acid accumulation in fish. *Harmful Algae* 26, 20–32. doi:10.1016/j.hal.2013.03.002.

Liu, H., Kelly, M. S., Campbell, D. A., Dong, S. L., Zhu, J. X., and Wang, S. F. (2007). Exposure to domoic acid affects larval development of king scallop *Pecten maximus* (Linnaeus, 1758). *Aquat. Toxicol.* 81, 152–158. doi:10.1016/j.aquatox.2006.11.012.

Lundholm, N., Hansen, P. J., and Kotaki, Y. (2004). Effect of pH on growth and domoic acid production by potentially toxic diatoms of the genera *Pseudo-nitzschia* and *Nitzschia*. *Mar. Ecol. Prog. Ser.* 273, 1–15. doi:10.3354/meps273001.

Lundholm, N., Krock, B., John, U., Skov, J., Cheng, J., Pančić, M., et al. (2018). Induction of domoic acid production in diatoms—Types of grazers and diatoms are important. *Harmful Algae* 79, 64–73. doi:10.1016/j.hal.2018.06.005.

Lundholm, N., Skov, J., Pocklington, R., and Moestrup, Ø. (1994). Domoic acid, the toxic amino acid responsible for amnesic shellfish poisoning, now in *Pseudonitzschia seriata* (Bacillariophyceae) in Europe. *Phycologia* 33, 475–478. doi:10.2216/i0031-8884-33-6-475.1.

Macintyre, H. L., Stutes, A. L., Smith, W. L., Dorsey, C. P., Annabraham, and Dickey, R. W. (2011). Environmental correlates of community composition and toxicity during a bloom of *Pseudo-nitzschia* spp. in the northern Gulf of Mexico. *J. Plankton Res.* 33, 273–295. doi:10.1093/plankt/fbq146.

Maeda, M., Kodama, T., Tanaka, T., Ohfune, Y., Nomoto, K., Nishimura, K., et al. (1984). Insecticidal and Neuromuscular Activities of Domoic Acid and Its Related Compounds. *J. Pestic. Sci.* 9, 27–32. doi:10.1584/jpestics.9.27.

Maeda, M., Kodama, T., Tanaka, T., Yoshizumi, H., Takemoto, T., Nomoto, K., et al. (1986). Structures of isodomoic acid A, B and C, novel insecticidal amino acids from the red alga *Chondria armata*. *Chem. Pharm. Bull.* 34, 4892–4895.

Maeno, Y., Kotaki, Y., Terada, R., Cho, Y., Konoki, K., and Yotsu-Yamashita, M. (2018). Six domoic acid related compounds from the red alga, *Chondria armata*, and domoic acid biosynthesis by the diatom, *Pseudo-nitzschia multiseries*. *Sci. Rep.* 8, 356. doi:10.1038/s41598-017-18651-w.

Maldonado, M. T., Hughes, M. P., Rue, E. L., and Wells, M. L. (2002). The effect of Fe and Cu on growth and domoic acid production by *Pseudo-nitzschia multiseries* and *Pseudo-nitzschia australis*. *Limnol. Oceanogr.* 47, 515–526. doi:10.4319/lo.2002.47.2.0515.

Marchetti, A., Catlett, D., Hopkinson, B. M., Ellis, K., and Cassar, N. (2015). Marine diatom proteorhodopsins and their potential role in coping with low iron availability. *ISME J.* 9, 2745–2748. doi:10.1038/ismej.2015.74.

Marchetti, A., Maldonado, M. T., Lane, E. S., and Harrison, P. J. (2006). Iron requirements of the pennate diatom *Pseudo-nitzschia*: Comparison of oceanic (high-nitrate, low-chlorophyll waters) and coastal species. *Limnol. Oceanogr.* 51, 2092–2101.

Marchetti, A., Schruth, D. M., Durkin, C. A., Parker, M. S., Kodner, R. B., Berthiaume, C. T., et al. (2012). Comparative metatranscriptomics identifies molecular bases for the physiological responses of phytoplankton to varying iron availability. *Proc. Natl. Acad. Sci. U. S. A.* 109. doi:10.1073/pnas.1118408109.

Martin, J. H., Gordon, R. M., and Fitzwater, S. E. (1990). Iron in Antarctic waters. *Nature* 345, 156–158. doi:10.1038/345156a0.

McCabe, R. M., Hickey, B. M., Kudela, R. M., Lefebvre, K. A., Adams, N. G., Bill, B. D., et al. (2016). An unprecedented coastwide toxic algal bloom linked to anomalous ocean conditions. *Geophys. Res. Lett.* 43, 10,366-10,376. doi:10.1002/2016GL070023.

Nash, S. M. B., Baddock, M. C., Takahashi, E., Dawson, A., and Cropp, R. (2017). Domoic Acid Poisoning as a Possible Cause of Seasonal Cetacean Mass Stranding Events in Tasmania, Australia. *Bull. Environ. Contam. Toxicol.* 98, 8–13. doi:10.1007/s00128-016-1906-4.

Nguyen, A. L., Luong, J. H. T., and Masson, C. (1990). Capillary electrophoresis for detection and quantitation of domoic acid in mussels. *Anal. Lett.* 23, 1621–1634. doi:10.1080/00032719008052513.

Ohfune, Y., and Tomita, M. (1982). Total Synthesis of (−)-Domoic Acid. A Revision of the Original Structure. *J. Am. Chem. Soc.* 104, 3511–3513. doi:10.1021/ja00376a048.

Pan, Y., Bates, S. S., and Cembella, A. D. (1998). Environmental stress and domoic acid production by *Pseudo-nitzschia*: A physiological perspective. *Nat. Toxins* 6, 127–135. doi:10.1002/(sici)1522-7189(199805/08)6:3/4<127::aid-nt9>3.3.co;2-u.

Pan, Y., Parsons, M., Busman, M., Moeller, P., Dortch, Q., Powell, C., et al. (2001). *Pseudo-nitzschia* sp. cf. *pseudodelicatissima* - a confirmed producer of domoic acid from the northern Gulf of Mexico. *Mar. Ecol. Prog. Ser.* 220, 83–92. doi:10.3354/meps220083.

Pan, Y., Subba Rao, D. V., and Mann, K. H. (1996a). Changes in domoic acid production and cellular chemical composition of the toxigenic diatom *Pseudo-nitschia multiseries* under phosphate limitation. *J. Phycol.* 32, 371–381. doi:10.1111/j.0022-3646.1996.00371.x.

Pan, Y., Subba Rao, D. V, Mann, K. H., Brown, R. G., and Pocklington, R. (1996b). Effects of silicate limitation on production of domoic acid, a neurotoxin, by the diatom *Pseudo-nitzschia multiseries*. I. Batch culture studies. *Mar. Ecol. Prog. Ser.* 131, 225/233. doi:10.3354/meps131225.

Piletska, E. V., Villoslada, F. N., Chianella, I., Bossi, A., Karim, K., Whitcombe, M. J., et al. (2008). Extraction of domoic acid from seawater and urine using a resin based on 2-(trifluoromethyl)acrylic acid. *Anal. Chim. Acta* 610, 35–43. doi:10.1016/j.aca.2008.01.032.

Pocklington, R., Milley, J. E., Bates, S. S., Bird, C. J., de Freitas, A. S. W., and Quilliam, M. A. (1989). Trace Determination of Domoic Acid in Seawater and Phytoplankton by High-Performance Liquid Chromatography of the Fluorenylmethoxycarbonyl (FMOC) Derivative. *Int. J. Environ. Anal. Chem.* 38, 351–368. doi:10.1080/03067319008026940.

Prince, E., Irmer, F., and Pohnert, G. (2013). Domoic Acid Improves the Competitive Ability of *Pseudo-nitzschia delicatissima* against the Diatom *Skeletonema marinoi*. *Mar. Drugs* 11, 2398–2412. doi:10.3390/md11072398.

Quilliam, M. A., and Wright, J. L. C. (1989). The Amnesic Shellfish Poisoning Mystery. *Anal. Chem.* 61, 1053A-1060A. doi:10.1021/ac00193a002.

Rhodes, L. L., Holland, P., Adamson, J., Selwood, A., and McNabb, P. (2004). Mass culture of New Zealand isolates of *Pseudo-nitzschia australis* for production of a new isomer of domoic acid. *Harmful Algae 2002*, 125–127.

Romero, M. L., Kotaki, Y., Relox, J. J., Lundholm, N., Takata, Y., Kodama, M., et al. (2012). Two new ASP toxin production types in strains of *Nitzschia navis-varingica* from the Philippines. *Coast. Mar. Sci.* 35, 67–69.

Rue, E., and Bruland, K. (2001). Domoic acid binds iron and copper: a possible role for the toxin produced by the marine diatom *Pseudo-nitzschia*. *Mar. Chem.* 76, 127–134. doi:10.1016/S0304-4203(01)00053-6.

Ryan, J. P., Kudela, R. M., Birch, J. M., Blum, M., Bowers, H. A., Chavez, F. P., et al. (2017). Causality of an extreme harmful algal bloom in Monterey Bay, California, during the 2014–2016 northeast Pacific warm anomaly. *Geophys. Res. Lett.* 44, 5571–5579. doi:10.1002/2017GL072637.

Schnetzer, A., Lampe, R. H., Benitez-Nelson, C. R., Marchetti, A., Osburn, C. L., and Tatters, A. O. (2017). Marine snow formation by the toxin-producing diatom, *Pseudo-nitzschia australis*. *Harmful Algae* 61, 23–30. doi:10.1016/j.hal.2016.11.008.

Schnetzer, A., Miller, P. E., Schaffner, R. A., Stauffer, B. A., Jones, B. H., Weisberg, S. B., et al. (2007). Blooms of *Pseudo-nitzschia* and domoic acid in the San Pedro Channel and Los Angeles harbor areas of the Southern California Bight, 2003-2004. *Harmful Algae* 6, 372–387. doi:10.1016/j.hal.2006.11.004.

Scholin, C. A., Gulland, F., Doucette, G. J., Benson, S., Busman, M., Chavez, F. P., et al. (2000). Mortality of sea lions along the central California coast linked to a toxic diatom bloom. *Nature* 403, 80–84. doi:10.1038/47481.

Sekula-Wood, E., Schnetzer, A., Benitez-Nelson, C. R., Anderson, C., Berelson, W. M., Brzezinski, M. A., et al. (2009). Rapid downward transport of the neurotoxin domoic acid in coastal waters. *Nat. Geosci.* 2, 272–275. doi:10.1038/ngeo472.

Shaw, B. A., Andersen, R. J., and Harrison, P. J. (1997). Feeding deterrent and toxicity effects of apo-fucoxanthinoids and phycotoxins on a marine copepod (*Tigriopus californicus*). *Mar. Biol.* 128, 273–280. doi:10.1007/s002270050092.

Silver, M. W., Bargu, S., Coale, S. L., Benitez-Nelson, C. R., Garcia, A. C., Roberts, K. J., et al. (2010). Toxic diatoms and domoic acid in natural and iron enriched waters of the oceanic Pacific. *Proc. Natl. Acad. Sci.* 107, 20762–20767. doi:10.1073/pnas.1006968107.

Silvert, W., and Subba Rao, D. V (1992). Dynamic Model of the Flux of Domoic Acid, a Neurotoxin, through a *Mytilus edulis* Population. *Can. J. Fish. Aquat. Sci.* 49, 400–405. Available at: www.nrcresearchpress.com.

Sison-Mangus, M. P., Jiang, S., Kudela, R. M., and Mehic, S. (2016). Phytoplankton-associated bacterial community composition and succession during toxic diatom bloom and non-bloom events. *Front. Microbiol.* 7, 1–12. doi:10.3389/fmicb.2016.01433.

Smida, D. B., Lundholm, N., Kooistra, W. H. C. F., Sahraoui, I., Ruggiero, M. V., Kotaki, Y., et al. (2014). Morphology and molecular phylogeny of *Nitzschia bizertensis* sp. nov.-A new domoic acid-producer. *Harmful Algae* 32, 49–63. doi:10.1016/j.hal.2013.12.004.

Smith, D. S., and Kitts, D. D. (1995). Enzyme Immunoassay for the Determination of Domoic Acid in Mussel Extracts. *J. Agric. Food Chem.* 43, 367–371. doi:10.1021/jf00050a020.

Sobrinho, B. F., De Camargo, L. M., Sandrini-Neto, L., Kleemann, C. R., Da Costa Machado, E., and Mafra, L. L. (2017). Growth, toxin production and allelopathic effects of *Pseudo-Nitzschia multiseries* under Iron-enriched conditions. *Mar. Drugs* 15. doi:10.3390/md15100331.

Stewart, J. E., Marks, L. J., Gilgan, M. W., Pfeiffer, E., and Zwicker, B. M. (1998). Microbial utilization of the neurotoxin domoic acid: blue mussels (*Mytilus edulis*) and soft shell clams (*Mya arenaria*) as sources of the microorganisms. *Can. J. Microbiol.* 44, 456–464. doi:10.1139/w98-028.

Subba Rao, D. V., Quilliam, M. A., and Pocklington, R. (1988). Domoic acid - A Neurotoxic Amino acid Produced by the Marine Diatom *Nitzschia pungens* in Culture. *Can. J. Fish. Aquat. Sci.* 45, 2076–2079. doi:10.1139/f88-241.

Sugie, K., Fujiwara, A., Nishino, S., Kameyama, S., and Harada, N. (2020). Impacts of Temperature, CO_2, and Salinity on Phytoplankton Community Composition in the Western Arctic Ocean. *Front. Mar. Sci.* 6. doi:10.3389/fmars.2019.00821.

Takemoto, T., and Daigo, K. (1958). Constituents of *Chondria armata*. *Chem. Pharm. Bull.* 6, 578–580. doi:10.1248/cpb.6.578b.

Tammilehto, A., Nielsen, T. G., Krock, B., Møller, E. F., and Lundholm, N. (2012). *Calanus* spp.-Vectors for the biotoxin, domoic acid, in the Arctic marine ecosystem? *Harmful Algae* 20, 165–174. doi:10.1016/j.hal.2012.10.004.

Tammilehto, A., Nielsen, T. G., Krock, B., Møller, E. F., and Lundholm, N. (2015). Induction of domoic acid production in the toxic diatom *Pseudo-nitzschia seriata* by calanoid copepods. *Aquat. Toxicol.* 159, 52–61. doi:10.1016/j.aquatox.2014.11.026.

Thorel, M., Claquin, P., Schapira, M., Le Gendre, R., Riou, P., Goux, D., et al. (2017). Nutrient ratios influence variability in *Pseudo-nitzschia* species diversity and particulate domoic acid production in the Bay of Seine (France). *Harmful Algae* 68, 192–205. doi:10.1016/j.hal.2017.07.005.

Thorel, M., Fauchot, J., Morelle, J., Raimbault, V., Le Roy, B., Miossec, C., et al. (2014). Interactive effects of irradiance and temperature on growth and domoic acid production of the toxic diatom *Pseudo-nitzschia australis* (Bacillariophyceae). *Harmful Algae* 39, 232–241. doi:10.1016/j.hal.2014.07.010.

Trainer, V. L., Adams, N. G., Bill, B. D., Stehr, C. M., Wekell, J. C., Moeller, P., et al. (2000). Domoic acid production near California coastal upwelling zones, June (1998). *Limnol Ocean.* 45, 1818–1833. doi:https://doi.org/10.4319/lo.2000.45.8.1818.

Trainer, V. L., Bates, S. S., Lundholm, N., Thessen, A. E., Cochlan, W. P., Adams, N. G., et al. (2012). *Pseudo-nitzschia* physiological ecology, phylogeny, toxicity, monitoring and impacts on ecosystem health. *Harmful Algae* 14, 271–300. doi:10.1016/j.hal.2011.10.025.

Trainer, V. L., Hickey, B. M., Lessard, E. J., Cochlan, W. P., Trick, C. G., Wells, M. L., et al. (2009a). Variability of *Pseudo-nitzschia* and domoic acid in the Juan de Fuca eddy region and its adjacent shelves. *Limnol. Oceanogr.* 54, 289–308. doi:10.4319/lo.2009.54.1.0289.

Trainer, V. L., Wells, M. L., Cochlan, W. P., Trick, C. G., Bill, B. D., Batgh, K. A., et al. (2009b). An ecological study of a massive bloom of toxigenic *Pseudo-nitzschia cuspidata* off the Washington State coast. *Limnol. Oceanogr.* 54, 1461–1474. doi:10.4319/lo.2009.54.5.1461.

Trick, C. G., Bill, B. D., Cochlan, W. P., Wells, M. L., Trainer, V. L., and Pickell, L. D. (2010). Iron enrichment stimulates toxic diatom production in high-nitrate, low-chlorophyll areas. *Proc. Natl. Acad. Sci. U. S. A.* 107, 5887–5892. doi:10.1073/pnas.0910579107.

Trick, C. G., Trainer, V. L., Cochlan, W. P., Wells, M. L., and Beall, B. F. (2018). The successional formation and release of domoic acid in a *Pseudo-nitzschia* bloom in the Juan de Fuca Eddy: A drifter study. *Harmful Algae* 79, 105–114. doi:10.1016/j.hal.2018.08.007.

Umhau, B. P., Benitez-Nelson, C. R., Anderson, C. R., McCabe, K., and Burrell, C. (2018). A Time Series of Water Column Distributions and Sinking Particle Flux of *Pseudo-Nitzschia* and Domoic Acid in the Santa Barbara Basin, California. *Toxins (Basel).* 10, 480. doi:10.3390/toxins10110480.

Van Dolah, F. M., Finley, E. L., Haynes, B. L., Doucette, G. J., Moeller, P. D., and Ramsdell, J. S. (1994). Development of rapid and sensitive high throughput pharmacologic assays for marine phycotoxins. *Nat. Toxins* 2, 189–196. doi:10.1002/nt.2620020407.

Van Dolah, F. M., Leighfield, T. A., Haynes, B. L., Hampson, D. R., and Ramsdell, J. S. (1997). A Microplate Receptor Assay for the Amnesic Shellfish Poisoning Toxin, Domoic Acid, Utilizing a Cloned Glutamate Receptor. *Anal. Biochem.* 245, 102–105.

Van Meerssche, E., and Pinckney, J. L. (2017). The influence of salinity in the domoic acid effect on estuarine phytoplankton communities. *Harmful Algae* 69, 65–74. doi:10.1016/j.hal.2017.10.003.

Walz, P. M., Garrison, D. L., Graham, W. M., Cattey, M. A., Tjeerdema, R. S., and Silver, M. W. (1994). Domoic acid-producing diatom blooms in Monterey Bay, California: 1991-1993. *Nat. Toxins* 2, 271–279. doi:10.1002/nt.2620020505.

Wang, Z., King, K. L., Ramsdell, J. S., and Doucette, G. J. (2007). Determination of domoic acid in seawater and phytoplankton by liquid chromatography-tandem mass spectrometry. *J. Chromatogr. A* 1163, 169–176. doi:10.1016/j.chroma.2007.06.054.

Wekell, J. C., Gauglitz, E. J., Bamett, H. J., Hatfield, C. L., Simons, D., and Ayres, D. (1994). Occurrence of Domoic Acid in Washington State Razor Clams (*Siliqua patula*) During 1991 -1993. *Nat. Toxins* 2, 197–205. doi:10.1002/nt.2620020408.

Wekell, J. C., Trainer, V. L., Ayres, D., and Simons, D. (2002). A study of spatial variability of domoic acid in razor clams: Recommendations for resource management on the Washington coast. *Harmful Algae* 1, 35–43. doi:10.1016/S1568-9883(02)00004-5.

Wells, M. L., Trick, C. G., Cochlan, W. P., Hughes, M. P., and Trainer, V. L. (2005). Domoic acid: The synergy of iron, copper, and the toxicity of diatoms. *Limnol. Oceanogr.* 50, 1908–1917. doi:10.4319/lo.2005.50.6.1908.

Windust, A. (1992). The Responses of Bacteria, Microalgae and Zooplankton to the Diatom *Nitzschia pungens* f. *multiseries* and Its Toxic Metabolite Domoic acid.

Work, T. M., Barr, B., Beale, A. M., Fritz, L., Michael, A., Wright, J. L. C., et al. (1993). Epidemiology of Domoic Acid Poisoning in Brown Pelicans (*Pelecanus occidentalis*) and Brandt's Cormorants (*Phalacrocorax penicillatus*) in California. *J. Zoo Wildl. Med.* 24, 54–62.

Wright, J. L. C., Boyd, R. K., de Freitas, A. S. W., Falk, M., Foxall, R. A., Jamieson, W. D., et al. (1989). Identification of domoic acid, a neuroexcitatory amino acid, in toxic mussels from eastern Prince Edward Island. *Can. J. Chem.* 67, 481–490. doi:10.1139/v89-075.

Wright, J. L. C., Falk, M., McInnes, A. G., and Walter, J. A. (1990). Identification of isodomoic acid D and two new geometrical isomers of domoic acid in toxic mussels. *Can. J. Chem.* 68, 22–25. doi:10.1139/v90-005.

Wu, W., Wu, X., Lin, X., Xie, Z., and Giesy, J. P. (2009). Quantification of domoic acid in shellfish tissues by pressurized capillary electrochromatography. *J. Sep. Sci.* 32, 2117–2122. doi:10.1002/jssc.200900017.

Zaman, L., Arakawa, O., Shimosu, A., Onoue, Y., Nishio, S., Shida, Y., et al. (1997). Two new isomers of domoic acid from a red alga, *Chondria armata*. *Toxicon* 35, 205–212. doi:10.1016/S0041-0101(96)00123-7.

Zhang, W., Lin, M., Tong, P., Lu, Q., and Zhang, L. (2016). Ferrite nanospheres-based magnetic solid-phase extraction for determination of domoic acid in seawater samples using high-performance liquid chromatography with tandem mass spectrometry. *J. Chromatogr. A* 1443, 54–61. doi:10.1016/j.chroma.2016.03.055.

Zhang, X. W., and Zhang, Z. X. (2012). Quantification of domoic acid in shellfish samples by capillary electrophoresis-based enzyme immunoassay with electrochemical detection. *Toxicon* 59, 626–632. doi:10.1016/j.toxicon.2012.02.011.